Conditional Chemoconnectomics: A Set of Libraries Targeting All Chemical Transmission Corresponding Genes Efficiently

Renbo Mao[a,b,#], Jianjun Yu[a,#], Bowen Deng[a], Xihuimin Dai[a], Yuyao Du[a], Sujie Du[a], Wenxia Zhang[a] and Yi Rao[a,1]

[a]Laboratory of Neurochemical Biology, Chinese Institute for Brain Research, Beijing; PKU-IDG/McGovern Institute for Brain Research, Peking-Tsinghua Center for Life Sciences, School of Life Sciences, Department of Chemical Biology, College of Chemistry and Chemical Engineering, School of Pharmaceutical Sciences, Peking University, Beijing 100871; Chinese Institutes for Medical Research, Capital Medical University; Changping Laboratory, Yard 28, Science Park Road, Changping District; and Research Unit of Medical Neurobiology, Chinese Academy of Medical Sciences, Beijing, China.

[b]National Institute of Biological Sciences, Chinese Academy of Medical Sciences & Peking Union Medical College, Beijing, China.

[#]Co-first authors

[1] Corresponding Author Yi Rao

Email: yrao@pku.edu.cn

Author Contributions: R.M. and J.Y. performed majority of experiments and data analysis. B.D., J.Y., and R.M. found advanced morning activity phenotype and carried out experiments of CNMa/CNMaR. R.M., Y.D., and S.D. carried out experiments of cCCTomics fly generation. R.M., J.Y., X.D., and Y.R. wrote the manuscript.

Competing Interest Statement: The authors declare no competing interest.

Keywords: chemoconnectome, CRISPR/Cas9, CNMa, circadian rhythm, morning anticipation

Abstract

Dissection of neural circuitry underlying behaviors is a central theme in neurobiology. Chemical transmission is the predominant model for signaling between neurons. Here we have created lines target all chemical transmission corresponding genes in Drosophila after modifying GFP RNA interference, Flp-out and CRISPR/Cas9 technologies. After thorough validation, all three strategies are demonstrated to be highly effective with the best using chromatin-peptide fused Cas9 variants and scaffold optimized sgRNAs. As a proof of principle, we conduct a comprehensive intersection analysis of chemoconnectome (CCT) genes expression profiles in the clock neurons using chemoconnectomics driver lines, leading to the finding of 45 CCT genes presented in clock neurons. Mutating these genes specifically in clock neurons revealed that loss of the neuropeptide CNMa in two posterior dorsal clock neurons (DN1p) or its receptor (CNMaR) caused advanced morning activity, opposite to the mutants of neuropeptide PDF or its receptor (PDFR). These results demonstrate the effectiveness of conditional chemoconnectomics libraries and indicate an antagonistic relationship between CNMa-CNMaR and PDF-PDFR signaling in regulating morning anticipation.

Introduction

Much research efforts have been made in uncovering the wiring and signaling pathways of neural circuits underlying specific behaviors. Multiple circuit dissection strategies have been developed, including genetic screening, genetic labelling, circuit tracing, live imaging, genetic sensors and central nervous system reconstruction via electron microscopy (EM) imaging. Recently, we have developed chemoconnectomics (CCTomics), focusing on building a comprehensive set of knockout and knockin tool lines of chemoconnectome (CCT) genes, to dissect neural circuitry based on chemical transmission (Deng et al., 2019).

Each strategy has advantages and disadvantages, for example: genetic screening is less biased but inefficient; circuit tracing with viruses provides information of connection, but is often prone to leaky expression and inaccurate labelling; and EM reconstruction is anatomically elaborate but does not allow for manipulation of corresponding neurons. CCTomics overcomes some limitations of previous strategies by allowing for behavioral screening of CCT genes and accurate labelling or manipulation of corresponding neurons. However, it is still limited in that knockout of some CCT genes can be lethal during development and that CCT genes may function differently in different neurons, which require a cell type-specific manipulation. Thus, we decided to invent a conditional CCTomics (cCCTomics) in which gene deletion was conditional.

There are three major strategies for somatic gene mutagenesis at the DNA/RNA level: RNA interference, DNA site-specific recombination enzymes, and CRISPR/Cas system. RNA interference targets RNAs conveniently and efficiently (Martin and Caplen, 2007; Oberdoerffer et al., 2005). Libraries of transgenic RNAi flies covering almost the entire fly genome have been

established (Ni et al., 2011; Perkins et al., 2015). DNA site specific recombination enzymes such as Flp, B3 and Cre mediate specific and efficient gene editing (Gaj et al., 2014; Grindley et al., 2006). These strategies require flies with reverse repetitive sequences knocked into the corresponding genes, which is time-consuming with relatively complex recombination for genetic assays. CRISPR/Cas systems, particularly CRISPR/Cas9, which targets DNA with a sgRNA/Cas protein complex, have been broadly applied in gene manipulation over the last decade. The widespread use of CRIPSR/Cas9 in Drosophila somatic gene manipulation began in 2014 (Xue et al., 2014). Later, tRNA-flanking sgRNAs was designed and applied, which enabled multiple sgRNAs to mature in a single transcript (Xie et al., 2015), accelerating the application of this strategy in conditional gene manipulation in flies with impressive efficiency (Delventhal et al., 2019; Port and Bullock, 2016; Port et al., 2020; Schlichting et al., 2019; Schlichting et al., 2022). Additionally, libraries of UAS-sgRNA targeting kinases (Port et al., 2020) and GPCRs (Schlichting et al., 2022) have been established, but no sgRNA libraries covering all the CCT genes exists yet. The efficiency of CRISPR/Cas9 has not been validated systematically in the Drosophila nervous system.

The circadian rhythm can be used for proof of principle testing of cCCTomics. Organisms evolve periodic behaviors and physiological traits in response to cyclical environmental changes. The rhythmic locomotor behavior of Drosophila, for instance, shows enhanced activity before the light is turned on and off in a light-dark (LD) cycle, referred to as morning and evening anticipations, respectively (Collins et al., 2005; Helfrich-Förster, 2001). Under dark-dark (DD) conditions, the activities peaks regularly about every 24 hours (h) (Konopka and Benzer, 1971). Approximately 150 clock neurons, circadian output neurons and extra-clock electrical

oscillators (xCEOs) coordinate Drosophila circadian behaviors (Dubowy and Sehgal, 2017; Tang et al., 2022). The regulation of morning and evening anticipations, the most prominent features in the LD condition, is primarily mediated by four pairs of sLNvs expressing pigment dispersing factor (PDF), six pairs of LNds and the 5th s-LNv (Grima et al., 2004; Rieger et al., 2006; Stoleru et al., 2004). At the molecular level, Pdf and Pdf receptor (PDFR) are well-known, with their mutants showing an advanced evening activity peak and no morning anticipation (Hyun et al., 2005; Lear et al., 2005; Renn et al., 1999). Other neuropeptides and their receptors, including AstC/AstC-R2 and neuropeptide F (NPF) and its receptor (NPFR), have also been reported to modulate evening activities (Díaz et al., 2019; He et al., 2013; Hermann et al., 2012), while CCHa1/CCHa1-R and Dh31 regulate morning activities (Fujiwara et al., 2018; Goda et al., 2019). To date, no advanced morning activity phenotype has been reported in flies.

To develop a more efficient approach for somatic gene manipulation, we have now generated two systems for conditional manipulation of CCT genes. One is GFPi/Flp-out-based conditional knockout system of CCT genes (cCCTomics) and another is CRISPR/Cas9-based (C-cCCTomics). Both systems have achieved high efficiency of gene mutagenesis in the Drosophila nervous system. C-cCCTomics, utilizing chromatin-peptide fused Cas9 and scaffold optimized sgRNA, makes efficient conditional gene knockout as simple as RNAi. Further application of C-cCCTomics in clock neurons revealed novel roles of CCT genes in circadian behavior: CNMa-CNMaR modulates morning anticipation as an antagonistic signal of PDF-PDFR.

Results

Complete Disruption of Target Genes by GFPi and Flp-out Based cCCTomics

For the purpose of conditional chemoconnectomics (cCCTomics), we initially leveraged the benefits of our previously generated CCTomics attP lines (Deng et al., 2019), which enabled us to fuse enhanced GFP coding sequence at the 3' end of each gene's coding region and flank most or entire gene span with FRT sequence through site-specific recombination (Fig 1A, Table S1). We designed this system so that it could be used to target genes tagged with GFP by RNAi (Neumüller et al., 2012) and at the same time to enable flippase(Flp) mediated DNA fragment excision between two FRT sequences when FRT sequences are in the same orientation (Vetter et al., 1983)（Fig1A）.

To validate the efficiency of cCCTomics, we performed pan-neuronal expression of either shRNA^{GFP} or flipase in cCCT flies. Immunofluorescent imaging showed that constitutive expression of shRNA^{GFP} (Fig 1B-1D, Fig S1A-S1I) or flipase (Fig 1E-1G, Fig S1J-S1U) almost completely eliminated GFP signals of target genes, indicating high efficiency. Knockout at the adult stage using either hsFLP driven Flp-out (Golic and Lindquist, 1989) (Fig 1H-1J) or neurally (elav-Switch) driven shRNA^{GFP} (Nicholson et al., 2008; Osterwalder et al., 2001) (Fig S2A-S2I) also showed high efficiency of suppression. Notably, control group of CCT$^{EGFP.FRT}$; elav-Switch/UAS-shRNAGFP flies fed with solvent (ethanol) showed obvious decreased GFP (Fig S2B, S2E, and S2H) comparing with UAS-shRNA^{GFP}/CCT$^{EGFP.FRT}$ flies fed with RU486 (Fig S2A, S2D, and S2G), indicating leaky expression of elav-Switch.

We then applied cCCTomics in pan-neuronal knockout of nAChRβ2 which is required for Drosophila sleep (Dai et al., 2021). Ablation of nAChRβ2 in the nervous system dramatically decreased both day and night sleep of flies, which was the same as shown in the previous

paper (Dai et al., 2021) (Fig 1K, 1L). Therefore, cCCTomics is an effective toolkit for manipulation of CCT genes and suitable for functional investigations of genes. Expression of in-frame fused eGFP-labelled CCT genes highly co-localized with signals revealed by immunocytochemistry (Fig S3A-S3I), allowing direct examination of gene expression without amplification, which is different from the GAL4/UAS binary system.

We then checked the viability of cCCT lines and found that cCCT lines including Capa$^{EGFP.FRT}$, ChAT$^{EGFP.FRT}$ and Eh$^{EGFP.FRT}$ were viable whereas their CCT mutants were lethal. Gad1$^{EGFP.FRT}$, GluRIID$^{EGFP.FRT}$ and CapaR$^{EGFP.FRT}$ were still lethal as their CCT mutants were (Table S2). This indicates that some of the cCCT knockin flies may functionally affect corresponding genes, which are not suitable for conditional gene manipulation. Combination of cCCT transgenic flies with UAS-flp, UAS-shRNA^{GFP} or specific drivers is complicated and unfriendly for screen work, despite the almost 100% efficiency of gene suppression. Because of the limitations of this method, we further created a CRISPR/Cas9 based conditional knockout system of chemoconnectomics (C-cCCTomics).

CRISPR/Cas9-Based Conditional Knockout System for CCTomics

To simplify effective manipulation of CCT genes, we designed a vector based on pACU2 (Han et al., 2011) with tRNA flanking sgRNAs (Port and Bullock, 2016; Xie et al., 2015) targeting CCT genes (Fig 2A). We also adopted an optimized sgRNA scaffold “E+F” (E, stem extension; F, A-U flip) (Chen et al., 2013), which facilitates Cas9-sgRNA complex formation and gene knockout efficiency (Dang et al., 2015; Poe et al., 2019; Zhao et al., 2016), to all sgRNAs to improve gene knockout efficiency. To balance efficiency and off-target effect, we selected three sgRNAs for

each CCT gene with highest predicted efficiency and no predicted off-target effect based on previously reported models (Chu et al., 2016; Doench et al., 2014; Graf et al., 2019; Gratz et al., 2014; Heigwer et al., 2014; Stemmer et al., 2015; Xu et al., 2015) (see Table S3 and details at Methods).

We generated UAS-sgRNA^{3x} transgenic lines for all 209 defined CCT genes (Abruzzi et al., 2017; Dai et al., 2019; Deng et al., 2019) and UAS-Cas9.HC (Cas9.HC) (Mali et al., 2013). We first verified that C-cCCTomics mediated precise target DNA breaking by ubiquitous expression of Cas9.P2 (Port et al., 2014) and sgRNA by targeting Pdf or Dh31. Sanger sequencing showed that indels were present exactly at the Cas9 cleavage sites (Fig S4A-S4H).

To determine the efficiency of C-cCCTomics, we employed pan-neuronal expression of Cas9.HC with sgRNA^{Dh31} or sgRNA^{pdf}. Targeting by Cas9.HC/sgRNA^{Dh31} eliminated most but not all of the GFP signal in Dh31$^{EGFP.FRT}$ (Fig 2B-2D), whereas all anti-PDF signals were eliminated by Cas9.HC/sgRNA^{pdf} (Fig 2E-2G). Furthermore, we used the C-cCCT strategy to conditionally knockout genes for pdfr, nAChRβ2 and nAChRα2, which were previously reported as essential for circadian rhythm or sleep (Dai et al., 2021; Renn et al., 1999). Pan-neuronal knockout of Pdfr phenocopied arrhythmicity of its null mutants (Fig 2H-2J) while there was no significant sleep decrease in these conditional knockout (cKO) flies (Fig 2K-2L) when we applied C-cCCTomics to manipulate nAChRβ2 or nAChRa2. Taken together, C-cCCTomics (with Cas9.HC) achieved a relatively high gene knockout efficiency, but it was not effective enough for all genes.

Evaluation of Cas9 with Different Chromatin-Modulating Peptides

Since the establishment of the CRISPR/Cas9 system a decade ago, many groups have attempted to improve its efficiency in gene manipulation. Most attempts have been focused on the two main components of this system, the Cas9 protein (Ding et al., 2019; Ling et al., 2020; Liu et al., 2019; Zhao et al., 2016; Zheng et al., 2020) and the single guide RNA (Chen et al., 2013; Chu et al., 2016; Dang et al., 2015; Doench et al., 2014; Filippova et al., 2019; Graf et al., 2019; Labuhn et al., 2018; Mu et al., 2019; Nahar et al., 2018; Scott et al., 2019; Xu et al., 2015). At the beginning of C-cCCTomics design, we adopted an optimized sgRNA scaffold and selected sgRNAs with predicted high efficiency. We tried to further improve the efficacy by modifying Cas9 protein. We fused a chromatin-modulating peptide (Ding et al., 2019), HMGN1 (High mobility group nucleosome binding domain 1), at the N-terminus of Cas9 and HMGB1 (High mobility group protein B1) at its C-terminus with GGSGP linker, termed Cas9.M9 (Fig 3A, Methods). We also obtained a modified Cas9.M6 with HMGN1 at the N-terminus and an undefined peptide (UDP) at the C-terminus (Fig 3A). We replaced the STARD linker between Cas9 and NLS in Cas9.HC with GGSGP the linker (Zhao et al., 2016), termed Cas9.M0 (Fig 3A). None of these modifications have been validated previously in flies.

To determine whether the modified Cas9 variants were more efficient, we first pan-neuronally expressed each Cas9 variant and sgRNA^{ple}, and assessed their efficiency by immunofluorescence imaging. By counting anti-TH positive neurons in the brain (anterior view) after targeting by Cas9/sgRNA^{ple}, we found that unmodified Cas9.HC/sgRNA^{ple} only achieved 69.58±3.04% (n=5) knockout efficiency (Fig 3G, 3K, 3L), while Cas9.M6/sgRNA^{ple} and Cas9.M9/sgRNA^{ple} significantly improved efficiency to 87.53±3.06% (n=7) and 97.19±2.15% (n=8), respectively (Fig 3I-3L). Fourteen additional CCT genes were subjected to pan-neuronal

196 knockout, and the mRNA levels of the target genes were evaluated using real-time quantitative
197 PCR with at least one primer overlapping the sgRNA targeting site (Fig S5). Cas9.M6 and
198 Cas9.M9 demonstrated significantly higher gene disruption efficiency compared to the
199 unmodified Cas9.HC, achieving average efficiencies of 87.51%±2.24% and 89.59%±2.39% for
200 Cas9.M6 and Cas9.M9, respectively, in contrast to 70.72%±3.82% for Cas9.HC. (Fig 3M, Fig
201 S5). To rule out the possibility of the observed variations in gene disruption efficiency being
202 attributed to differential Cas9 expression levels, we quantified the Cas9 expression levels and
203 noted that both Cas9.M6 and Cas9.M9 exhibited lower mRNA levels than Cas9.HC under the
204 experiment condition (Fig 3N). Subsequently, genomic DNA of Drosophila head was extracted,
205 and libraries encompassing target sites were constructed for high-throughput sequencing to
206 verify disparities in genetic editing efficiency among these three Cas9 variants (Fig 3O). In
207 almost all nineteen sites tested, the mutation ratio consistently showed a trend towards
208 Cas9.M6 and Cas9.M9 having a higher gene disruption efficiency than Cas9.HC (Fig 3P, Fig
209 S6). The single-site mutation rates varied from 5.81% to 43.47% for Cas9.HC, 22.40% to 53.54%
210 for Cas9.M6, and 19.90% to 63.57% for Cas9.M9 (Fig 3P, Fig S6). It should be noted that
211 genomic DNA extracted from fly heads contained glial cells, which did not express Cas9/sgRNA,
212 leading to a larger denominator and consequently reducing the observed mutation rates.
213 Unmodified Cas9 displayed mutation rates comparable to those previously reported by
214 Schlichting et al., 2022. The findings indicated that both Cas9.M6 and Cas9.M9 displayed
215 elevated efficiency compared to Cas9.HC, with Cas9.M9 exhibiting the highest mutagenesis
216 proficiency. These results suggest that the implementation of modified C-cCCTomics using
217 Cas9.M6 and Cas9.M9 achieved an elevated level of efficiency. While unmodified C-

cCCTomics was not efficient enough to knockout nAChRβ2 and nAChRα2 to phenocopy their mutants, we employed Cas9.M9 in conditional knockout of these genes to verify its efficiency. Pan-neuronal knocking out of nAChRβ2 or nAChRa2 by Cas9.M9/sgRNA showed significant sleep decrease which was similar to their mutants (Fig 3Q-3R) (Dai et al., 2021).

Taken together, our results support that we have created a high efficiency toolkit for CCT gene manipulation in the nervous system, as well as more efficient Cas9 variants, Cas9.M6 and Cas9.M9, which can also be applied to genes other than those in the CCT.

45 CCT Genes Found in Clock Neurons by Genetic Intersection

We analyzed the expression profile of CCT genes in circadian neurons with CCTomics driver lines in all clock neurons expressing Clk856 (Gummadova et al., 2009). With the Flp-out or split-lexA intersection strategy (Fig 4A, 4B), we found 45 out of 148 analyzed CCT genes expressed in circadian neurons (Fig 4C, Fig S7-S8, Table S4, Table S5). In all eight subsets of clock neurons, 24 CCT genes were expressed in DN1s, 20 in DN2s, 21 in DN3s, 29 in LNds, 15 in l-LNvs, 11 in s-LNvs, 5 in 5^{th} s-LNv and 3 in LPNs, with a total of 128 gene-subsets.

Prior to transcriptomic analysis (Ma et al., 2021), 23 CCT genes had been reported in clock neurons (Díaz et al., 2019; Duhart et al., 2020; Erion et al., 2016; Frenkel et al., 2017; Fujiwara et al., 2018; Goda et al., 2016; Hamasaka et al., 2007; He et al., 2013; Hermann-Luibl et al., 2014; Hermann et al., 2012; Hyun et al., 2005; Renn et al., 1999; Selcho et al., 2017). In our intersection dissection, expression profiles of 15 CCT genes were similar but not identical to previously reported 18 CCT genes in clock neurons (Fig 4C, Table S4). An additional 22 out of 30 CCT genes identified in our genetic intersection were also detected in the transcriptome

240 analysis (Ma et al., 2021). Among the 45 CCT genes expressed in eight clock neuron subsets,
241 128 gene-subsets, ~36% (46 out 128) were found in the transcriptome analysis (Ma et al., 2021)
242 (Fig 4C, Table S4). This suggests that the expression profile obtained through genetic
243 dissection overlapped with transcriptome results (see DISCUSSION).
244
245 **Conditional Knockout of CCT Genes in Circadian Neurons**
246 To investigate the function of CCT genes in circadian neurons with our conditional knockout
247 system, we knocked out all 67 (45 genes identified above and additional 22 genes reported
248 previously) CCT genes in Clk856-labeled clock neurons by C-cCCTomics.
249 In the pilot screen, we monitored fly activity by video recording (Dai et al., 2019) and analyzed
250 rhythmic behavior under LD and DD conditions. We analyzed morning anticipation index (MAI)
251 and evening anticipation index (EAI) under the LD condition (Harrisingh et al., 2007; Im and
252 Taghert, 2010)(Fig 5A), power, period and arrhythmic rate (AR) under the DD condition. Fly
253 activities tended to rise rapidly after ZT22.5 at dawn and ZT10 at dusk. Thus, we added two
254 more parameters to describe the anticipatory activity patterns of LD condition. Morning
255 anticipation pattern index (MAPI) was defined as the difference between
256 Pi_a[arctan(ZT20.5~ZT22.5 activity increasing slope)] and Pi_p[arctan(ZT22.5 ~ZT24 activity
257 increasing slope)], M(Pi_a-Pi_p). Evening anticipation pattern index (EAPI) was defined similar to
258 MAPI (Fig 5A, see Methods). Pi_a and Pi_p were positive, while MAPI and EAPI were negative,
259 for wild type (wt) flies as their activities gradually increases at dawn or dusk at increasing rates.
260 Knocking out Pdf or Pdfr in clock neurons phenocopied their mutants with lower MAI,
261 advanced evening activity, low power, high arrhythmic rate and shorter period (Hyun et al.,

2005; Lear et al., 2005; Renn et al., 1999) (Table S6, Fig S9A-S9D). The MAI-decreasing phenotype of Dh31 knockout was also reproduced in this pilot screen (Goda et al., 2019) (Table S6). All the above results verified the effectiveness of C-cCCTomics. Unexpectedly, additional experimental replications with full controls using Cas9.M9 revealed that leaky expression of Cas9.M9 and sgRNA might have caused disruption of Dh31, Dh44, Pdf and Pdfr (Fig S9A-S9D) (see DISCUSSION), which was not suitable for neuronal specific mutagenesis of some genes. Therefore, in the following work we primarily focused on Cas9.M6 instead.

Analysis of the newly defined parameters MAPI and EAPI showed that control flies (Clk856-GLA4>UAS-Cas9.M9) had negative EAPI but slightly positive MAPI. The positive MAPI of control flies in this screen might be caused by Cas9.M9 toxicity. Only the Pdf and Pdfr clock-neuron knockout flies showed positive EAPIs, indicating an advanced evening activity (Table S6, Fig S9A, S9C). nAChRα1, MsR1, mAChR-B, and CNMa cKO flies had highest MAPI values (Table S6). We further confirmed their phenotypes using Cas9.M6 which revealed that CNMa plays a role in regulating morning anticipatory activity (Fig S10A).

Regulation of Morning Anticipation by CNMa-positive DN1p Neurons

Conditionally knocking out CNMa in clock neurons advanced morning activity (Fig 5B, Fig S10B) and increased MAPI (Fig 5C, Fig S10A, S10C), leaving the power and period intact in male flies (Fig 5D, 5E). The same advanced morning activity phenotype were also observed in female flies (Fig S10D-S10G). To further validate this phenotype, we generated a CNMa knockout ($CNMa^{KO}$) line by replacing its whole coding region with an attP-splicing adaptor element (Deng et al., 2019) (Fig 5F). Both male and female $CNMa^{KO}$ flies exhibited the same phenotypes as

284 seen in the CNMa cKO (Fig 5G-5I).

285 Previous studies have found CNMa expression in DN1 neurons (Abruzzi et al., 2017; Jin et
286 al., 2021; Ma et al., 2021). Our intersection showed four DN1p and one DN3 CNMa positive
287 neurons in Clk856 labelled neurons (Fig S8 - 16, Fig 4C, Table S4). Analysis with an
288 endogenous CNMa-KI-GAL4 knockin driver showed that six pairs of CNMa neurons located in
289 the DN1p region and three pairs located in the subesophageal ganglion (SOG) had the brightest
290 GFP signals (Fig 6A). The anatomical features of CNMa neurons were further confirmed using
291 stingerRed and more neurons were found in regions, the anterior ventrolateral protocerebrum
292 (AVLP), and the antennal mechanosensory and motor center (AMMC) (Fig S11A). Dendrites of
293 CNMa neurons were concentrated in DN1p and SOG, with their axons distributed around DN1p
294 region, lateral horn (LH), and prow region (PRW) (Fig 6B, 6C). Using the Trans-tango strategy
295 (Talay et al., 2017), we also found that downstream of CNMa neurons were about fifteen pairs
296 of neurons in the SOG, five pairs of LNd neurons, one pair of DN3 neurons and six pars
297 intercerebralis (PI) neurons (Fig 6D, arrowhead).

298 Because we had found that knocking out CNMa in Clk856-GAL4 labeled neurons produced
299 advanced morning activity, and that CNMa intersected with Clk856-Gal4 labeled neurons in 4
300 pairs of DN1ps and one pair of DN3 neurons (Fig S8-16), we focused on these neurons and
301 performed more intersections. Taking advantage of a series of clock neuron subset-labeled
302 drivers (Sekiguchi et al., 2020), we intersected CNMa-p65AD with 4 DN1 labelling drivers:
303 GMR51H05-GAL4, GMR91F02-GAL4, Pdfr-KI-GAL4 and GMR79A11-GAL4 (Fig 6E-6H). We
304 found two arborization patterns: Type I with two neurons whose branches projecting to the
305 anterior region, as in CNMa∩GMR51H05, CNMa∩Pdfr, and CNMa∩GMR79A11 (Fig 6E, 5G,

306 6H), and type II with four neurons branching on the posterior side with few projections to the
307 anterior region, as in CNMa∩GMR91F02 (Fig 6F).

308 CNMa knockout in Type I or Type II neurons (GMR51H05-GAL4, GMR91F02-GAL4, and
309 GMR79A11-GAL4) all reproduced the MAPI-increased phenotype of clk856 specific CNMa
310 knockout (Fig 6I). However, Type II neurons-specific CNMa knockout (CNMa ∩ GMR91F02)
311 showed no advanced morning activity peak (Fig 6K), while Type I neurons-specific CNMa
312 knockout did (Fig 6J), indicating that these two type I CNMa neurons are the main functional
313 subset regulating the morning anticipation activity of fruit fly.

314 Pdf or Pdfr mutants have weak or no morning anticipation, which is in reversely related to
315 the phenotype of CNMa knockout flies. We also identified two Pdfr and CNMa double-positive
316 DN1ps, which have a type I projection pattern (Fig 6G). Reintroduction of Pdfr in Pdfr knockout
317 background revealed that GMR51H05 and GMR79A11Gal4 drivers, which covered the main
318 functional CNMa-positive subset, could partially rescue the morning anticipation and power
319 phenotype of Pdfr knockout flies to a considerably larger extent than the GMR91F02 driver (Fig
320 6L-6M). Moreover, knocking out Pdfr in type I CNMa neurons decreased morning anticipation
321 of flies (Fig 6N). Because the main subset of functional CNMa is also PDFR-positive, it is
322 possible that CNMa secretion is regulated by PDF/PDFR signal.

323

324 **Role of Neuronal CNMaR in Morning Anticipation**

325 There is only one CNMa receptor reported in the fly genome (Jung et al., 2014). We generated
326 a $CNMaR^{KO\text{-}p65AD}$ line by CRISPR/Cas9 (Fig 7A) and this knockout showed advanced morning
327 activity (Fig 7B, 7D) and increased MAPI (Fig 7C, 7E) in both sexes. $CNMaR^{KI\text{-}Gal4}$/UAS-

328 mCD8::GFP and CNMaR$^{KI\text{-}Gal4}$/UAS-stinger::Red showed expression of CNMaR across the
329 whole brain (Fig 7F, Fig S11B), especially in DN1p, DN3 , the PI and the SOG. The dendrite
330 arborization and synaptic projections of CNMaR neurons also covered broad regions (Fig 7G,
331 7H), at the PI, the SOG, the posterior ventrolateral protocerebrum (PVLP) and the central
332 complex (CC). Further conditional knockout of CNMaR in neurons by C-cCCTomics
333 phenocopied CNMaR$^{KO\text{-}p65AD}$ phenotype (Fig 7I-7L). These results indicate that CNMaR is
334 similar to CNMa in regulating morning anticipation.
335
336 **DISCUSSION**
337 **Conditional CCTomics Strategies and Toolkit**
338 We have generated conditional gene manipulation systems based on Flp-out/GFPi or
339 CRISPR/Cas9. cCCT based gene deletion after heat-shock or mifepristone (RU486) eliminated
340 most GFP signals, and pan-neuronal constitutive expression of shRNA^{GFP} or flippase disrupted
341 seven out of eight tested genes completely while targeting of SIFa$^{EGFP.FRT}$ achieved 96±3%
342 efficiency. Although the recombination of genetic elements is relatively cumbersome when
343 using cCCTomics, it is worthwhile to apply this method to specific genes given its high level of
344 efficiency. While two UAS-sgRNA libraries have been established, one primarily targeting
345 kinases (Port et al., 2020) and the other targeting GPCRs (Schlichting et al., 2022), both
346 libraries only cover a portion of CCT genes, and are thus insufficient for manipulating all CCT
347 genes. The development of C-cCCTomics, however, makes CCT gene manipulation as simple
348 as RNA interference. Furthermore, the use of modified Cas9.M6 or Cas9.M9 highly enhances
349 the efficiency of gene disruption in the nervous system, allowing for efficient manipulation of all

CCT genes in a cell-specific manner.

The toxicity of CRISPR/Cas9 depends on the Cas9 protein (Port et al., 2014). When expressed pan-neuronally in nSyb-GAL4 (R57C10-GAL4, attP40) , Cas9.M9 slightly reduced viability, while the expression of other Cas9 variants had no significant effect on viability (Fig S12). Although Cas9.M9 showed leaky-expression- efficiency, this was not a problem with Cas9.M6, which successfully disrupted Dh31, Dh44, Pdf, and Pdfr (Fig S9). A more restricted expression of Cas9.M9 with lower toxicity is necessary for better somatic gene manipulation in the future.

CCT of Clock Neurons

Intersecting Clk856-Gal4 or Clk856-p6AD with CCTomics, we identified 45 CCT genes in Clk856 labelled clock neurons. Clock neurons appear highly heterogeneous both in our intersection dissection and in a previous transcriptomic analysis (Abruzzi et al., 2017; Ma et al., 2021). Comparing these two CCT gene expression profiles in clock neurons, 45 out of 128 gene-subsets are identical. The accuracy of our genetic intersection is limited by two possibilities: 1) KI-LexA may not fully represent the expression pattern of the corresponding gene, and 2) the efficiency of STOP cassette removal in the Flp-out strategy is limited. Moreover, the leakage of LexAop-GFP may result in unreliable labelling in split-lexA strategy.

We have also observed that the expression profile of Pdfr in clock neurons is inconsistent across studies, with different clock subsets being identified(Hyun et al., 2005; Im and Taghert, 2010; Lear et al., 2005; Ma et al., 2021; Mertens et al., 2005; Shafer et al., 2008) . The variability in labelling clock neurons with Pdfr transgenic GAL4s, KI-myc tag, antibodies, and

372 transcriptomic anatomy reflects the limitations of each approach. The expression of Pdfr in
373 LNds and DN1s is considered reliable as they are labeled by all strategies. Our intersection
374 dissection is most closely aligned to Pdfr antibody-labelled neurons (Hyun et al., 2005). Both
375 genetic drivers and transcriptomic analysis contribute to our knowledge of the expression profile
376 of neurons. The physiological significance of each gene in a particular neuron should be further
377 investigated by genetic manipulation.
378
379 **Regulation of Rhythmic Behavior by CCT genes**
380 Multiple attractive genes have been identified in our functional screen of CCT genes in clock
381 neurons: for example, knocking out of VGlut weakens both morning anticipation and rhythmic
382 strength (Table S7). In further screening of brain regions, we have narrowed down the morning
383 anticipation regulation role of VGlut in R18H11-GAL4 labeled neurons (Table S8). VGlut in
384 these neurons has also been reported to regulate sleep in Drosophila (Guo et al., 2016). Its
385 downstream neurons may be the PI neurons or LNvs (Barber et al., 2021; Guo et al., 2016).
386 Moreover, the deficiency of the neuropeptide CNMa results in advanced morning activity.
387 We have validated that two Pdfr and CNMa double-positive DN1p neurons mainly regulate this
388 process through intersectional manipulation of CNMa. Knockout and reintroduction of Pdfr in
389 these neurons have verified that Pdfr partially functions in DN1p CNMa neurons, and PDF
390 increases cAMP level in Pdfr positive neurons (Shafer et al., 2008), suggesting the regulation
391 of CNMa signaling by PDF signaling. Furthermore, given that the morning anticipation vanishing
392 phenotype of Pdf or Pdfr mutant is opposite to that of CNMa knockout flies, we consider the
393 two signals to be antagonistic. However, knocking out CNMaR in Clk856 labelled clock neurons

394 showed no significant phenotype (Table S7), whereas the mutant and pan-neuronal knockout
395 flies had similar phenotypes to CNMa knockout flies, suggesting its role in the circadian output
396 neurons. Previous studies have indicated that CNMa integrate thermosensory inputs to
397 promote wakefulness, and CNMaR is thought to function in Dh44 positive PI neurons (Jin et al.,
398 2021), a subset of circadian output neurons. To gain a deeper understanding of the downstream
399 effects of DN1p CNMa postive neurons, further analysis focusing on specific brain regions is
400 necessary.

401 We have also reproduced phenotypes of Pdf, Pdfr, and Dh31 mutant flies with C-
402 cCCTomics as previous studies. Surprisingly, only five genes are functional among all sixty-
403 seven CCT genes in this prior screen. This may be caused by limitations of the simple
404 behavioral paradigm, single gene manipulation, and single GAL4 driver. For example, switching
405 of light condition from L: D = 12h: 12h to L: D = 6h:18h, AstC/AstC-R2 would suppress flies'
406 evening activity intensity to adapt to the environmental change (Díaz et al., 2019), and only
407 double knockout of AChRs and mGluRs in PI neurons can possibly result in alteration in
408 behavioral rhythms (Barber et al., 2021). Further diversified functional analysis of CCT genes
409 in clock neurons is required for clock circuit dissection.

Methods

Fly Lines and Rearing Conditions

Flies were reared on standard corn meal at 25 ℃, 60% humidity, 12 h light: 12 h dark (LD) cycle. For flies used in behavior assays, they were backcrossed into our isogenized Canton S background for 5 to 7 generations. For heat induced assays, flies were reared at 20℃. All CCT attP KO lines and CCT KI driver lines were previous generated at our lab (Deng et al., 2019). Clk856-GAL4 and GMR57C10-GAL4 driver lines were gifts from Donggen Luo Lab (Peking University). 13XLexAop2 (FRT.stop) myr::GFP was gift from Rubin Lab.

C-cCCTomics sgRNAs design

All sgRNAs target at or before functional coding regions (e.g. GPCR transmembrane domain, synthetase substrate binding domain) of each CCT genes. For each gene, about 20 sgRNAs with specific score ≥ 12 were firstly designed at CRISPRgold website (Chu et al., 2016; Graf et al., 2019), then their specificity and efficacy were further valued in Optimal CRISPR target finder(Gratz et al., 2014), E-CRISPR(Heigwer et al., 2014) and CCTop (Stemmer et al., 2015) system. The first three highest efficacy sgRNAs with no predicted off-target effect were selected. All selected sgRNAs are listed in Table S3.

Molecular Biology

All cCCTomics knockin (KI) lines and C-cCCTomics transgenic flies were generated through phiC31 mediated attB/attP recombination, and the miniwhite gene was used as selection marker.

For cCCTomics KI lines, backbone pBSK-attB-FRT-*Hpa*I-T2A-EGFP-FRT was modified

433 from pBSK-attB-loxP-myc-T2A-Gal4-GMR-miniwhite (Deng et al., 2019). Myc-T2A-GAL4
434 cassette was removed by PCR amplification while first FRT cassette was introduced. Second
435 FRT cassette was inserted by T4 ligation between *SpeI* and *BamHI*. T2A-EGFP was cloned
436 from pEC14 and was inserted into the backbone between two FRT cassettes. All gene spans,
437 except for stop codon, deleted in CCT attP KO lines were cloned into pBSK-attB-FRT-*Hpa*I-
438 T2A-EGFP-FRT at *Hpa*I site.

439 For C-cCCTomics UAS-sgRNA lines, backbone pMsgNull was modified from pACU2 (Han
440 et al., 2011). Synthetic partial fly $tRNA^{Gly}$ sequence was inserted between *EcoR*I and *Kpn*I. An
441 irrelevant 1749 bp cassette amplified from pAAV-Efla-DIO-mScarlet (addgeen#130999) was
442 inserted between *Eag*I and *Kpn*I. All sgRNA spacers were synthesized at primers, and "E+F"
443 sgRNA scaffold and rice $tRNA^{Gly}$ was amplified from a synthetic backbone PM04. Finally, gRNA-
444 $tRNA^{Gly}$ cassettes were cloned into pMsgNull between *Eag*I and *Kpn*I by Gibson Assembly.

445 All UAS-Cas9 variants generated in this research were cloned into vector pACU2 and all
446 Cas9 sequence were amplified from hCas9 (addgene#41815). Human codon optimized Cas9
447 was cloned into pACU2 to generate UAS-Cas9.HC. UAS-Cas9.M0 was modified from UAS-
448 Cas9.HC by introduce a 3x HA tag after NSL and replace the SARD linker with the 3×GGSGP
449 linker (Zhao et al., 2016). UAS-Cas9.M6 and UAS-Cas9.M9 were designed as HMGN1-Cas9-
450 UPD and HMGN1-Cas9-HB1 respectively. All these chromatin-modulating peptides were linked
451 with Cas9 by 3x GGSGP linker.

452 $CNMaR^{KO\text{-}p65AD}$ is generated by replace the coding region of the first exon with T2A-p65AD
453 by CRISPR/Cas9, the T2A-p65AD was linked in frame after first ten amino acids. Spacers of
454 gRNAs used to break the targeted CNMaR region were 5'-GCAGATTTCAGTTCATCTTT-3', 5'-

455 GGCTTGGCAATGAC TATATA-3'.

456

457 **Gene expression quantitation and high-throughput sequencing**

458 Female flies were gathered six to eight days post-eclosion for gene expression quantification
459 and high-throughput sequencing. Fly heads were isolated by chilling them on liquid nitrogen
460 and subsequent shaking. mRNA extraction was performed using Trizol according to a
461 previously established protocol (Green and Sambrook, 2020). Genomic DNA was removed,
462 and cDNA was synthesized using a commercial kit (TIANGEN#DP419). For real-time
463 quantitative PCR, at least one PCR primer was designed to overlap with the sgRNA target site.

464 Genomic DNA from fly heads was extracted using a standard alkali lysis protocol(Huang
465 et al., 2009). Genomic regions approximately 130 to 230 bp in length, centered around the
466 sgRNA target site, were amplified by PCR employing Q5 polymerase (NEB#M0494).
467 Subsequently, libraries were prepared using the BTseq kit (Beijing Tsingke Biotech Co., Ltd.).
468 These libraries were pooled and subjected to sequencing on the MiSeq platform (Illumina).
469 Analysis of the libraries was conducted using Crispresso2(Clement et al., 2019).

470 **Generation of KI and Transgenic lines**

471 Generation of cCCTomics KI, CNMa$^{KI\text{-}p65AD}$, and CNMaR$^{KO\text{-}p65AD}$ lines are the same as
472 generation of CCTomics KI driver lines as previously described (Deng et al., 2019). To generate
473 C-cCCTomics UAS-sgRNA or UAS-Cas9 variants lines, attB vectors were injected and
474 integrated into the attP40, attP2 or VK00005 through phiC31 mediated gene integration.

475 All flies generated in this research were selected by mini-white and confirmed by PCR.

476

Behavioral assays

Unmated male or female flies of 4 to 5 days were used in circadian rhythm assays. Before measurement, flies were entrained under 12 h light: 12 h dark cycle at 25℃ for at least 3 days and then transferred to dark-dark condition for 7 days.

Virgin flies of 4 to 5 days were used in sleep assays. Flies were entrained to a 12 h light: 12 h dark cycle at 25℃ for 2 days to eliminate the effect of CO2 anesthesia before sleep record. Sleep was defined as 5 min or longer immobility (Hendricks et al., 2000; Shaw et al., 2000) and analyzed by in-house scripts as previously described ((Dai et al., 2021; Dai et al., 2019; Deng et al., 2019).

Locomotion was obtained as previously described (Dai et al., 2021). Locomotion activity was measured and analyzed by Actogram J plugin (Dai et al., 2019). Morning anticipation index and evening anticipation index were defined as the ratio of last 3 hours activity before light-on or light-off accounts to last 6 hours activity before light-on or light-off (Index=sum(3hrs)/sum(6hrs)) (Harrisingh et al., 2007; Im and Taghert, 2010) and analyzed by an in-house python script.

Heat Shock and Drug Treatment

For hsFLP mediated conditional knockout, flies of 4 to 6 days were heat shock at 37℃ during ZT10 to ZT12 for 4 days. And they were reared at 20℃ for another 4-days and then dissected.

For mifepristone (RU486) induced conditional knockout, flies of 4 to 6 days were treated with 500 μM RU486 mixed in corn food and then dissected 4 days later.

Immunohistochemistry and Confocal Imaging

For all imaging without staining, adult flies were anesthetized on ice and dissected in cold phosphate-buffer saline (PBS). Brains or ventral nerve codes (VNC) were fixed in 2% paraformaldehyde (weight/volume) for 30 min, washed with washing buffer (PBS with 1% Triton X-100, v/v, 3% NaCl, g/mL) for 7 min three times and mounted in Focusclear (Cell Explorer Labs, FC-101).

For imaging with staining, brains and VNCs were fixed for 30 min, washed for 15 min three times. Then they were blocked in PBSTS, incubated with primary antibodies, washed with washing buffer, incubated with second antibodies and mounted as described previously(Dai et al., 2021; Dai et al., 2019).

All brains or VNCs were imaged on Zeiss LSM710 or Zeiss LSM880 confocal microscope and processed by Imaris.

The following primary antibodies were used: mouse anti-PDF (1:200, DSHB), rabbit anti-TH (1:1000, Novus Biologicals), rabbit anti-LK (1:1000, RaoLab, this paper). Rabbit anti-DSK (1:1000) was a gift from Dr. C. Zhou Lab (Institute of Zoology, Chinese Academy of Science) (Wu et al., 2020). The following secondary antibodies were used: AlexaFluor goat anti-mouse 488 (1:1000, Invitrogen), AlexaFlour goat anti-rabbit 488/633 (1:1000, Invitrogen).

For Fig 2, number of TH positive neurons were counted with Imaris Spots plugin.

Quantification and Statistics

MAI, MAPI, EAI, EAPI, power and period were calculated by python or R scripts. ZT0 was set as the time point when light was on and ZT12 was set as the time point for light-off. Activity bins

started at ZT0 and each was calculated as a sum of the total activity within 30min. Flies were regarded as death and removed if their activity value within last 2 bins was 0. A representative 24hr activity pattern was the average between corresponding activity bins from 2 consecutive days. To minimize effects from singular values, each flies` activity was normalized using the following formula:

$$Nor\_b_i = \frac{b_i - \min(b_0, \dots, b_{48})}{\max(b_0, \dots, b_{48}) - \min(b_0, \dots, b_{48})}$$

bi means the activity value for a certain bin. min(b0,...,b48) means the minimal bin value within 24hr and max(b0,...,b48) means the maximal bin value within 24hr. Nor_bi means the final normalized bin value for a certain bin from a given fly. Normalized activity was used for following analysis.

Morning activity arise (M_arise) was defined as the radian between the activity curve (ZT21-ZT22) and the time coordinate. Morning activity plateau (M_plateau) was defined as the radian between the activity curve (ZT22.5-ZT24) and the time coordinate. Evening activity arise (E_arise) was defined as the radian between the activty curve (ZT8-ZT11.5) and the time coordinate. Evening activity plateau (E_plateau) was defined as the radian between the activity curve (ZT10.5-ZT12) and the time coordinate. Morning anticipation pattern index (MAPI) was calculated by subtracting M_arise from M_plateau and Evening anticipation pattern index (EAPI) was calculated by subtracting E_arise from E_plateau.

The original activity data from 7 consecutive days in dark-dark condition was used for power and period calculation as described (Geissmann et al., 2019). Each flies` periodogram was calculated based on Chi-Square algorithm (Sokolove and Bushell, 1978) and flies with a null power value were regarded as arrhythmic.

543 All statistical analyses were carried out with Prism 8 (Graphpad software). The Kruskal-
544 Wallis ANOVA test followed by Dunn's posttest was used to compare multiple columns.
545
546 **ACKNOWLEDGEMENTS.**
547 We are grateful to Xiaofei Liu, Xueying Wang and Yile Jiao for sgRNA design and cloning, to
548 Linyi Zhang, Wenli Xu, Yuqing Gong and Quiquan Chen for assistance with behavior assays,
549 to Xiao Dong for cloning, to Xinwei Gao for assistance with imaging, to Pingping Yan, Lan
550 Wang, Yonghui Zhang and Haixia Zeng for fly rearing, to Enxing Zhou and Wei Yang for
551 Drosophila activity tracing scripts, to Donggen Luo, Chuan Zhou, Gerald M. Rubin, Vienna
552 Drosophila RNAi Center and Bloomington Drosophila Stock Center for flies, to Yuh-Nung Jan
553 for pACU2 construct.
554

REFERENCES

Abruzzi, K.C., Zadina, A., Luo, W., Wiyanto, E., Rahman, R., Guo, F., Shafer, O., and Rosbash, M. (2017). RNA-seq analysis of Drosophila clock and non-clock neurons reveals neuron-specific cycling and novel candidate neuropeptides. PLoS genetics *13*, e1006613.

Barber, A.F., Fong, S.Y., Kolesnik, A., Fetchko, M., and Sehgal, A. (2021). Drosophila clock cells use multiple mechanisms to transmit time-of-day signals in the brain. Proc Natl Acad Sci USA *118*, e2019826118.

Chen, B., Gilbert, L.A., Cimini, B.A., Schnitzbauer, J., Zhang, W., Li, G.W., Park, J., Blackburn, E.H., Weissman, J.S., Qi, L.S.*, et al.* (2013). Dynamic imaging of genomic loci in living human cells by an optimized CRISPR/Cas system. Cell *155*, 1479-1491.

Chu, V.T., Graf, R., Wirtz, T., Weber, T., Favret, J., Li, X., Petsch, K., Tran, N.T., Sieweke, M.H., Berek, C.*, et al.* (2016). Efficient CRISPR-mediated mutagenesis in primary immune cells using CrispRGold and a C57BL/6 Cas9 transgenic mouse line. Proc Natl Acad Sci USA *113*, 12514-12519.

Clement, K., Rees, H., Canver, M.C., Gehrke, J.M., Farouni, R., Hsu, J.Y., Cole, M.A., Liu, D.R., Joung, J.K., Bauer, D.E.*, et al.* (2019). CRISPResso2 provides accurate and rapid genome editing sequence analysis. Nature Biotechnology *37*, 224-226.

Collins, B.H., Dissel, S., Gaten, E., Rosato, E., and Kyriacou, C.P. (2005). Disruption of Cryptochrome partially restores circadian rhythmicity to the arrhythmic period mutant of Drosophila. Proc Natl Acad Sci USA *102*, 19021-19026.

Dai, X., Zhou, E., Yang, W., Mao, R., Zhang, W., and Rao, Y. (2021). Molecular resolution of a behavioral paradox: sleep and arousal are regulated by distinct acetylcholine receptors in different neuronal types in Drosophila. Sleep *44*, zsab017.

Dai, X., Zhou, E., Yang, W., Zhang, X., Zhang, W., and Rao, Y. (2019). D-Serine made by serine racemase in Drosophila intestine plays a physiological role in sleep. Nat Commun *10*, 1986.

Dang, Y., Jia, G., Choi, J., Ma, H., Anaya, E., Ye, C., Shankar, P., and Wu, H. (2015). Optimizing sgRNA structure to improve CRISPR-Cas9 knockout efficiency. Genome Biol *16*, 280.

Delventhal, R., O'Connor, R.M., Pantalia, M.M., Ulgherait, M., Kim, H.X., Basturk, M.K., Canman, J.C., and Shirasu-Hiza, M. (2019). Dissection of central clock function in Drosophila through cell-specific CRISPR-mediated clock gene disruption. eLife *8*, e48308.

Deng, B., Li, Q., Liu, X., Cao, Y., Li, B., Qian, Y., Xu, R., Mao, R., Zhou, E., Zhang, W.*, et al.* (2019). Chemoconnectomics: mapping chemical transmission in Drosophila. Neuron *101*, 876-893.e874.

Díaz, M.M., Schlichting, M., Abruzzi, K.C., Long, X., and Rosbash, M. (2019). Allatostatin-C/AstC-R2 is a novel pathway to modulate the circadian activity pattern in Drosophila. Curr Biol *29*, 13-22.

Ding, X., Seebeck, T., Feng, Y., Jiang, Y., Davis, G.D., and Chen, F. (2019). Improving CRISPR-Cas9 genome editing efficiency by fusion with chromatin-modulating peptides. Crispr j *2*, 51-63.

Doench, J.G., Hartenian, E., Graham, D.B., Tothova, Z., Hegde, M., Smith, I., Sullender, M., Ebert, B.L., Xavier, R.J., and Root, D.E. (2014). Rational design of highly active sgRNAs for CRISPR-Cas9-mediated gene inactivation. Nat Biotechnol *32*, 1262-1267.

Dubowy, C., and Sehgal, A. (2017). Circadian Rhythms and Sleep in Drosophila melanogaster.

598 Genetics *205*, 1373-1397.
599 Duhart, J.M., Herrero, A., de la Cruz, G., Ispizua, J.I., Pírez, N., and Ceriani, M.F. (2020).
600 Circadian Structural Plasticity Drives Remodeling of E Cell Output. Curr Biol *30*, 5040-
601 5048.e5045.
602 Erion, R., King, A.N., Wu, G., Hogenesch, J.B., and Sehgal, A. (2016). Neural clocks and
603 Neuropeptide F/Y regulate circadian gene expression in a peripheral metabolic tissue. eLife *5*,
604 e13552.
605 Filippova, J., Matveeva, A., Zhuravlev, E., and Stepanov, G. (2019). Guide RNA modification
606 as a way to improve CRISPR/Cas9-based genome-editing systems. Biochimie *167*, 49-60.
607 Frenkel, L., Muraro, N.I., Beltrán González, A.N., Marcora, M.S., Bernabó, G., Hermann-Luibl,
608 C., Romero, J.I., Helfrich-Förster, C., Castaño, E.M., Marino-Busjle, C.*, et al.* (2017).
609 Organization of circadian behavior relies on glycinergic transmission. Cell Rep *19*, 72-85.
610 Fujiwara, Y., Hermann-Luibl, C., Katsura, M., Sekiguchi, M., Ida, T., Helfrich-Förster, C., and
611 Yoshii, T. (2018). The CCHamide1 neuropeptide expressed in the anterior dorsal neuron 1
612 conveys a circadian signal to the ventral lateral neurons in Drosophila melanogaster. Front
613 Physiol *9*, 1276.
614 Gaj, T., Sirk, S.J., and Barbas, C.F., 3rd (2014). Expanding the scope of site-specific
615 recombinases for genetic and metabolic engineering. Biotechnol Bioeng *111*, 1-15.
616 Geissmann, Q., Garcia Rodriguez, L., Beckwith, E.J., and Gilestro, G.F. (2019). Rethomics: An
617 R framework to analyse high-throughput behavioural data. PLoS One *14*, e0209331.
618 Goda, T., Tang, X., Umezaki, Y., Chu, M.L., Kunst, M., Nitabach, M.N.N., and Hamada, F.N.
619 (2016). Drosophila DH31 neuropeptide and PDF receptor regulate night-onset temperature
620 preference. J Neurosci *36*, 11739-11754.
621 Goda, T., Umezaki, Y., Alwattari, F., Seo, H.W., and Hamada, F.N. (2019). Neuropeptides PDF
622 and DH31 hierarchically regulate free-running rhythmicity in Drosophila circadian locomotor
623 activity. Sci Rep *9*, 838.
624 Golic, K.G., and Lindquist, S. (1989). The FLP recombinase of yeast catalyzes site-specific
625 recombination in the Drosophila genome. Cell *59*, 499-509.
626 Graf, R., Li, X., Chu, V.T., and Rajewsky, K. (2019). sgRNA Sequence Motifs Blocking Efficient
627 CRISPR/Cas9-Mediated Gene Editing. Cell Rep *26*, 1098-1103.e1093.
628 Gratz, S.J., Ukken, F.P., Rubinstein, C.D., Thiede, G., Donohue, L.K., Cummings, A.M., and
629 O'Connor-Giles, K.M. (2014). Highly specific and efficient CRISPR/Cas9-catalyzed homology-
630 directed repair in Drosophila. Genetics *196*, 961-971.
631 Green, M.R., and Sambrook, J. (2020). Total RNA Isolation from Drosophila melanogaster.
632 *2020*, pdb.prot101675.
633 Grima, B., Chélot, E., Xia, R., and Rouyer, F. (2004). Morning and evening peaks of activity rely
634 on different clock neurons of the Drosophila brain. Nature *431*, 869-873.
635 Grindley, N.D., Whiteson, K.L., and Rice, P.A. (2006). Mechanisms of site-specific
636 recombination. Annu Rev Biochem *75*, 567-605.
637 Gummadova, J.O., Coutts, G.A., and Glossop, N.R. (2009). Analysis of the Drosophila clock
638 promoter reveals heterogeneity in expression between subgroups of central oscillator cells and
639 identifies a novel enhancer region. J Biol Rhythms *24*, 353-367.
640 Guo, F., Yu, J., Jung, H.J., Abruzzi, K.C., Luo, W., Griffith, L.C., and Rosbash, M. (2016).
641 Circadian neuron feedback controls the Drosophila sleep--activity profile. Nature *536*, 292-297.

Hamasaka, Y., Rieger, D., Parmentier, M.L., Grau, Y., Helfrich-Förster, C., and Nässel, D.R. (2007). Glutamate and its metabotropic receptor in Drosophila clock neuron circuits. J Comp Neurol *505*, 32-45.

Han, C., Jan, L.Y., and Jan, Y.-N. (2011). Enhancer-driven membrane markers for analysis of nonautonomous mechanisms reveal neuron-glia interactions in Drosophila. Proc Natl Acad Sci USA *108*, 9673-9678.

Harrisingh, M.C., Wu, Y., Lnenicka, G.A., and Nitabach, M.N. (2007). Intracellular Ca2+ regulates free-running circadian clock oscillation in vivo. J Neurosci *27*, 12489-12499.

He, C., Cong, X., Zhang, R., Wu, D., An, C., and Zhao, Z. (2013). Regulation of circadian locomotor rhythm by neuropeptide Y-like system in Drosophila melanogaster. Insect Mol Biol *22*, 376-388.

Heigwer, F., Kerr, G., and Boutros, M. (2014). E-CRISP: fast CRISPR target site identification. Nat Methods *11*, 122-123.

Helfrich-Förster, C. (2001). The locomotor activity rhythm of Drosophila melanogaster is controlled by a dual oscillator system. J Insect Physiol *47*, 877-887.

Hendricks, J.C., Finn, S.M., Panckeri, K.A., Chavkin, J., Williams, J.A., Sehgal, A., and Pack, A.I. (2000). Rest in Drosophila Is a Sleep-like State. Neuron *25*, 129-138.

Hermann-Luibl, C., Yoshii, T., Senthilan, P.R., Dircksen, H., and Helfrich-Förster, C. (2014). The ion transport peptide is a new functional clock neuropeptide in the fruit fly Drosophila melanogaster. J Neurosci *34*, 9522-9536.

Hermann, C., Yoshii, T., Dusik, V., and Helfrich-Förster, C. (2012). Neuropeptide F immunoreactive clock neurons modify evening locomotor activity and free-running period in Drosophila melanogaster. J Comp Neurol *520*, 970-987.

Huang, A.M., Rehm, E.J., and Rubin, G.M. (2009). Quick preparation of genomic DNA from Drosophila. Cold Spring Harb Protoc *2009*, pdb.prot5198.

Hyun, S., Lee, Y., Hong, S.T., Bang, S., Paik, D., Kang, J., Shin, J., Lee, J., Jeon, K., Hwang, S.*, et al.* (2005). Drosophila GPCR Han is a receptor for the circadian clock neuropeptide PDF. Neuron *48*, 267-278.

Im, S.H., and Taghert, P.H. (2010). PDF receptor expression reveals direct interactions between circadian oscillators in Drosophila. J Comp Neurol *518*, 1925-1945.

Jin, X., Tian, Y., Zhang, Z.C., Gu, P., Liu, C., and Han, J. (2021). A subset of DN1p neurons integrates thermosensory inputs to promote wakefulness via CNMa signaling. Curr Biol.

Jung, S.H., Lee, J.H., Chae, H.S., Seong, J.Y., Park, Y., Park, Z.Y., and Kim, Y.J. (2014). Identification of a novel insect neuropeptide, CNMa and its receptor. FEBS Lett *588*, 2037-2041.

Konopka, R.J., and Benzer, S. (1971). Clock mutants of Drosophila melanogaster. Proc Natl Acad Sci USA *68*, 2112-2116.

Labuhn, M., Adams, F.F., Ng, M., Knoess, S., Schambach, A., Charpentier, E.M., Schwarzer, A., Mateo, J.L., Klusmann, J.H., and Heckl, D. (2018). Refined sgRNA efficacy prediction improves large- and small-scale CRISPR-Cas9 applications. Nucleic Acids Res *46*, 1375-1385.

Lear, B.C., Merrill, C.E., Lin, J.-M., Schroeder, A., Zhang, L., and Allada, R. (2005). A G protein-coupled receptor, groom-of-PDF, is required for PDF neuron action in circadian behavior. Neuron *48*, 221-227.

Ling, X., Xie, B., Gao, X., Chang, L., Zheng, W., Chen, H., Huang, Y., Tan, L., Li, M., and Liu, T. (2020). Improving the efficiency of precise genome editing with site-specific Cas9-

oligonucleotide conjugates. Sci Adv *6*, eaaz0051.

Liu, G., Yin, K., Zhang, Q., Gao, C., and Qiu, J.L. (2019). Modulating chromatin accessibility by transactivation and targeting proximal dsgRNAs enhances Cas9 editing efficiency in vivo. Genome Biol *20*, 145.

Ma, D., Przybylski, D., Abruzzi, K.C., Schlichting, M., Li, Q., Long, X., and Rosbash, M. (2021). A transcriptomic taxonomy of Drosophila circadian neurons around the clock. Elife *10*.

Mali, P., Yang, L., Esvelt, K.M., Aach, J., Guell, M., DiCarlo, J.E., Norville, J.E., and Church, G.M. (2013). RNA-guided human genome engineering via Cas9. Science *339*, 823-826.

Martin, S.E., and Caplen, N.J. (2007). Applications of RNA interference in mammalian systems. Annu Rev Genomics Hum Genet *8*, 81-108.

Mertens, I., Vandingenen, A., Johnson, E.C., Shafer, O.T., Li, W., Trigg, J.S., De Loof, A., Schoofs, L., and Taghert, P.H. (2005). PDF receptor signaling in Drosophila contributes to both circadian and geotactic behaviors. Neuron *48*, 213-219.

Mu, W., Zhang, Y., Xue, X., Liu, L., Wei, X., and Wang, H. (2019). 5' capped and 3' polyA-tailed sgRNAs enhance the efficiency of CRISPR-Cas9 system. Protein Cell *10*, 223-228.

Nahar, S., Sehgal, P., Azhar, M., Rai, M., Singh, A., Sivasubbu, S., Chakraborty, D., and Maiti, S. (2018). A G-quadruplex motif at the 3' end of sgRNAs improves CRISPR-Cas9 based genome editing efficiency. Chem Commun (Camb) *54*, 2377-2380.

Neumüller, R.A., Wirtz-Peitz, F., Lee, S., Kwon, Y., Buckner, M., Hoskins, R.A., Venken, K.J., Bellen, H.J., Mohr, S.E., and Perrimon, N. (2012). Stringent analysis of gene function and protein-protein interactions using fluorescently tagged genes. Genetics *190*, 931-940.

Ni, J.Q., Zhou, R., Czech, B., Liu, L.P., Holderbaum, L., Yang-Zhou, D., Shim, H.S., Tao, R., Handler, D., Karpowicz, P.*, et al.* (2011). A genome-scale shRNA resource for transgenic RNAi in Drosophila. Nat Methods *8*, 405-407.

Nicholson, L., Singh, G.K., Osterwalder, T., Roman, G.W., Davis, R.L., and Keshishian, H. (2008). Spatial and temporal control of gene expression in Drosophila using the inducible GeneSwitch GAL4 system. I. Screen for larval nervous system drivers. Genetics *178*, 215-234.

Oberdoerffer, P., Kanellopoulou, C., Heissmeyer, V., Paeper, C., Borowski, C., Aifantis, I., Rao, A., and Rajewsky, K. (2005). Efficiency of RNA interference in the mouse hematopoietic system varies between cell types and developmental stages. Mol Cell Biol *25*, 3896-3905.

Osterwalder, T., Yoon, K.S., White, B.H., and Keshishian, H. (2001). A conditional tissue-specific transgene expression system using inducible GAL4. Proc Natl Acad Sci USA *98*, 12596-12601.

Perkins, L.A., Holderbaum, L., Tao, R., Hu, Y., Sopko, R., McCall, K., Yang-Zhou, D., Flockhart, I., Binari, R., Shim, H.S.*, et al.* (2015). The Transgenic RNAi project at harvard medical school: resources and validation. Genetics *201*, 843-852.

Poe, A.R., Wang, B., Sapar, M.L., Ji, H., Li, K., Onabajo, T., Fazliyeva, R., Gibbs, M., Qiu, Y., Hu, Y.*, et al.* (2019). Robust CRISPR/Cas9-mediated tissue-specific mutagenesis reveals gene redundancy and perdurance in Drosophila. Genetics *211*, 459-472.

Port, F., and Bullock, S.L. (2016). Augmenting CRISPR applications in Drosophila with tRNA-flanked sgRNAs. Nature Methods *13*, 852-854.

Port, F., Chen, H.M., Lee, T., and Bullock, S.L. (2014). Optimized CRISPR/Cas tools for efficient germline and somatic genome engineering in Drosophila. Proc Natl Acad Sci USA *111*, E2967-2976.

Port, F., Strein, C., Stricker, M., Rauscher, B., Heigwer, F., Zhou, J., Beyersdörffer, C., Frei, J., Hess, A., Kern, K.*, et al.* (2020). A large-scale resource for tissue-specific CRISPR mutagenesis in Drosophila. eLife *9*, e53865.

Renn, S.C., Park, J.H., Rosbash, M., Hall, J.C., and Taghert, P.H. (1999). A pdf neuropeptide gene mutation and ablation of PDF neurons each cause severe abnormalities of behavioral circadian rhythms in Drosophila. Cell *99*, 791-802.

Rieger, D., Shafer, O.T., Tomioka, K., and Helfrich-Förster, C. (2006). Functional analysis of circadian pacemaker neurons in Drosophila melanogaster. J Neurosci *26*, 2531-2543.

Schlichting, M., Díaz, M.M., Xin, J., and Rosbash, M. (2019). Neuron-specific knockouts indicate the importance of network communication to Drosophila rhythmicity. eLife *8*, e48301.

Schlichting, M., Richhariya, S., Herndon, N., Ma, D., Xin, J., Lenh, W., Abruzzi, K., and Rosbash, M. (2022). Dopamine and GPCR-mediated modulation of DN1 clock neurons gates the circadian timing of sleep. Proc Natl Acad Sci USA *119*, e2206066119.

Scott, T., Urak, R., Soemardy, C., and Morris, K.V. (2019). Improved Cas9 activity by specific modifications of the tracrRNA. Sci Rep *9*, 16104.

Sekiguchi, M., Inoue, K., Yang, T., Luo, D.G., and Yoshii, T. (2020). A Catalog of GAL4 Drivers for Labeling and Manipulating Circadian Clock Neurons in Drosophila melanogaster. J Biol Rhythms *35*, 207-213.

Selcho, M., Millán, C., Palacios-Muñoz, A., Ruf, F., Ubillo, L., Chen, J., Bergmann, G., Ito, C., Silva, V., Wegener, C.*, et al.* (2017). Central and peripheral clocks are coupled by a neuropeptide pathway in Drosophila. Nat Commun *8*, 15563.

Shafer, O.T., Kim, D.J., Dunbar-Yaffe, R., Nikolaev, V.O., Lohse, M.J., and Taghert, P.H. (2008). Widespread receptivity to neuropeptide PDF throughout the neuronal circadian clock network of Drosophila revealed by real-time cyclic AMP imaging. Neuron *58*, 223-237.

Shaw, P.J., Cirelli, C., Greenspan, R.J., and Tononi, G. (2000). Correlates of sleep and waking in Drosophila melanogaster. Science *287*, 1834-1837.

Sokolove, P.G., and Bushell, W.N. (1978). The chi square periodogram: Its utility for analysis of circadian rhythms. Journal of Theoretical Biology *72*, 131-160.

Stemmer, M., Thumberger, T., Del Sol Keyer, M., Wittbrodt, J., and Mateo, J.L. (2015). CCTop: An Intuitive, Flexible and Reliable CRISPR/Cas9 Target Prediction Tool. PLoS One *10*, e0124633.

Stoleru, D., Peng, Y., Agosto, J., and Rosbash, M. (2004). Coupled oscillators control morning and evening locomotor behaviour of Drosophila. Nature *431*, 862-868.

Talay, M., Richman, E.B., Snell, N.J., Hartmann, G.G., Fisher, J.D., Sorkaç, A., Santoyo, J.F., Chou-Freed, C., Nair, N., Johnson, M.*, et al.* (2017). Transsynaptic Mapping of Second-Order Taste Neurons in Flies by trans-Tango. Neuron *96*, 783-795.e784.

Tang, M., Cao, L.-H., Yang, T., Ma, S.-X., Jing, B.-Y., Xiao, N., Xu, S., Leng, K.-R., Yang, D., Li, M.-T.*, et al.* (2022). An extra-clock ultradian brain oscillator sustains circadian timekeeping. Sci Adv *8*, eabo5506.

Vetter, D., Andrews, B.J., Roberts-Beatty, L., and Sadowski, P.D. (1983). Site-specific recombination of yeast 2-micron DNA in vitro. Proc Natl Acad Sci U S A *80*, 7284-7288.

Wu, F., Deng, B., Xiao, N., Wang, T., Li, Y., Wang, R., Shi, K., Luo, D.G., Rao, Y., and Zhou, C. (2020). A neuropeptide regulates fighting behavior in Drosophila melanogaster. Elife *9*, e54229.

Xie, K., Minkenberg, B., and Yang, Y. (2015). Boosting CRISPR/Cas9 multiplex editing

capability with the endogenous tRNA-processing system. Proc Natl Acad Sci U S A *112*, 3570-3575.

Xu, H., Xiao, T., Chen, C.H., Li, W., Meyer, C.A., Wu, Q., Wu, D., Cong, L., Zhang, F., Liu, J.S., *et al.* (2015). Sequence determinants of improved CRISPR sgRNA design. Genome Res *25*, 1147-1157.

Xue, Z., Wu, M., Wen, K., Ren, M., Long, L., Zhang, X., and Gao, G. (2014). CRISPR/Cas9 mediates efficient conditional mutagenesis in Drosophila. G3 (Bethesda) *4*, 2167-2173.

Zhao, P., Zhang, Z., Lv, X., Zhao, X., Suehiro, Y., Jiang, Y., Wang, X., Mitani, S., Gong, H., and Xue, D. (2016). One-step homozygosity in precise gene editing by an improved CRISPR/Cas9 system. Cell Res *26*, 633-636.

Zheng, X., Qi, C., Yang, L., Quan, Q., Liu, B., Zhong, Z., Tang, X., Fan, T., Zhou, J., and Zhang, Y. (2020). The Improvement of CRISPR-Cas9 system with ubiquitin-associated domain fusion for efficient plant genome editing. Front Plant Sci *11*, 621.

788 **FIGURES**

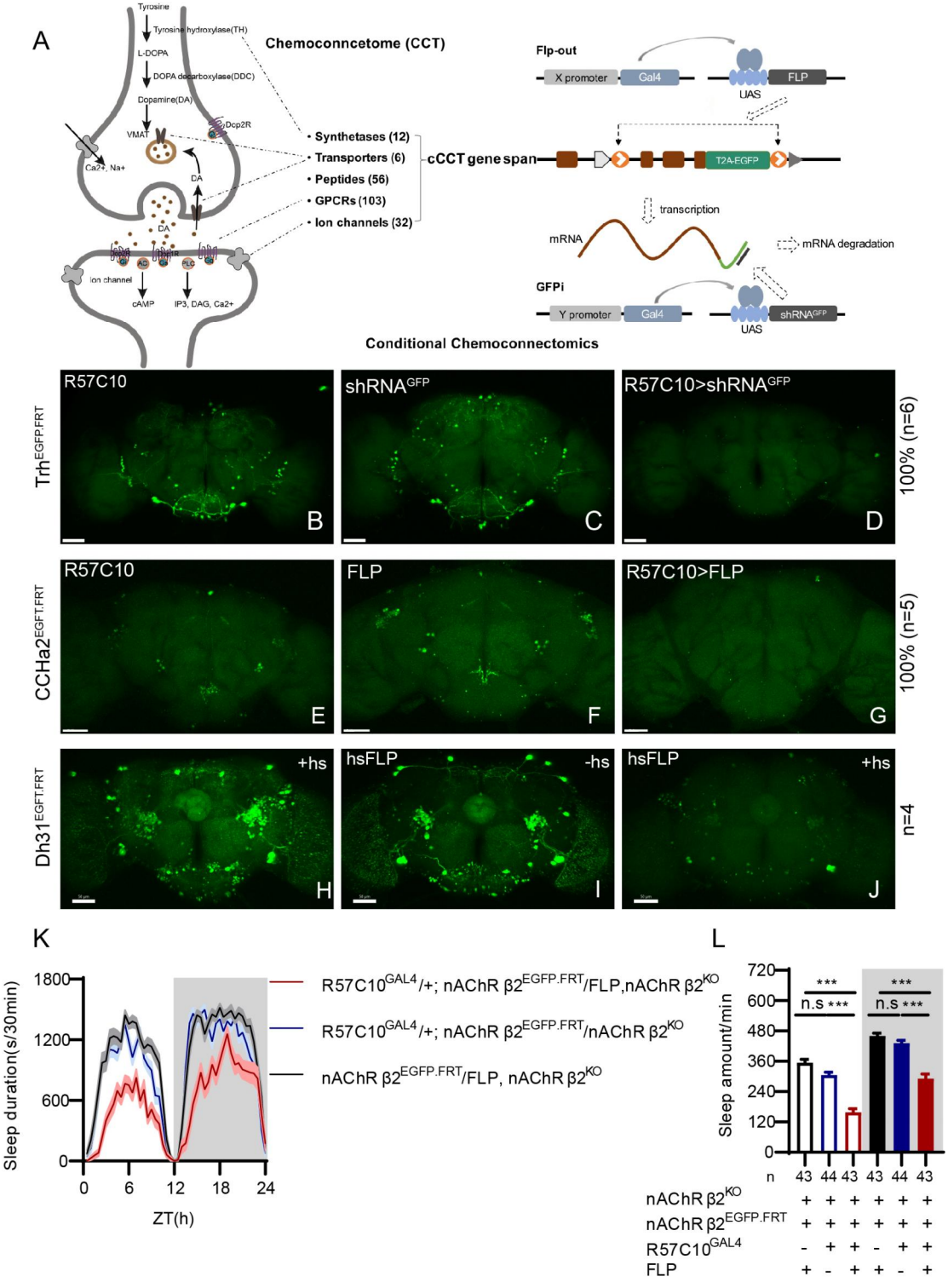

789

790 **Fig 1. cCCTomics Mediates Efficient Conditional Disruption of CCT Genes**

791 (A) Schematic of cCCT gene span and principle of cCCTomics. A T2A-EGFP sequence was

792 induced at the 3' end of CCT genes and their most or all coding regions (depending on attP-

KO lines) were flanked by 34 bp FRT sequence. Both Flp-out (top) and GFP RNAi (down) could mediate CCT gene manipulation. (B-J) Expression of Trh (B-D), CCHa2 (E-G), and Dh31 (H-J) are efficiently disrupted by pan-neuronal expression of GFP-RNAi (B-D), pan-neuronal expression of Flp-out (E-G), and heatshock-Flp (H-J) respectively. Representative fluorescence images of R57C10-Gal4/+;$Trh^{EGFP.FRT}$/+ (B), UAS-$shRNA^{GFP}$/$Trh^{EGFP.FRT}$ (C), R57C10-Gal4/+; UAS-$shRNA^{GFP}$/$Trh^{EGFP.FRT}$ (D), R57C10-Gal4/+;$CCHa2^{EGFP.FRT}$/+; (E), UAS-Flp/$CCHa2^{EGFP.FRT}$ (F), R57C10-Gal4/+; UAS-Flp/$CCHa2^{EGFP.FRT}$ (G), $Dh31^{EGFP.FRT}$ with heatshock (H), hs-Flp/$Dh31^{EGFP.FRT}$ without heatshock (I), and hs-Flp/$Dh31^{EGFP.FRT}$ with heatshock are shown. Manipulation efficiency and experiment group fly number is noted on the right. Scale bar, 50um. (K-L) sleep profiles (K) and statistical analysis (L) of Flp-out induced nAChRβ2 neuronal knockout flies (red) and genotype controls (dark and blue). Sleep profiles are plotted in 30 min bins. In this and other figures, blank background indicates the light phase (ZT 0-12); shaded background indicates the dark phase (ZT 12-24). Both daytime sleep (open bars) and nighttime sleep (filled bars) duration were significantly reduced in nAChRβ2 neuronal knockout files.

In all statistical panels, unless otherwise noted, 1) Numbers below each bar represent the number of flies tested. 2) Mean ± SEM is shown. 3) The Kruskal-Wallis test followed by Dunn's post test was used. ***$p < 0.001$. ** $p < 0.01$. * $p < 0.05$. n.s. $p > 0.05$. Male flies were used unless otherwise noted.

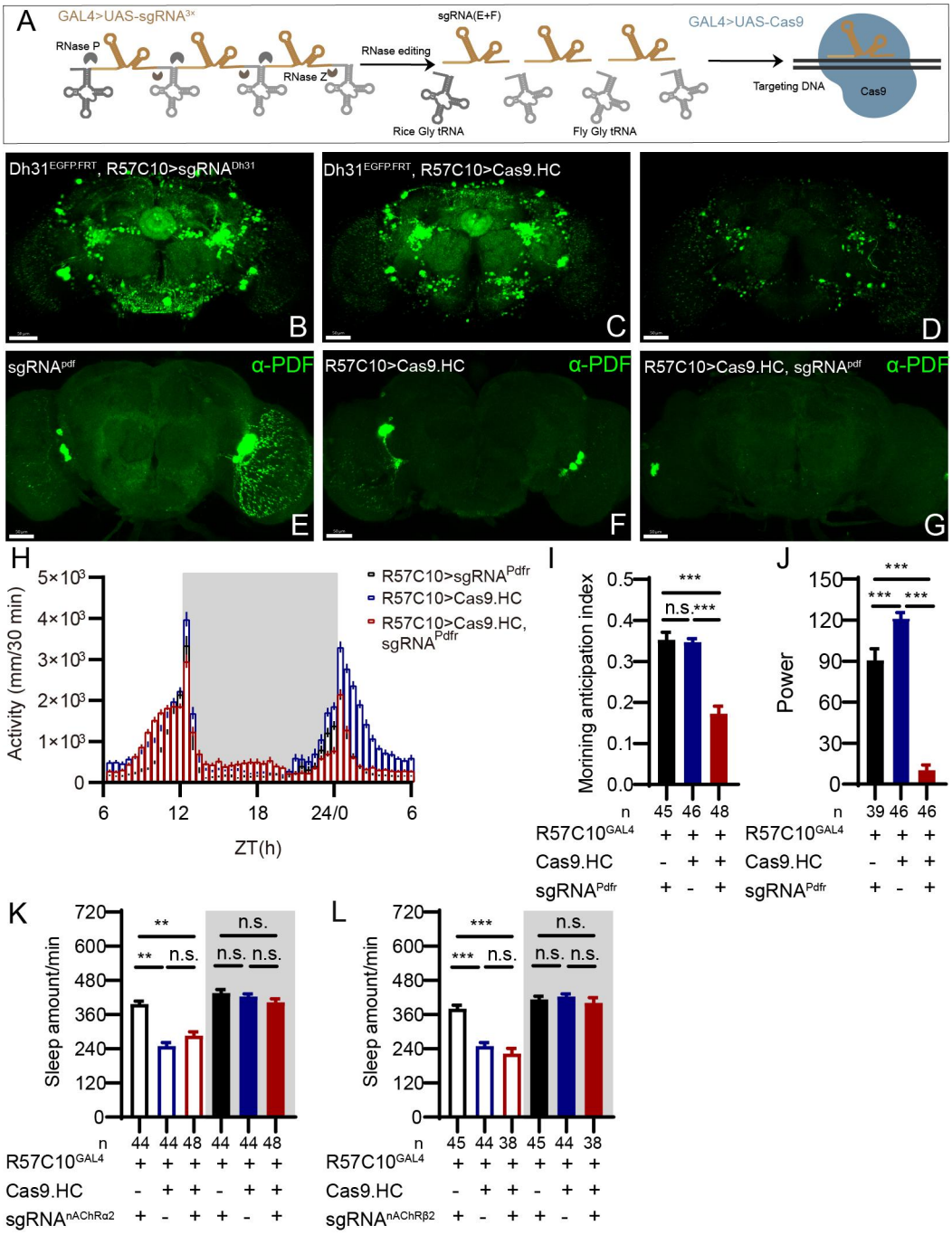

Fig 2. C-cCCTomics Mediates Efficient Conditional Knockout of CCT Genes

(A) Schematic of C-cCCTomics principle. Cas9 and three sgRNAs are driven by GAL4/UAS system. Three tandem sgRNAs are segregated by fly $tRNA^{Gly}$ and matured by RNase Z and RNase P. (B-G) Pan-neuronal knockout of Dh31 (D) and Pdf (G) by C-cCCTomics strategy. Representative fluorescence images presented expression of Dh31 (B-D) or anti-PDF (E-G). Pan-neuronal expression of Cas9 and sgRNA eliminated most (D) or all (G) fluorescent signal

819 compared to control fly brains (B-C, E-F). Scale bar, 50 μm. (H) Activity profiles of pan-neuronal
820 knockout of Pdf. Plotted in 30 min bins. (I-J) Statistical analysis of morning anticipation index (I)
821 and power (J) for pan-neuronal Pdf knockout flies. Knocking out of Pdf in neurons reduced both
822 morning anticipation index and power significantly. (K-L) Statistical analysis of nAChRα2 (K)
823 and nAChRβ2 (L) pan-neuronal knockout flies' sleep phenotype. Sleep of these flies were not
824 disrupted.

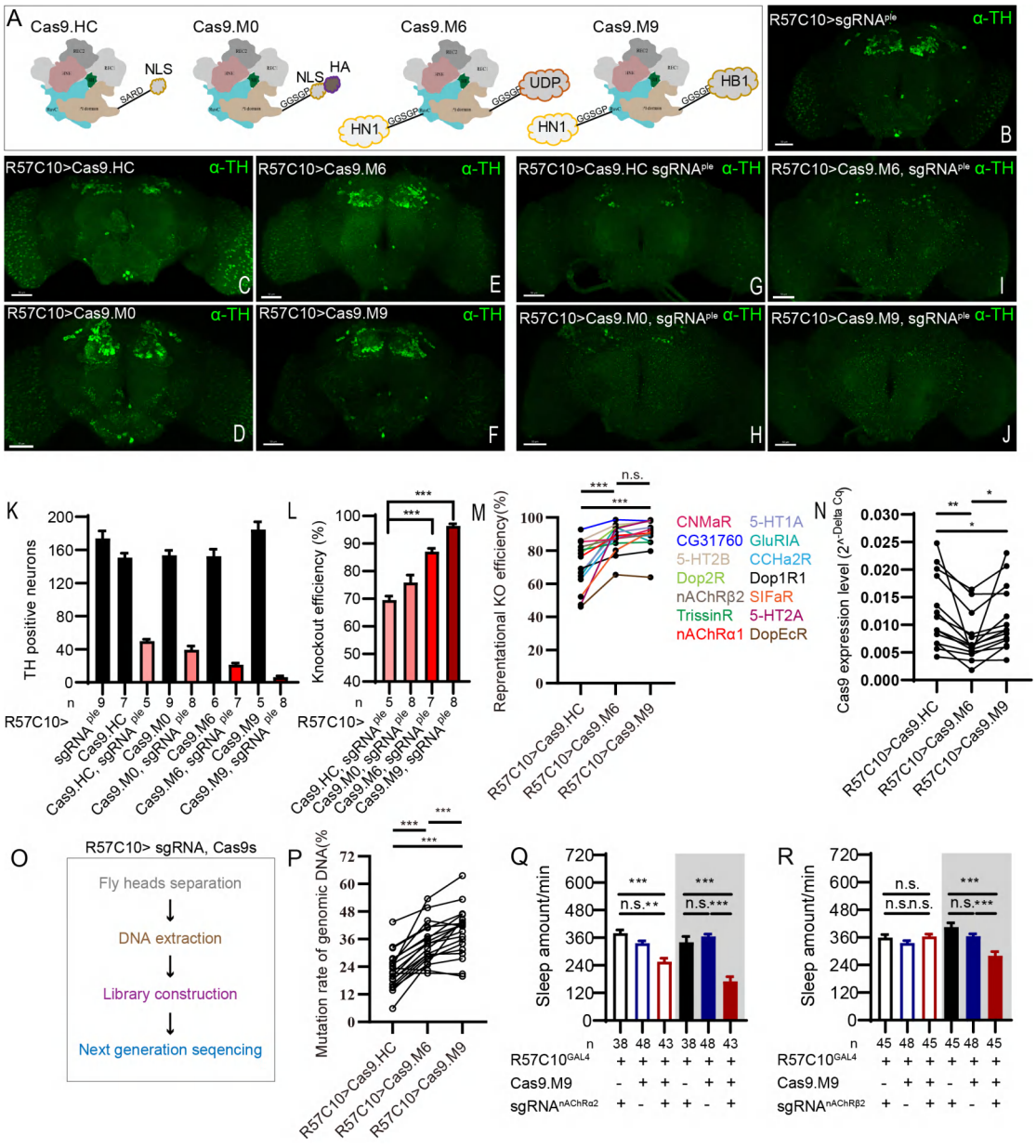

Figure 3. Efficiency Evaluation of Variations of Chromatin-Modulating Peptides Modified Cas9.

(A) Schematics of chromatin-modulating peptides modified Cas9. (B-J) Efficiency evaluation of Cas9 variants. Fluorescence imaging of R57C10-Gal4>UAS-sgRNA^{ple} (B), R57C10-Gal4>UAS-Cas9 (C-F), and R57C10-Gal4>UAS-Cas9, UAS-sgRNA^{ple} (G-J) flies are shown. Brains were stained with anti-TH (green). Scale bar is 50μm. (K) Anterior TH positive neurons numbers of (K-U). (L) Statistical analysis of ple knockout efficiency related to (K). Modified

833 Cas9.M6 and Cas9.M9 showed an improved efficiency comparing to Cas9.HC. Student's t

834 test was used. (M) Statistical analysis of representational KO efficiency of Cas9 variants as

835 related to Figure S5. Gene symbols on the right indicate tested genes. (N) Statistical analysis

836 of Cas9 expression level. (O-P) Workflow of efficiency validation by next-generation

837 sequencing (O) and Statistical analysis of single-site mutation ratios induced by Cas9 variants

838 (P). Paired t test was used in (M), (N) and (P). (Q-R) Statistical analysis of sleep amount for

839 nAChRα2 (X) or nAChRβ2 (Y) pan-neuronal knockout flies. Knockout of nAChRα2 and

840 nAChRβ2 by modified Cas9.M9 significantly decreased flies' sleep amount.

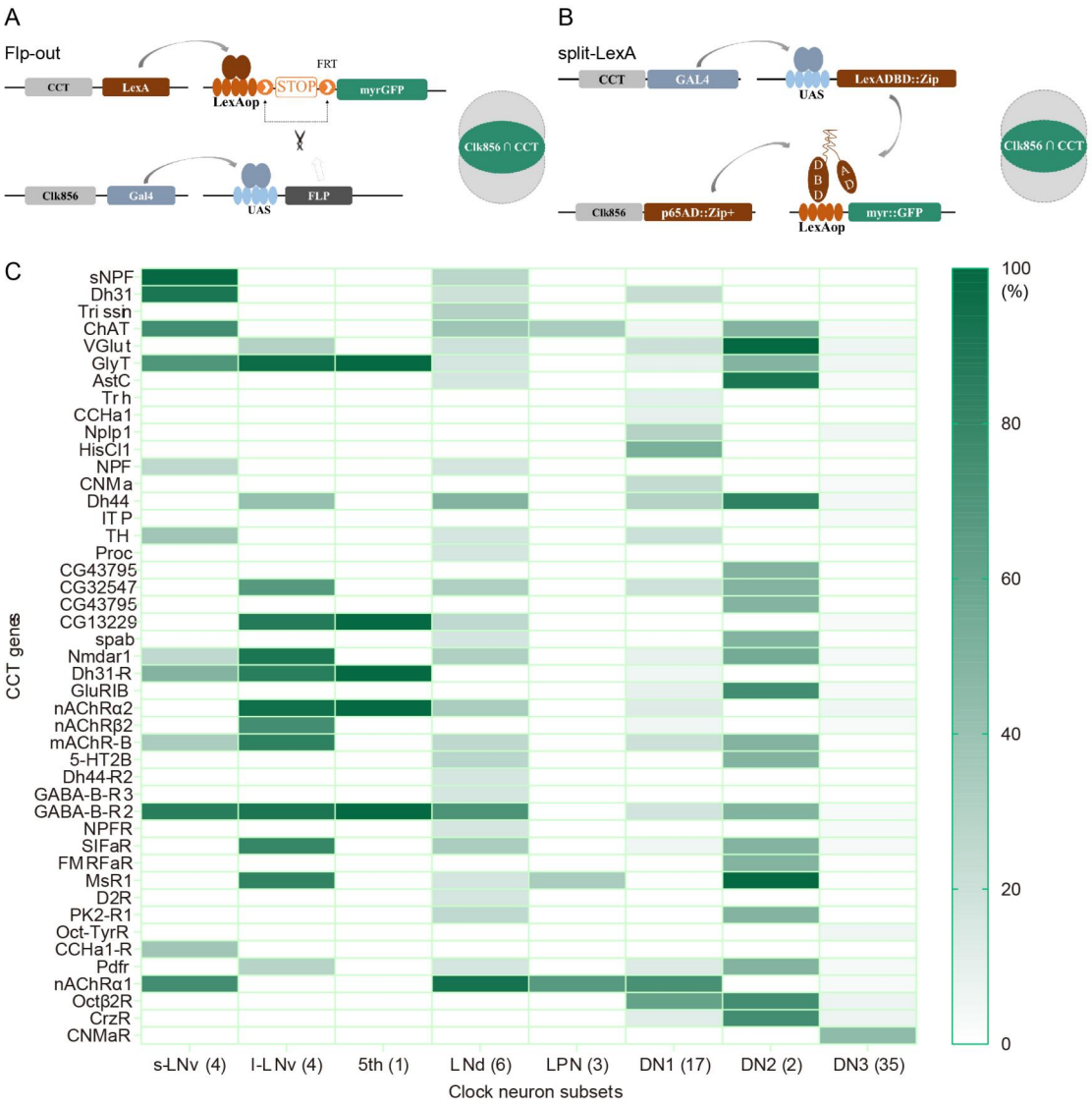

Fig 4. Genetic Dissection of Clk856 Labelled Clock Neurons.

(A-B) Schematic of intersection strategies used in Clk856 labelled clock neurons dissection, Flp-out strategy (A) and split-LexA strategy (B). (C) Expression profiles of CCT genes in clock neurons. Gradient color denotes proportion of neurons that were positive for the CCT gene within each subset. This figure is corresponding to Table S4.

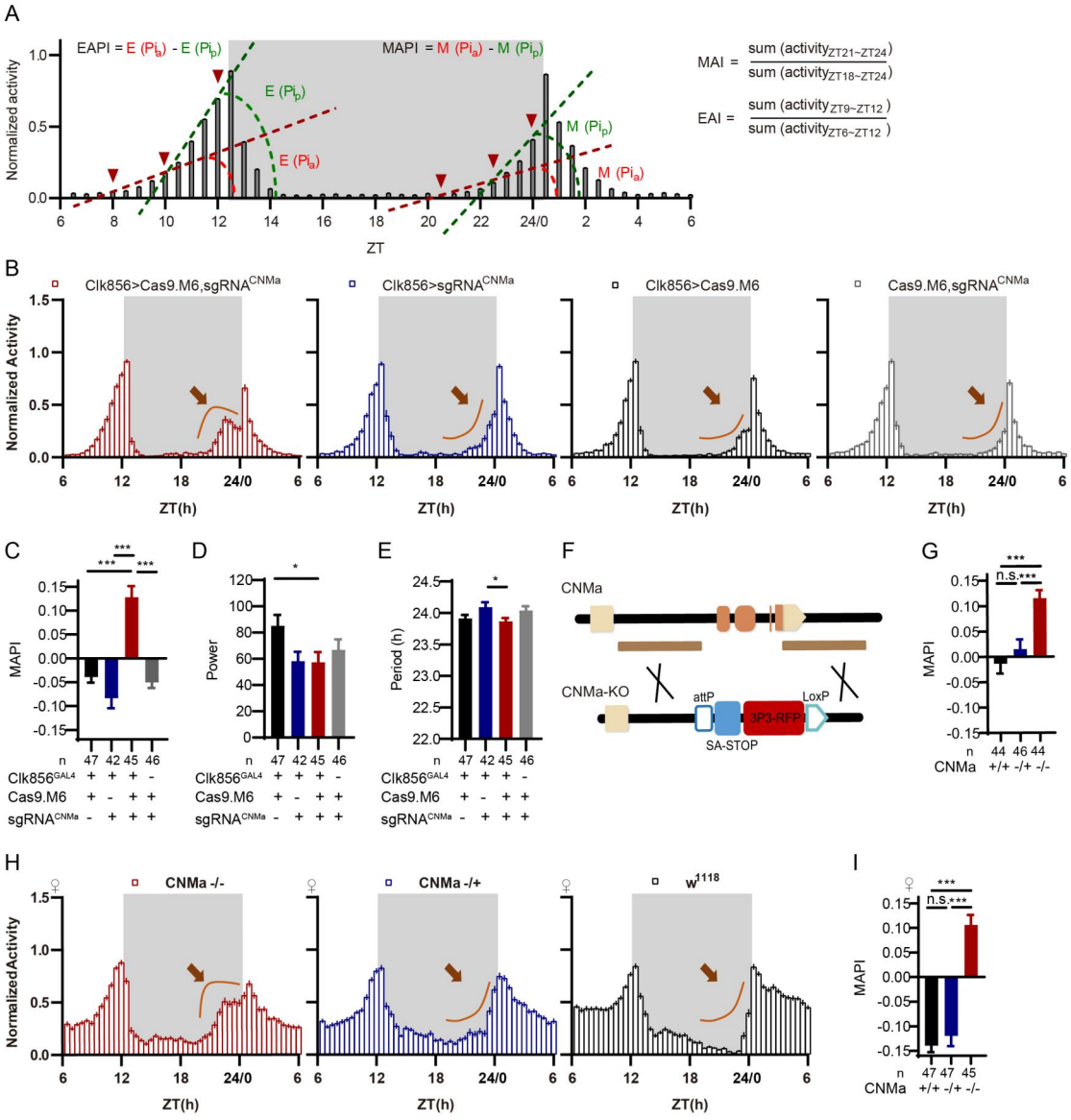

Fig 5. CNMa Regulation of Morning Anticipation in Clock Neuron

(A) Schematic of MAI, EAI, MAPI and EAPI definition. (B) Activity plots of male flies with CNMa knockout in clock neurons (red) and controls (blue, black and grey), plotted in 30 min bins. An advancement of morning activity peak was presented in CNMa clock-neuron-specific mutants (brown arrowhead). (C-E) Statistical analyses of MAPI, power, and period of flies in (B). MAPI was significantly increased in clock neurons-specific CNMa deficient flies (C) while power (D) and period (E) were not changed. (F) Schematic of $CNMa^{KO}$ generation. The entire encoding region of CNMa was replaced by an attP-SAstop-3P3-RFP-loxP cassette using CRISPR-Cas9

856 strategy. (G) Statistical analysis of MAPI of male CNMa^{KO} flies (red) and controls (blue and

857 black). MAPI significantly increased in male CNMa^{KO} flies. (H) Activity plots of female CNMa^{KO}

858 flies (red) and controls (blue and black). (I) Statistical analysis of MAPI of female CNMa^{KO} flies

859 (red) and controls (blue and black). MAPI was significantly increased in female CNMa^{KO} flies.

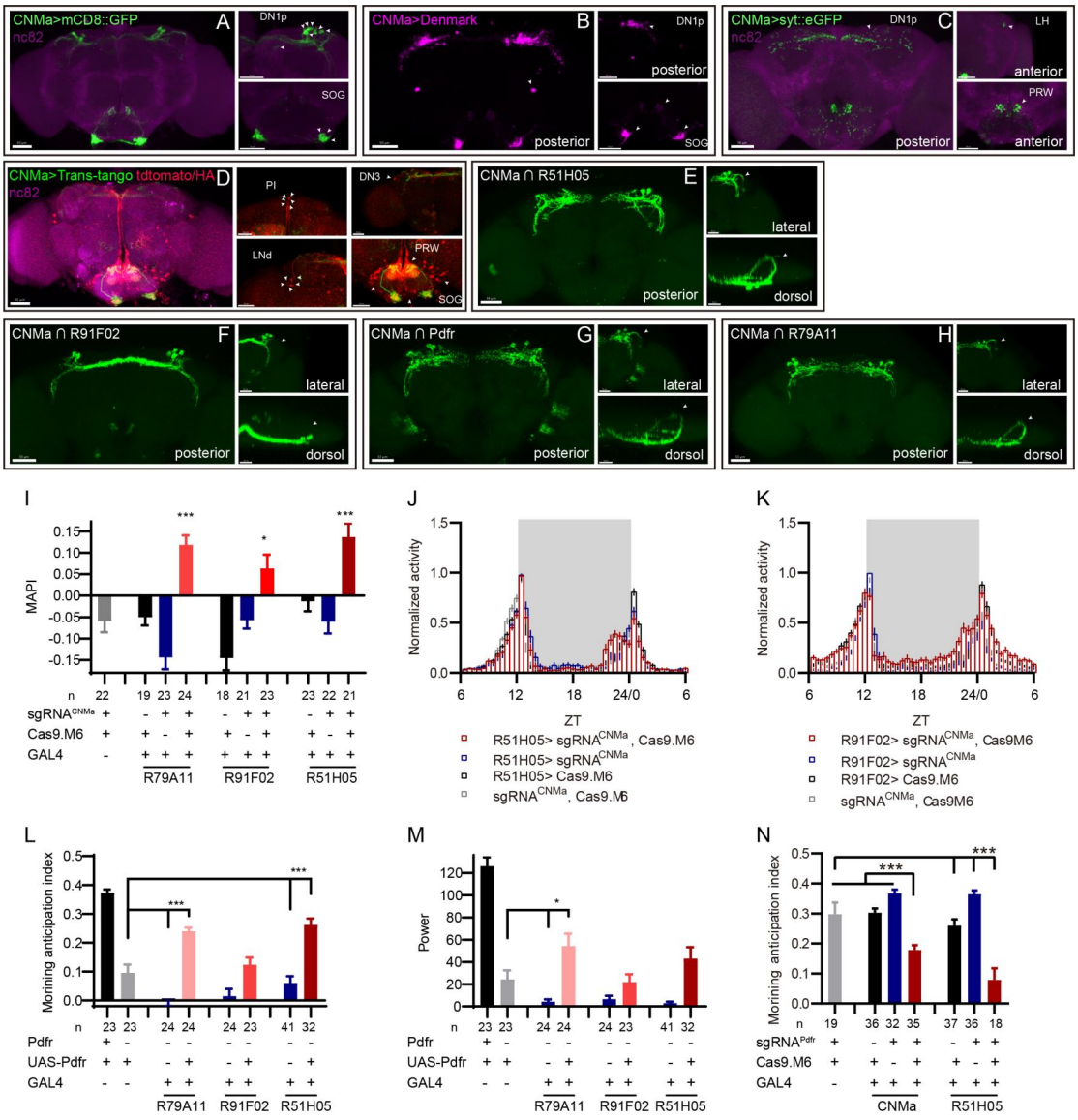

Fig 6. Expression, Projection and Trans-projection Feature of CNMa Neurons and Its Functional Subset

(A-C) Expression and projection patterns of CNMa-KI-Gal4 in the brain. Membrane, dendrites, and axon projections are labelled by mCD8::GFP (A), Denmark (B), and syt::eGFP (C) respectively. (D) Downstream neurons labelled through trans-tango driven by CNMa-KI-GAL4. Arrowheads indicate candidate downstream neurons: six neurons in PI, one pair in DN3, five pairs in LNd and about 15 pairs in SOG. (E-H) Intersection of DN1p CNMa neurons with DN1p labelled drivers. GMR51H05-GAL4 (E), GMR91F02-GAL4 (F), Pdfr-KI-GAL4 (G) and

869 GMR79A11-GAL4 (H) were intersected with CNMa-p65AD, UAS-LexADBD, LexAop-myr::GFP.
870 Two type I (E, G, H) neurons projected to anterior region and four type II (F) neurons had fewer
871 projections to anterior region. Scale bar, 50μm. (I) MAPIs were significantly increased in all
872 three DN1p drivers mediated CNMa knockout. (J-K) Activity plots of CNMa knockout in
873 R51H05-GAL4 (J) and R91F02-GAL4 (K) neurons. R51H05-GAL4 mediated CNMa knockout
874 flies showed an advanced morning activity peak (J), while R91F02-Gal4 mediated CNMa
875 knockout flies did not (K). (L-M) Statistical analyses of MAI and power. Pdfr reintroduction in
876 R79A11 and R51H05 neurons could partially rescue the MAI-decreased phenotype of Pdfr
877 knockout flies. (N) Statistical analyses of MAI of Pdfr knocking out in CNMa-KI-GAL4 and
878 R51H05-GAL4 labelled neurons.

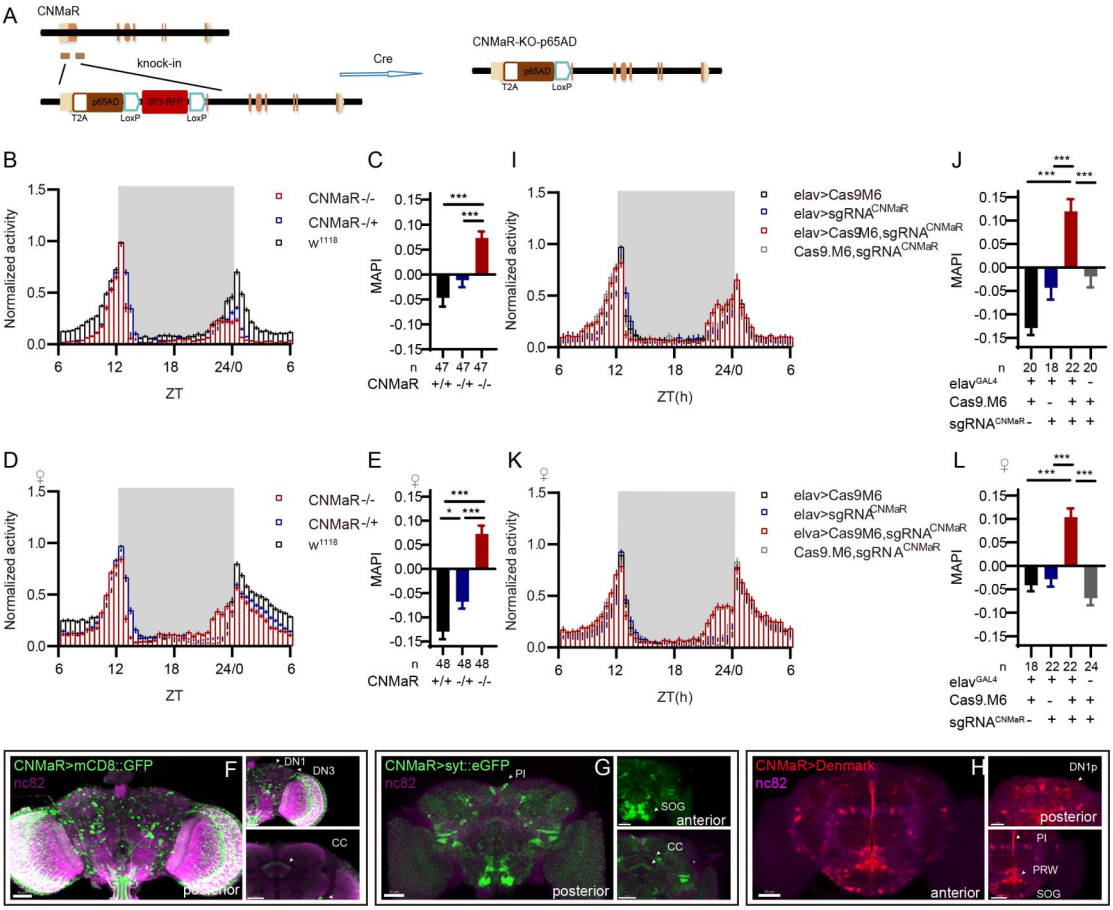

Fig 7. CNMaR Regulation of Morning Anticipation

(A) Schematic of CNMaR$^{KO\text{-}p65AD}$ generation. Most of the first exon in CNMaR was replaced by a T2A-p65AD-loxP-3P3-RFP-loxP cassette using CRISPR-Cas9 strategy and the T2A-p65AD was inserted in the reading frame of the remaining CNMaR codon. 3P3-RFP was removed latterly by Cre mediated recombination. (B-E) Activity plot (B, D) and statistical analysis (C, E) of male (B-C) or female (D-E) CNMaR$^{KO\text{-}p65AD}$ flies (red) and genotypical controls (blue and black). MAPI was significantly increased in both male and female CNMaR$^{KO\text{-}p65AD}$ flies. In this and other figures, "♀" denotes female flies. (F-H) Expression and projection patterns of CNMaR-KI-Gal4 in the brain. Scale bars, 50μm. (I-L) Activity plots (I, K) and statistical analyses (J, L) of CNMaR pan-neuronal knockout flies. Neuronal knockout of CNMaR increased MAPI (K).

Supplementary Information

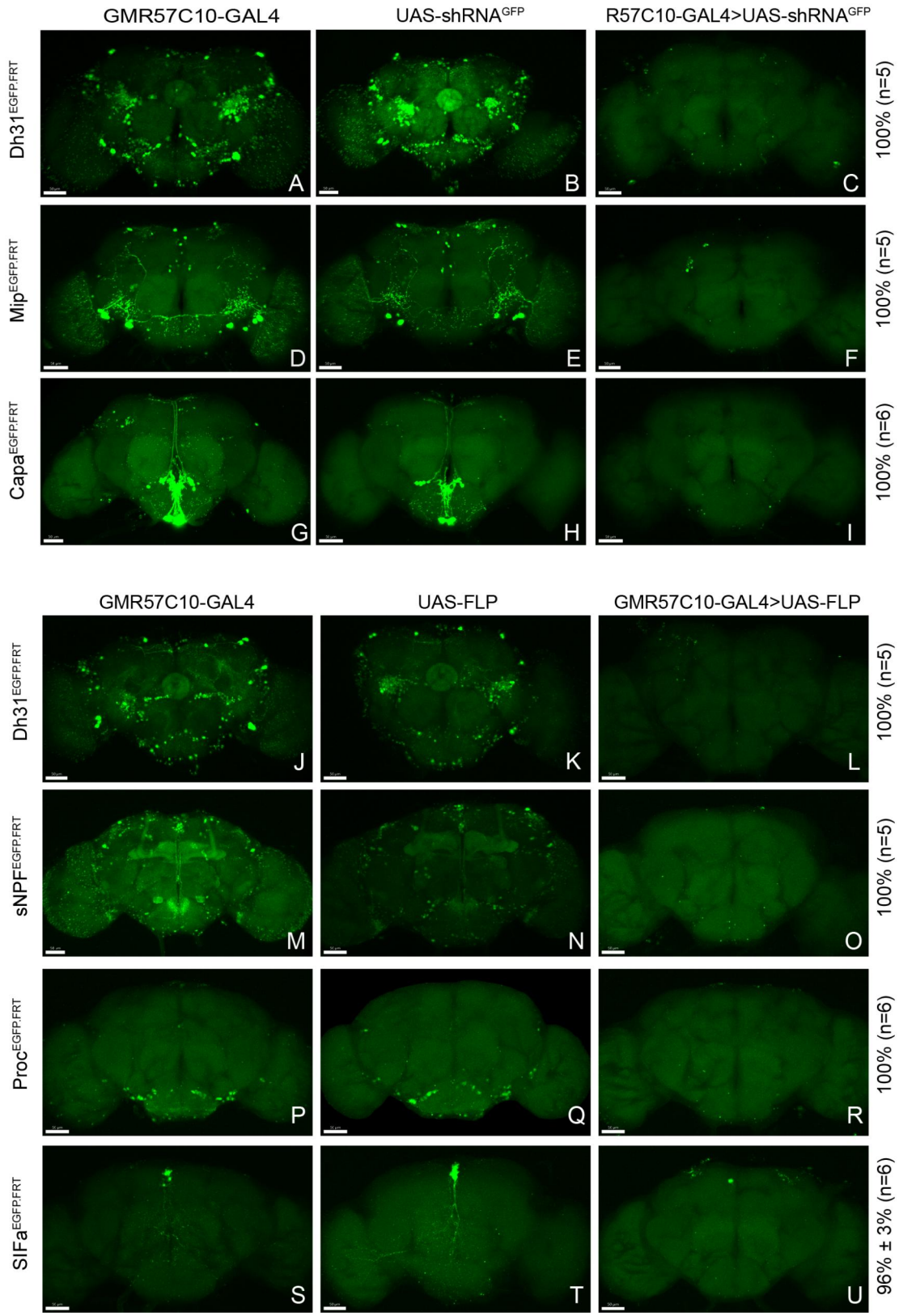

Fig S1. Efficient Conditional Disruption of CCT Genes by cCCTomics

(A-I) Pan-neuronal knockdown of Dh31 (A-C), Mip (D-F) and Capa (G-I) by GFPi. All

895 experimental fly brains (C, F, I) showed no GFP signal after knockdown by GFPi. As described

896 in Fig 1, all percentages in the right represent gene disruption efficiency and n represent number

897 of experimental flies. (J-U) Pan-neuronal knock out of Dh31, sNPF, Proc and SIFa by Flp-out

898 strategy. No obvious GFP signal was found in the experimental fly brains (L, O, R), excepting

899 one GFP positive neurons in SIFa flp-out group (U).

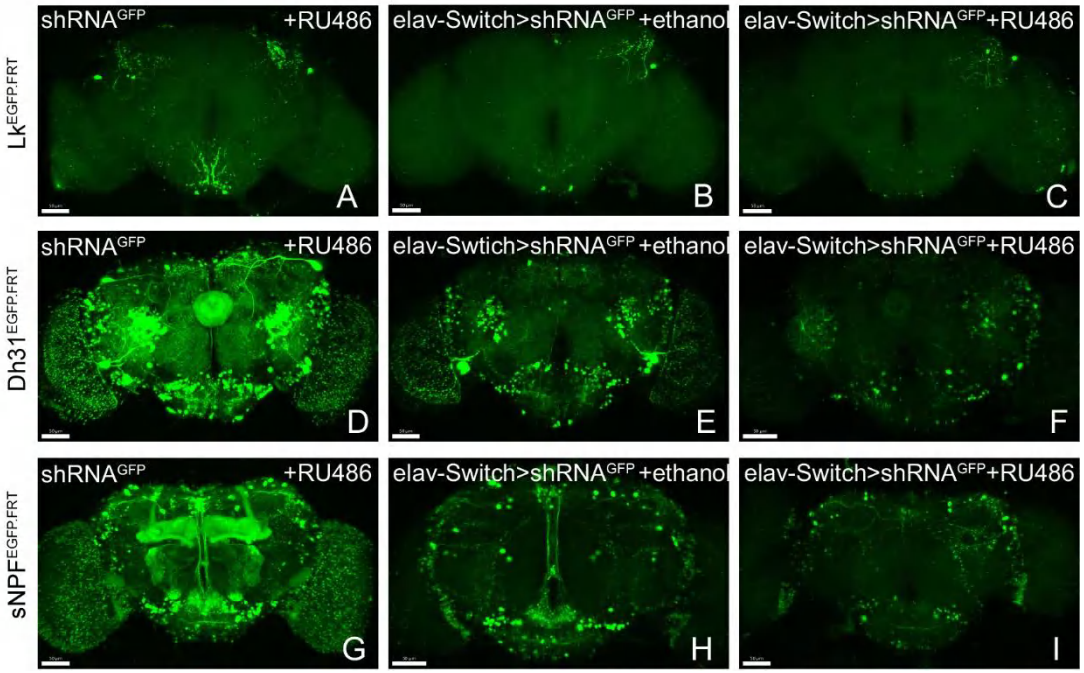

Fig S2. Gene Disruption of Target Genes by Induced shRNA

(A-J) Knockdown of Lk, Dh31 and sNPF by elav-Switch. Most GFP signal is lost in the experimental group (C, F, I).

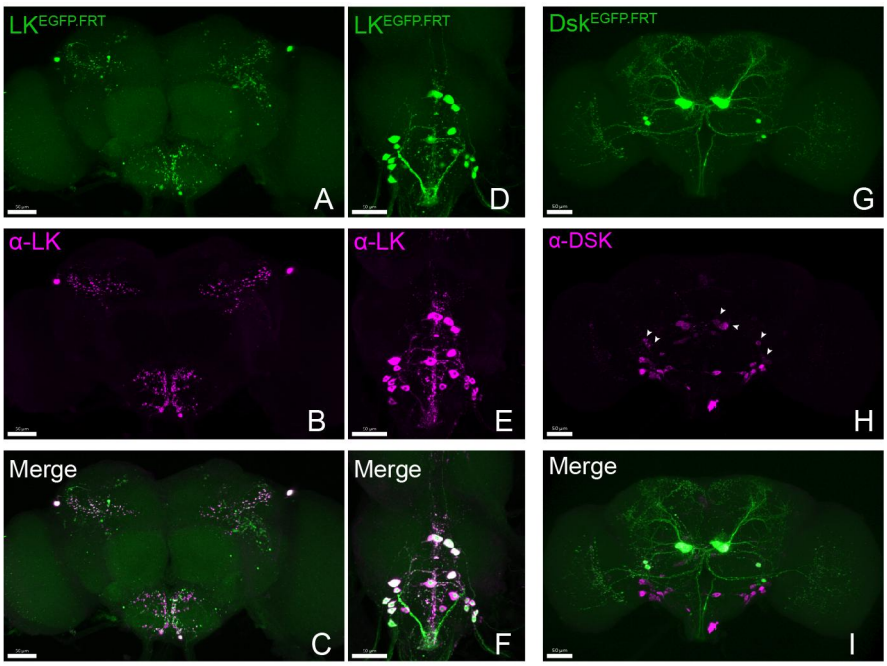

Fig S3. Accurate Labeling of Target Genes by cCCT Lines

(A-J) Co-localization of fused EGFP labelled CCT genes and corresponding antibodies. All the EGFP labelled Lk (A, D) and Dsk (G) neurons (Green) were co-localized with anti-LK (B, E; merge C, F) and anti-DSK (H, merge I) signal (purple). Arrowheads represent specific anti-DSK signal (Wu et al., 2020).

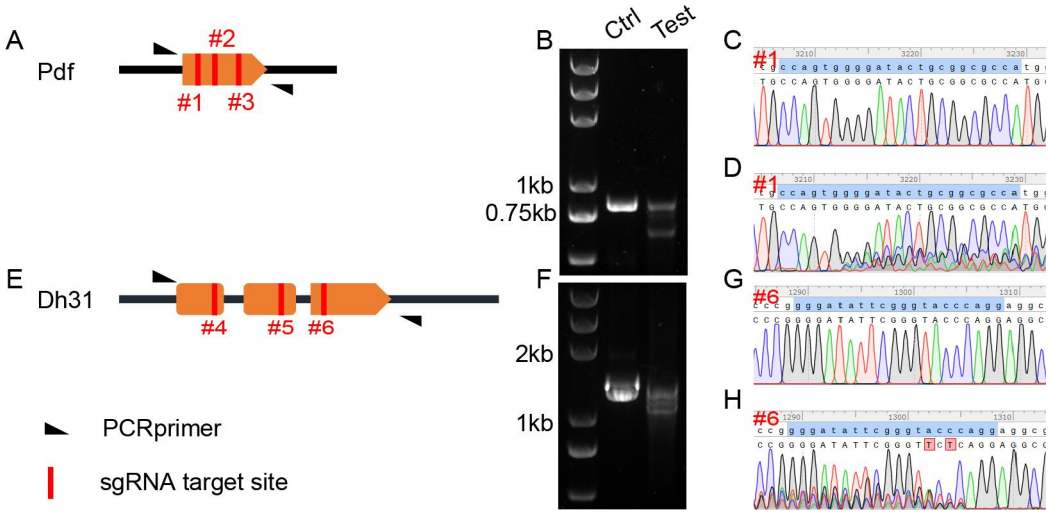

Fig S4. Validation of Primary C-cCCTomics

(A) Gene span of Pdf. #1, #2 and #3 with red lines denote sgRNA targets regions in Pdf coding sequence. (B) DNA gel electrophoresis of PCR products after *pdf* KO by C-cCCTomics. “Ctrl” denotes PCR products from genomic DNA mixture of Act5C-GAL4/+; UAS-Cas9.P2/+ flies and UAS-sRNA^{Pdf} flies. “Test” denotes PCR products from Act5C-GAL4/ UAS-sRNA^{Pdf}; UAS-Cas9.P2 flies. (C-D) Sanger sequencing results of Ctrl (C) and Test (D) PCR products at #1 sgRNA target site. (E-H) Similar to (A-D) with Dh31 as target. (I-J) Statistical analysis of nAChRα2 (I) and nAChRβ2 (J) pan-neuronal knockout flies’ sleep phenotype. Sleep of these flies were not disrupted.

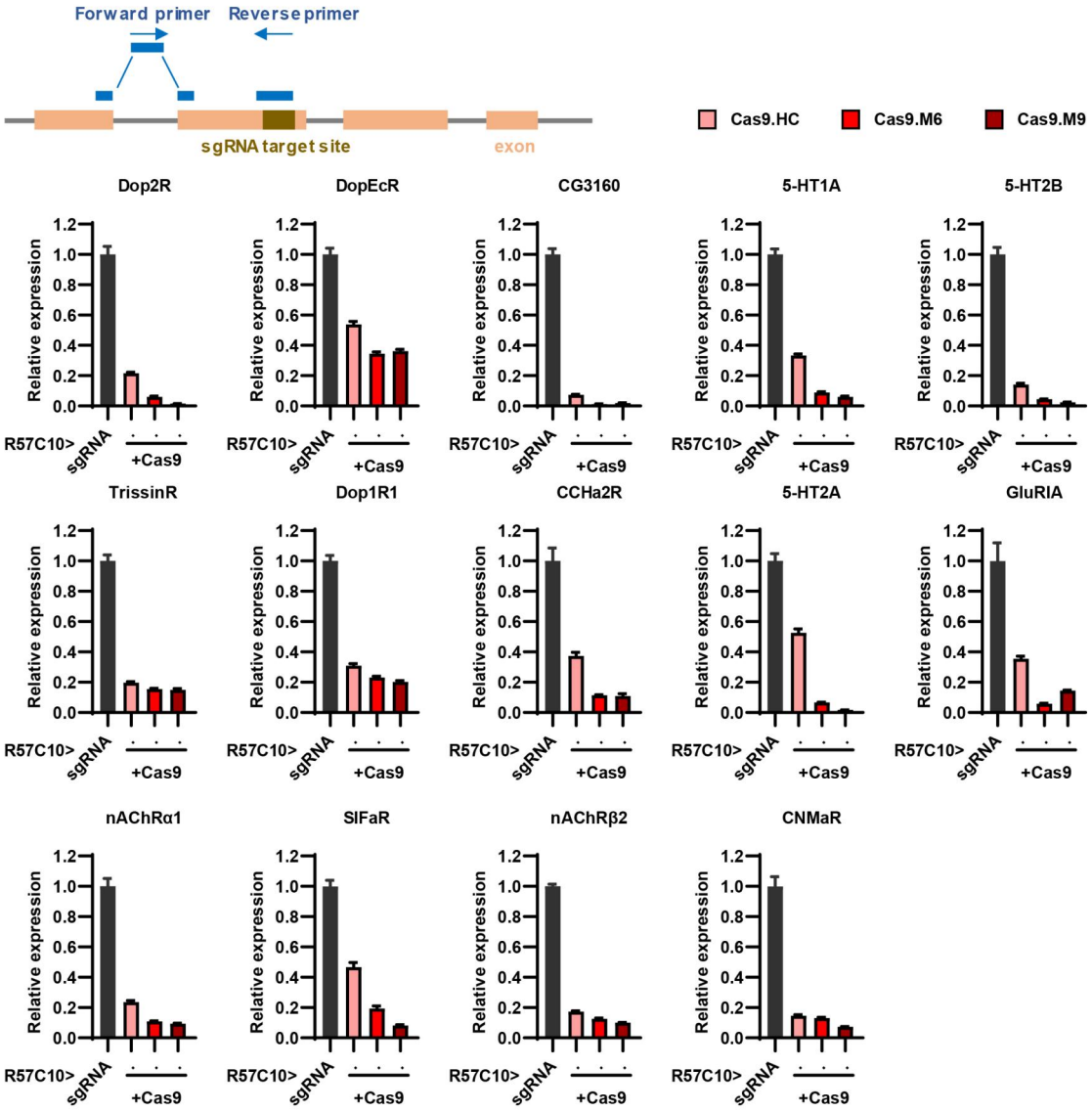

Fig S5. Efficiency validation by real-time quantitative PCR.

This figure corresponds to Fig 3M. The schematic at the top illustrates the principle of primer design. The gene symbol above each panel indicates the target of sgRNAs. The expression of the target gene in the experimental groups (where R57C10-GAL4 drives the expression of both Cas9 variants and sgRNA) was normalized to the control group (where R57C10-GAL4 drives sgRNA expression only).

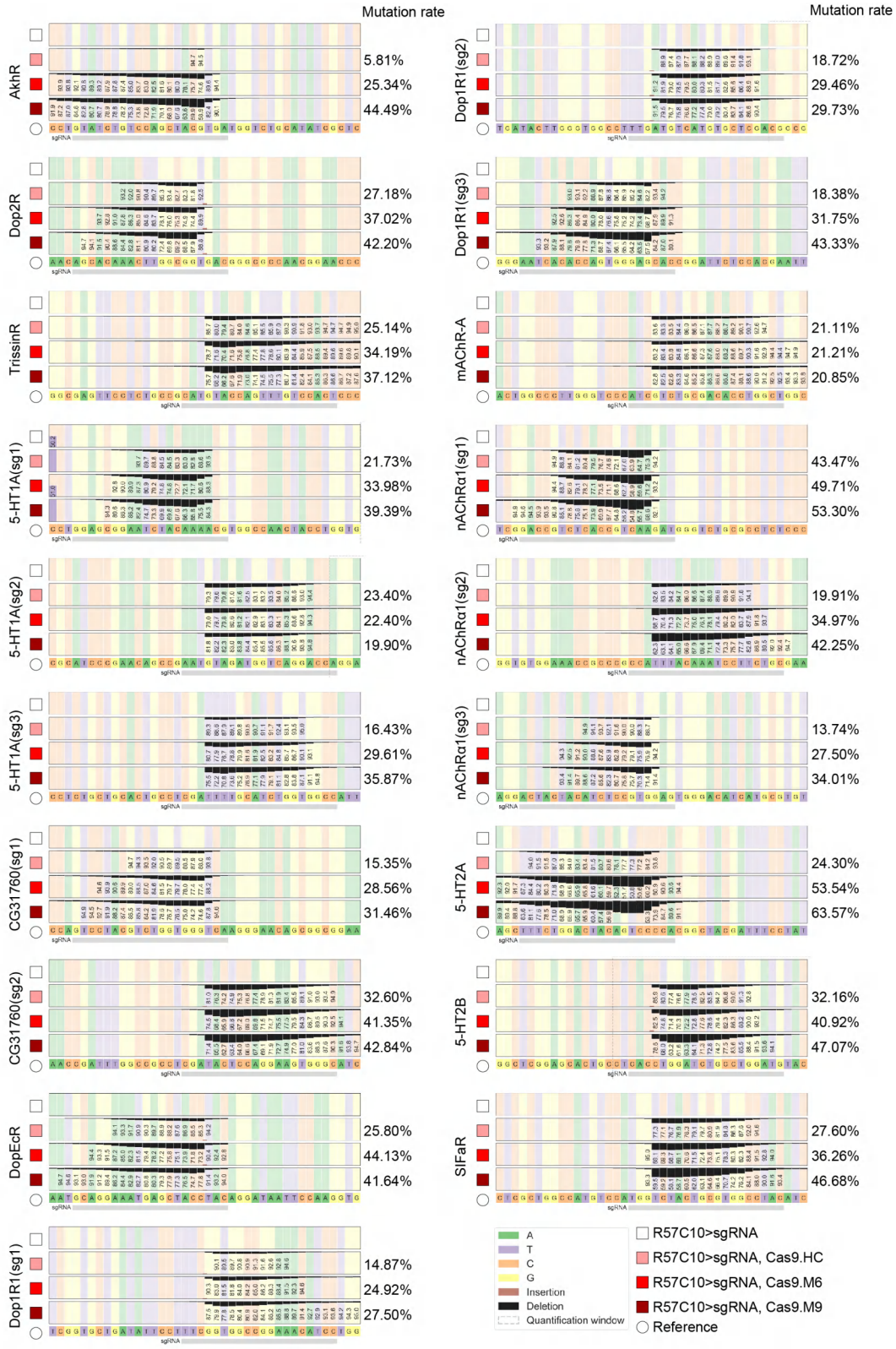

Fig S6. Efficiency validation by high-throughput sequencing

This figure corresponds to Fig 3P. Gene symbol on the left side of each panel denotes the target gene, while the percentages on the right denotes mutation rate as calculated by CRISPResso2.

931 A minimum of 10,000 reads were analyzed for each genotype.

932

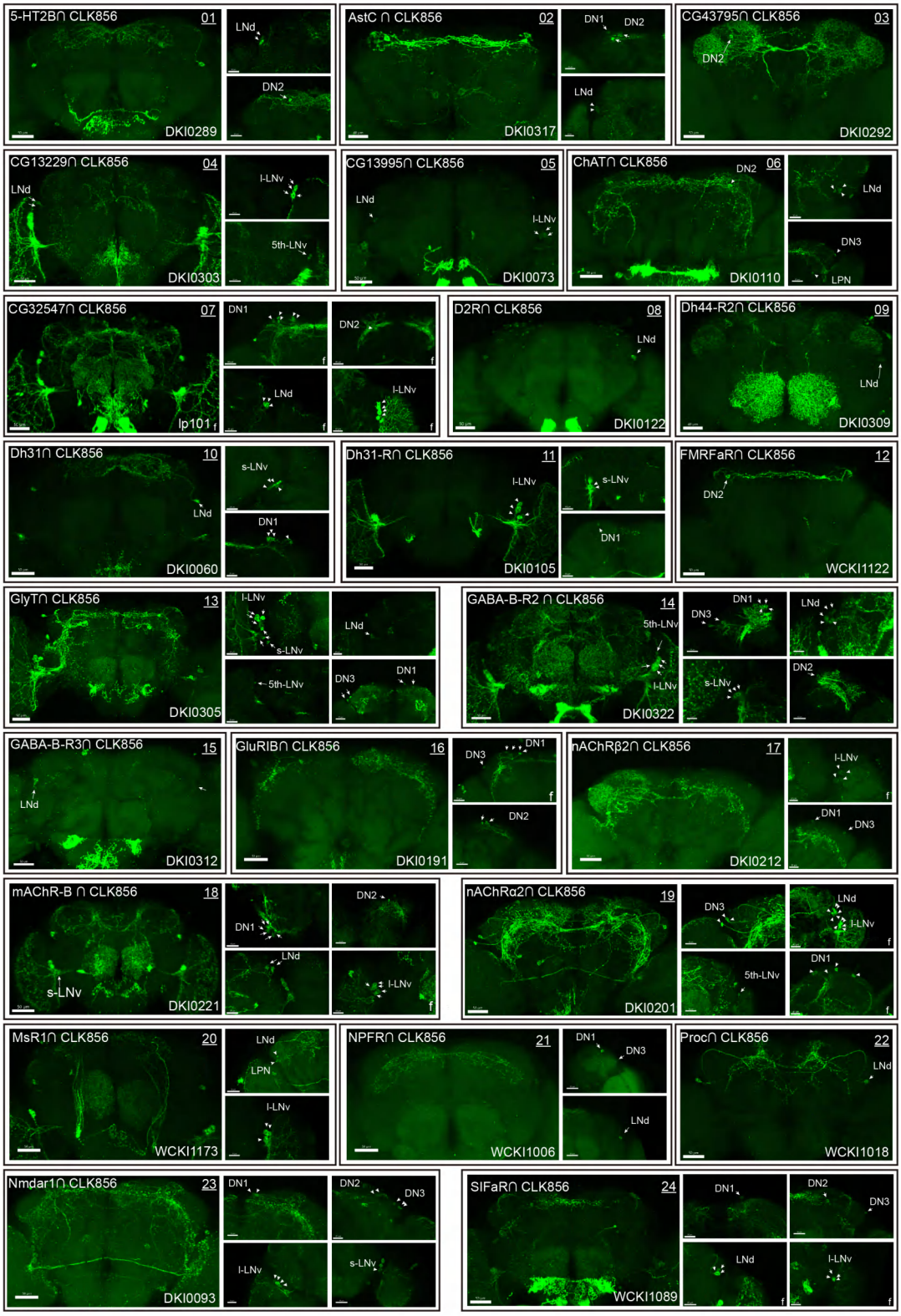

933

934 **Fig S7. Co-expression of Clk856 with CCT Genes**

935 (01-24) Intersectional expression patterns of CCT drivers with Clk856. Maximum neuron

936 numbers were presented in each image. Note at the bottom right corner is category ID of CCT

937 drivers in Rao Lab fly stock library. “f” denotes female fly brain, otherwise male brain is shown.

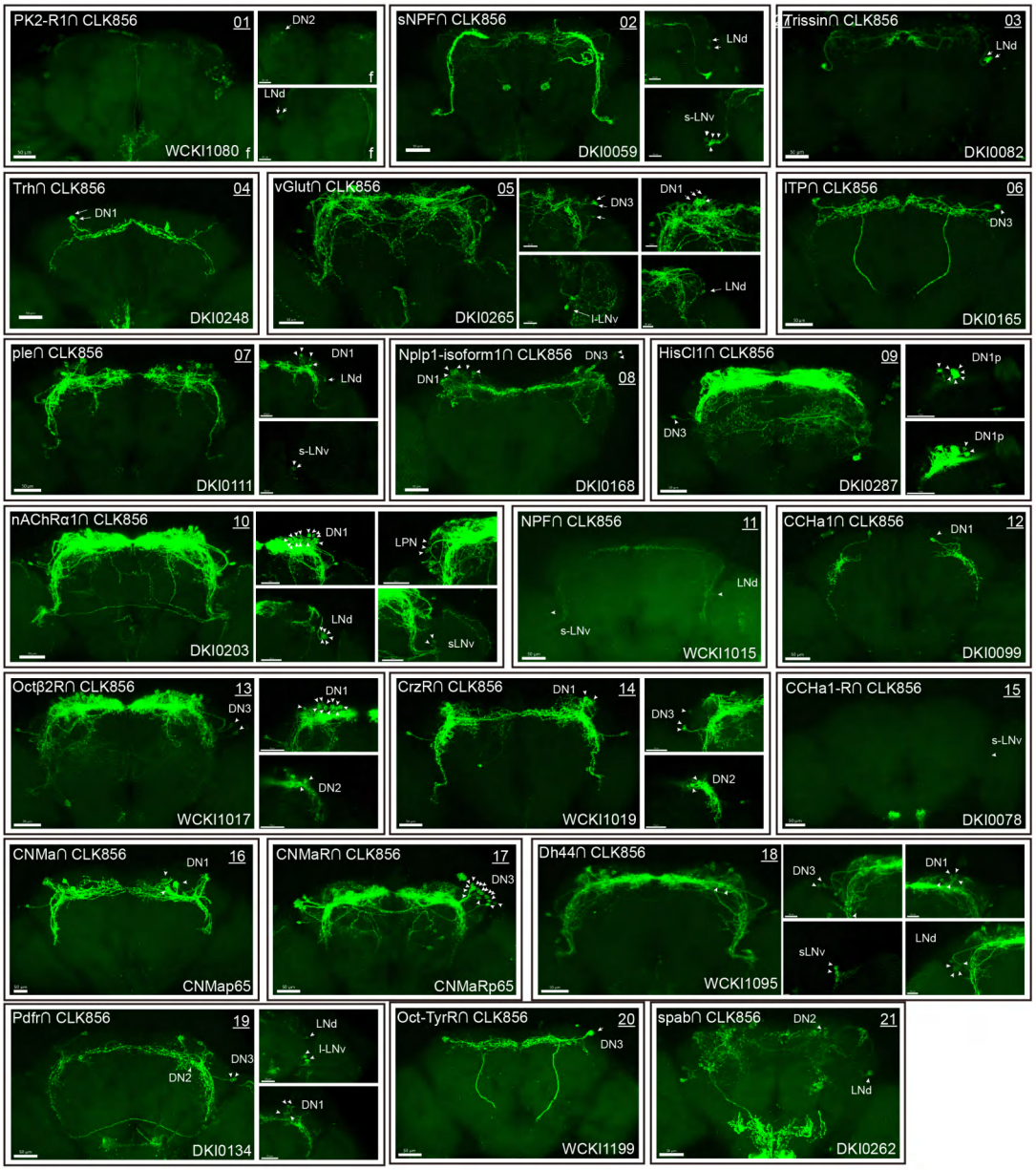

938

939 **Fig S8 Co-expression of Clk856 with CCT Genes**

940 (01-21) Intersectional expression patterns of CCT drivers with Clk856, similar to Fig S5.

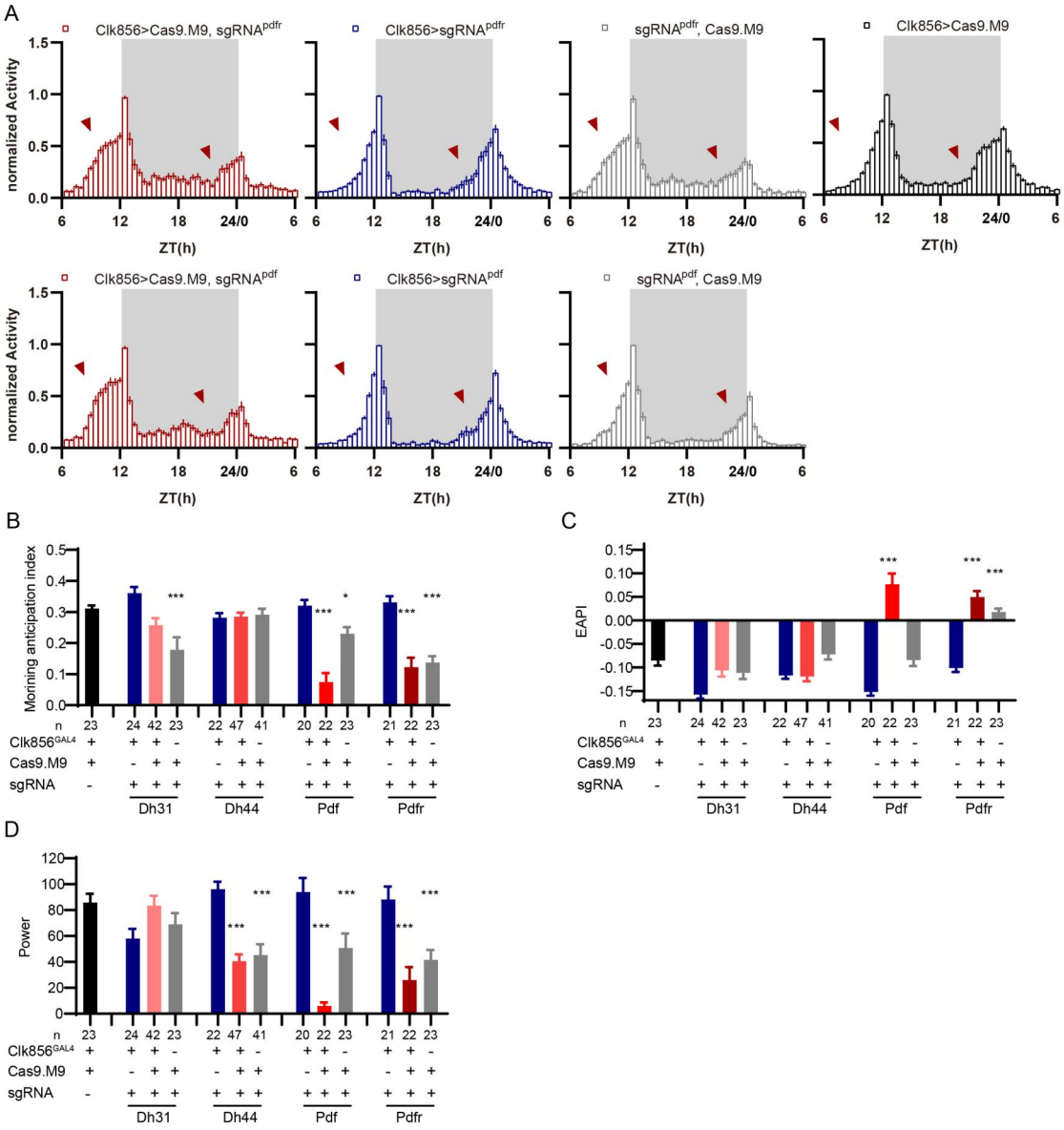

941

942 **Fig S9. Disruption of CCT Genes due to Leaky Expression of Cas9.M9**

943 (A) Activity plots of Pdfr or Pdf clock-neuron knockout flies (red) and control groups (blue, black,

944 and gray). (B-D) Statistical analyses of morning anticipation index (B), EAPI (C) and power (D)

945 after CCT genes were knockdown by Cas9.M9/sgRNAs. Leakage expression of Cas9.M9 and

946 sgRNAs might disrupt target genes at certain levels (grey bar). Cas9.M9 denotes UAS-

947 Cas9.M9. sgRNA denotes UAS-sgRNA.

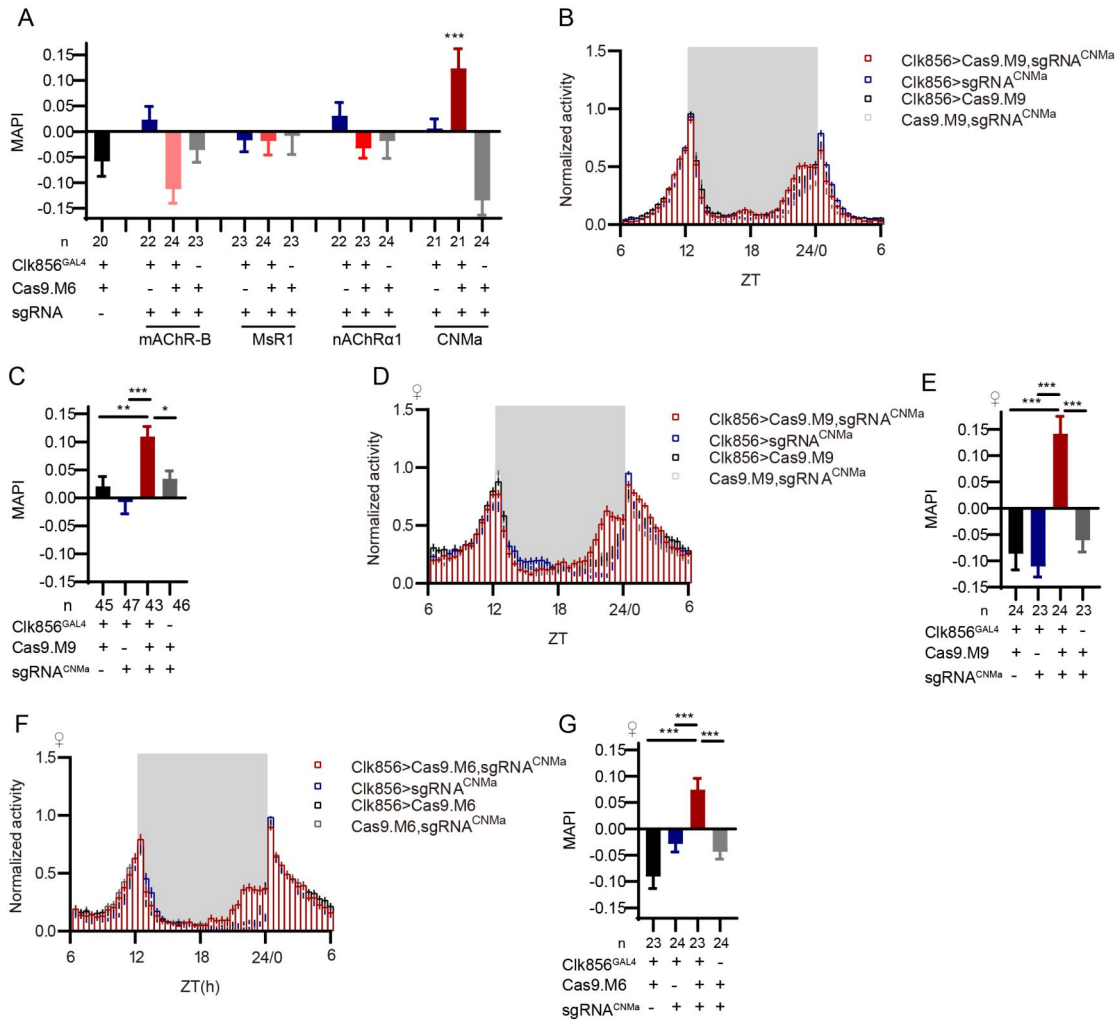

Fig S10. Morning Activity Advanced by Loss of CNMa

(A) MAPI statistical analyses after mAChR-B, MsR1, nAChRα1 and CNMa knockout in clock neurons. Only the CNMa knockout in clock neurons increased MAPI significantly. (B-E) Activity plots (B, D) and statistical analyses (C, E) of male (B, C) and female (D, E) flies with CNMa knockout in clock neurons. Both male and female flies showed advanced morning activity patterns B, C) and increased MAPIs (D, E). UAS-sgRNA^{CNMa}/UAS-Cas9.M9 flies showed a slightly increased MAPI which indicate possible leakage expression. (F-G) Activity plots (F) and statistical analyses (G) of female flies with CNMa deficient in clock neurons with Cas9.M6 used.

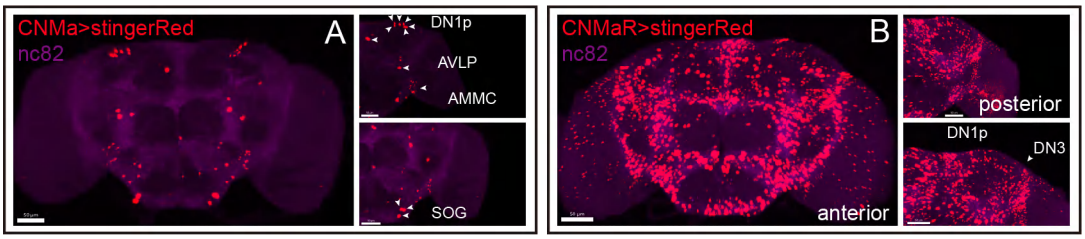

Fig S11. Expression of CNMa and CNMaR

(A-B) Stinger::Red labeled neurons in brain driven by CNMa-KI-GAL4 (A) and CNMaR-KI-GAL4 (B)

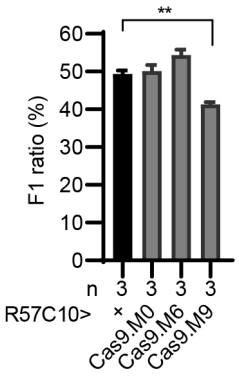

Fig S12. Impact on Viability of Cas9 Variants Expression by GMR57C10-GAL4

F1 ratio of UAS-Cas9 variants (male) cross GMR57C10-GAL4/cyo (virgin female). Expression of Cas9.M9 decreased progeny viability slightly.

** $p < 0.01$. Two-student test was used.

Table S1 cCCT Knockin fly list

cCCT NO.	CG number	Gene Symbol	cCCT NO.	CG number	Gene Symbol
CCT1002C	CG11325	AkhR	CCT1087C	CG42244	Octβ3R
CCT1003C	CG14375	CCHa2	CCT1088C	CG7411	Ort
CCT1004C	CG14593	CCHa2-R	CCT1089C	CG1543	TβH
CCT1007C	CG6936	mth	CCT1093C	CG13968	sNPF
CCT1008C	CG31147	mthl11	CCT1097C	CG15520	Capa
CCT1009C	CG17084	mthl9	CCT1098C	CG4910	CCAP
CCT1010C	CG6496	Pdf	CCT1099C	CG11318	CG11318
CCT1011C	CG8784	PK2-R1	CCT1102C	CG13229	CG13229
CCT1012C	CG13687	Ptth	CCT1103C	CG15556	CG15556
CCT1013C	CG14734	Tk	CCT1107C	CG30340	CG30340
CCT1014C	CG6515	TkR86C	CCT1108C	CG32447	CG32447
CCT1016C	CG13633	AstA	CCT1109C	CG33639	CG33639
CCT1019C	CG3302	Crz	CCT1110C	CG33696	CNMaR
CCT1020C	CG10698	CrzR	CCT1111C	CG34411	Lgr4
CCT1021C	CG2902	Nmdar1	CCT1113C	CG43795	CG43795
CCT1024C	CG32540	CCKLR-17D3	CCT1114C	CG44153	CG44153
CCT1025C	CG33517	D2R	CCT1117C	CG12345	Cha
CCT1026C	CG13094	Dh31	CCT1118C	CG13936	CNMamide
CCT1027C	CG32843	Dh31-R	CCT1119C	CG8380	DAT
CCT1028C	CG18090	Dsk	CCT1120C	CG9887	dVGLUT
CCT1029C	CG6440	Ms	CCT1121C	CG5400	Eh
CCT1030C	CG43745	MsR2	CCT1122C	CG18105	ETH
CCT1034C	CG13480	Lk	CCT1123C	CG5911	ETHR
CCT1035C	CG10626	Lkr	CCT1124C	CG2346	FMRFa
CCT1036C	CG4128	nAChR α6	CCT1126C	CG15274	GABA-B-R1
CCT1037C	CG33976	Octβ2R	CCT1128C	CG14994	gad1
CCT1039C	CG14358	CCHa1	CCT1129C	CG8442	GluRIA
CCT1040C	CG30106	CCHa1-R	CCT1130C	CG43743	GluRIB
CCT1041C	CG13575	CG13575	CCT1131C	CG6992	GluRIIA
CCT1042C	CG13995	CG13995	CCT1133C	CG4226	GluRIIC
CCT1043C	CG33495	Dup99B	CCT1134C	CG18039	GluRIID
CCT1044C	CG31720	mthl15	CCT1135C	CG31201	GluRIIE
CCT1047C	CG1147	NPFr	CCT1136C	CG14723	HisCl1
CCT1050C	CG16752	SPR	CCT1137C	CG13586	ITP
CCT1051C	CG14871	Trissin	CCT1138C	CG7665	Lgr1
CCT1052C	CG34381	TrissinR	CCT1143C	CG8985	MsR1
CCT1053C	CG16720	5-HT1A	CCT1145C	CG32853	mthl12
CCT1055C	CG12073	5HT7	CCT1147C	CG30018	mthl13
CCT1056C	CG14919	AstC	CCT1148C	CG17795	mthl2
CCT1057C	CG14575	CapaR	CCT1149C	CG6536	mthl4
CCT1058C	CG33344	CCAP-R	CCT1150C	CG6965	mthl5
CCT1059C	CG13579	CG13579	CCT1151C	CG16992	mthl6

CCT1060C	CG31760	CG31760	CCT1152C	CG7476	mthl7
CCT1061C	CG32547	CG32547	CCT1153C	CG32475	mthl8
CCT1062C	CG18314	DopEcR	CCT1156C	CG32538	nAChR α7
CCT1065C	CG3454	HDC	CCT1158C	CG34388	natalisin
CCT1066C	CG4395	hec	CCT1159C	CG3441	Nplp1
CCT1068C	CG6456	Mip	CCT1161C	CG15361	Nplp4
CCT1070C	CG6530	mthl3	CCT1164C	CG13565	Orcokinin
CCT1071C	CG5610	nAChR α1	CCT1165C	CG15284	Pburs
CCT1072C	CG6844	nAChR α2	CCT1166C	CG31660	pog
CCT1073C	CG2302	nAChR α3	CCT1167C	CG7105	Proc
CCT1074C	CG11348	nAChRβ1	CCT1168C	CG6986	Proc-R
CCT1075C	CG6798	nAChRβ2	CCT1169C	CG10537	Rdl
CCT1076C	CG6919	oa2	CCT1170C	CG8930	rk
CCT1078C	CG7395	sNPF-R	CCT1172C	CG5811	RYa-R
CCT1079C	CG11895	stan	CCT1174C	CG33527	SIFa
CCT1080C	CG9122	TRH	CCT1175C	CG10823	SIFaR
CCT1081C	CG1056	5-HT2A	CCT1176C	CG3171	Tre1
CCT1082C	CG42796	5HT2B	CCT1177C	CG7431	TyrR
CCT1083C	CG9753	AdoR	CCT1179C	CG8394	vGAT
CCT1084C	CG18208	Octα2R	CCT1183C	CG5621	Grik
CCT1085C	CG18741	DopR2	CCT1186C	CG8681	clumsy
CCT1086C	CG32476	mthl14	CCT1189C	CG12344	CG12344

Table S2 cCCT knockin strategy can't rescue all knockout phenotype

CG No.	Gene Symbol	attP KO phenotype	cCCT phenotype
CG15520	Capa	lethal	viable
CG12345	ChAT	lethal	viable
CG5400	Eh	lethal	viable
CG5911	ETHR	lethal	viable
CG10537	Rdl	lethal	viable
CG14575	CapaR	lethal	lethal
CG14994	gad1	lethal	lethal
CG18039	GluRIID	lethal	lethal
CG33976	Octβ2R	sterile	fertile
Rescue Rate		6/9	

Table S3 C-cCCTomics sgRNAs list

CCTsgEF No.	CG No.	Spacer + PAM	CCTsgEF No.	CG No.	Spacer + PAM
CCT1001sgEF	CG1171	GGCCAGCAGCATGAAGAGCACGG	CCT1108sgEF	CG32447	GATGGCCCCCAAACTAGCGCAGG
CCT1001sgEF	CG1171	TTGACCTTCTCGCCGGATTGGGG	CCT1108sgEF	CG32447	TGGGTGGACACTATACTGGGCGG
CCT1001sgEF	CG1171	TGCAATGAGGACTTCGCTCTTGG	CCT1108sgEF	CG32447	CACGCCCCGTCGGAGTTCAGGGG
CCT1002sgEF	CG11325	GTATCTGTCCAGCTACGTGATGG	CCT1109sgEF	CG33639	TCCCTCAGCGATTCCGTCCGCGG
CCT1002sgEF	CG11325	ACACGGTGATGGACAATCGGTGG	CCT1109sgEF	CG33639	GCCCAGATAAAGCTCCAGGTGGG
CCT1002sgEF	CG11325	CTTGGTCAGCAGATACAGCACGG	CCT1109sgEF	CG33639	CCGTCTTCAGCAGCGACCTGAGG
CCT1003sgEF	CG14375	ACTGGTCGTTATCTGCACCGTGG	CCT1110sgEF	CG33696	TGTATTGTATTCCGTGACATTGG
CCT1003sgEF	CG14375	TTTCGCTTGGCTCTGTTGCGCGG	CCT1110sgEF	CG33696	CTGCTCCGTCTGGTTTGTGGTGG
CCT1003sgEF	CG14375	TCAGAGGGATGCCAGGCCTACGG	CCT1110sgEF	CG33696	AGTGAGCGACACCTGCTTCCTGG
CCT1004sgEF	CG14593	ACGGTGACAATGTACGTCTCCGG	CCT1111sgEF	CG34411	GCCGGAACACTTCTTCCCCGAGG
CCT1004sgEF	CG14593	GCCGTCGCTATCCGCCAGCCTGG	CCT1111sgEF	CG34411	ACTGTGCCGTTGTATTGCAGTGG
CCT1004sgEF	CG14593	CTCCTGCTCCAGACCTTGTCCGG	CCT1111sgEF	CG34411	CTAAGCTCTCTGCTCCTAACGGG
CCT1005sgEF	CG4313	GATGCACGGCACCATGAAGGCGG	CCT1113sgEF	CG43795	GGAGAGCTCATTCGTGACGGCGG
CCT1005sgEF	CG4313	GATCAGGAAAAGGTCAGCCTGGG	CCT1113sgEF	CG43795	AATGCGACCGAGAGCGCCCGTGG
CCT1005sgEF	CG4313	GATCGCAGGACGACCCTTTGTGG	CCT1113sgEF	CG43795	GGAACCTGTCCTGAGCATACCGG
CCT1006sgEF	CG6371	AGCAGGTAATAGGTCAGTGGCGG	CCT1114sgEF	CG44153	GGTATGCTAAAGGCACGCCATGG
CCT1006sgEF	CG6371	GGCACGTCAAAAGCGCGCCATGG	CCT1114sgEF	CG44153	CCTCGGTGAGCGTGAAGACGCGG
CCT1006sgEF	CG6371	TTGCACACTGCTGCTAATCGCGG	CCT1114sgEF	CG44153	CGAAATAAACGAGACTACGCAGG
CCT1007sgEF	CG6936	GCCATCAATTACCGGTCAGACGG	CCT1115sgEF	CG7497	TTTGCATAGAGCGCTTTCGGAGG
CCT1007sgEF	CG6936	GACCTACCGATGCCGTGTGACGG	CCT1115sgEF	CG7497	ATGCATTGCAGCAGTTATGGCGG
CCT1007sgEF	CG6936	TATCCATGATATGGTCGTGAGGG	CCT1115sgEF	CG7497	CCACTCGGATGAACGACTGCAGG
CCT1008sgEF	CG31147	AATGAATAGTGTCTCTCGCAGGG	CCT1116sgEF	CG8216	GTTTGCGTCAGCACATACGGCGG
CCT1008sgEF	CG31147	GCAAACTGAAGACATGCATCCGG	CCT1116sgEF	CG8216	GATGCGGACGCCGCGAGCGAGGG
CCT1008sgEF	CG31147	TAGTTCTTACCGGTACTTGTCGG	CCT1116sgEF	CG8216	CTGGGCCTTGACGAATACCTGGG
CCT1009sgEF	CG17084	GCTCCACGTGAGTGGACTCGCGG	CCT1117sgEF	CG12345	AGGCAGTTCTCGGCTCCCCAGGG
CCT1009sgEF	CG17084	TGAGTATTGCTTTAGCCCGTTGG	CCT1117sgEF	CG12345	GGCCGACTATATCCGCGCCCTGG
CCT1009sgEF	CG17084	CACTACTCCAGCGTATGAGTAGG	CCT1117sgEF	CG12345	TTGAACAGGCCTATTACTACTGG
CCT1010sgEF	CG6496	GTTGCGCTTCCTGATGGGCACGG	CCT1118sgEF	CG13936	GATTGGACCGGGAGACGCCATGG
CCT1010sgEF	CG6496	CCTCGACTGGTTCAACAACGTGG	CCT1118sgEF	CG13936	GAGCAACAGATCCCTCAGCGAGG
CCT1010sgEF	CG6496	TGGCGCCGCAGTATCCCCACTGG	CCT1118sgEF	CG13936	CACAGGCTCGGCGATAATGGAGG
CCT1011sgEF	CG8784	GTATTAAGTCGGAAACCGCCAGG	CCT1119sgEF	CG8380	GACGAGCGCGAAACATGGAGCGG
CCT1011sgEF	CG8784	GATACATATCCGGATACCAAAGG	CCT1119sgEF	CG8380	CTTACGATTGTGCTGACCCAGGG
CCT1011sgEF	CG8784	GCTCGCATTTGTGCCGTTCGTGG	CCT1119sgEF	CG8380	GGTGCTGATAGCCTTCTATGTGG
CCT1012sgEF	CG13687	GAGTCTGGAACACCGCGCGGAGG	CCT1120sgEF	CG9887	CACGAAGAGATGCAGCGTGGCGG
CCT1012sgEF	CG13687	GCCATTGCCATAATGGAAATGGG	CCT1120sgEF	CG9887	TCTGACGGCGTTTAAGGAGAAGG
CCT1012sgEF	CG13687	GTACATGGGCGGCAGCTGATGGG	CCT1120sgEF	CG9887	TCATGATCGCCTTCGGCATGAGG
CCT1013sgEF	CG14734	GCTGACGGCACCATCGAGTGCGG	CCT1121sgEF	CG5400	GTGCGTATAATGACTTATGGCGG
CCT1013sgEF	CG14734	CATCCAATGCGCCCTCTGAGCGG	CCT1121sgEF	CG5400	TTTCTTGCAGACTCCATGGGTGG
CCT1013sgEF	CG14734	GCCCGCTTTACCACCCGACGCGG	CCT1121sgEF	CG5400	CTTGATTTTGTGCACCTTTGTGG
CCT1014sgEF	CG6515	ATTGTGAACACCACGCTCCTGGG	CCT1122sgEF	CG18105	TGCTCACTGCGTCCTATGCGAGG
CCT1014sgEF	CG6515	CAACGTCACGGTCTCTACGTCGG	CCT1122sgEF	CG18105	ACCAAGAACGTACCGCGGCTGGG
CCT1014sgEF	CG6515	CAAGACCGTACGAGTTGCCATGG	CCT1122sgEF	CG18105	CTGTCTGTTTCGCTCTTGGTGGG

CCT1015sgEF	CG7887	ATGGTCATTGTGGCGACGGGCGG	CCT1123sgEF	CG5911	GACTATGCAGAAGAACATGGCGG
CCT1015sgEF	CG7887	GTCTTCCACGTCCCCGACGGCGG	CCT1123sgEF	CG5911	CACGCCCACCGTCCTCGTGGAGG
CCT1015sgEF	CG7887	GTTGAAGGTGACGTTCAGGCTGG	CCT1123sgEF	CG5911	CATCTCGTGGCCAAGTACCCAGG
CCT1016sgEF	CG13633	GACGAGATGGCCGACAACGGTGG	CCT1124sgEF	CG2346	ACTTCATGCACTTCGGCAAGAGG
CCT1016sgEF	CG13633	GCAGTAGGAGGTGGGCGTGAAGG	CCT1124sgEF	CG2346	CGATGCCAATCACAGAGATGGGG
CCT1016sgEF	CG13633	CAGCTCCCCGGTAATTGGCCAGG	CCT1124sgEF	CG2346	GGCCGACTGCATCTGGTACAGGG
CCT1017sgEF	CG2872	CGAATGATCCGTGTGTTCCGAGG	CCT1125sgEF	CG2114	AATCGTCCTTAACCACACGGAGG
CCT1017sgEF	CG2872	GACGAACAGAATGTCCGAGACGG	CCT1125sgEF	CG2114	AGAACAATCGCATTGAGTTCTGG
CCT1017sgEF	CG2872	TTGTGGATACGATCCGTTCGAGG	CCT1125sgEF	CG2114	TGGATTGGCCCGCTGTGATACGG
CCT1018sgEF	CG10001	ACTGGCCATATGGAAGGTTCTGG	CCT1126sgEF	CG15274	GGATCTCGAGAATCGATGCATGG
CCT1018sgEF	CG10001	GATTACGAACATCAGATCAGCGG	CCT1126sgEF	CG15274	GCCTGCCGCAAGACTGGCGTTGG
CCT1018sgEF	CG10001	AAGAAGAATCCCACTATCCACGG	CCT1126sgEF	CG15274	TGCAGGATGAGCTTGAAGCCCGG
CCT1019sgEF	CG3302	TCTTGCCGTTGGTCCATCCGCGG	CCT1127sgEF	CG6706	GGCGTGGAAAACTCCTACACCGG
CCT1019sgEF	CG3302	GAAGGTCTGGCCCATGCACATGG	CCT1127sgEF	CG6706	GAAGGACGTGAGGATCATTCTGG
CCT1019sgEF	CG3302	CCATCCGCGGGAGTACTGGAAGG	CCT1127sgEF	CG6706	TCTACGTAATACATCCTTCGAGG
CCT1020sgEF	CG10698	CTCCCCGATAATGCAGAACCAGG	CCT1128sgEF	CG14994	CGAGTAATGGCACTGATCCGAGG
CCT1020sgEF	CG10698	TGGTGCTTCATGGCGACTATTGG	CCT1128sgEF	CG14994	ACGGGTATAAACTGTCCGAGAGG
CCT1020sgEF	CG10698	GGTCAGCAATTGGTCCACACTGG	CCT1128sgEF	CG14994	GCTTCATGTCCTCGGGATGGTGG
CCT1021sgEF	CG2902	AATGGTGACCGAATCTACGCCGG	CCT1129sgEF	CG8442	GCCAAAGCCAGAACGCAGGGGGG
CCT1021sgEF	CG2902	ACGAGAGTACTCGATCGTGACGG	CCT1129sgEF	CG8442	GTACACCTACGGAGAATCATTGG
CCT1021sgEF	CG2902	GAATCCGCTTGTATAACTCACGG	CCT1129sgEF	CG8442	ATCGATACCATCCAGTACTACGG
CCT1022sgEF	CG33513	GGACGGGGACCTGCGCTCGGCGG	CCT1130sgEF	CG43743	ATTCGTCCGGATACAGACCTCGG
CCT1022sgEF	CG33513	CACTGTTAACAAGCTCCATGAGG	CCT1130sgEF	CG43743	GCCGTGCAGCTTCTCACCAAAGG
CCT1022sgEF	CG33513	GGAGGCCTACCTAACGGATCCGG	CCT1130sgEF	CG43743	GGGGAACCAGGGCGTCACGAAGG
CCT1023sgEF	CG42301	AGCTGTAACCGTCAGGACACCGG	CCT1131sgEF	CG6992	AAGCTTGCTAATGAGATCCACGG
CCT1023sgEF	CG42301	GCTCGGCGTATTCTGCATGCCGG	CCT1131sgEF	CG6992	TCTGCACTACAAGAGTCCTCCGG
CCT1023sgEF	CG42301	CTTAGGTCGGGATTGAGTGTCGG	CCT1131sgEF	CG6992	ACGCGAGAGTACTGACAAGGAGG
CCT1024sgEF	CG32540	GTAGTCGAGCAGTGCCCTATAGG	CCT1132sgEF	CG7234	CCTTAATCCGTATAATGCCGAGG
CCT1024sgEF	CG32540	TGGACTTGAACTGGTGCCCAGGG	CCT1132sgEF	CG7234	GCATCCCCAGCAGTCGAACAGGG
CCT1024sgEF	CG32540	GAGCAGGAACACGTTGGTTATGG	CCT1132sgEF	CG7234	AGTCATATTATATCCAATCGAGG
CCT1025sgEF	CG33517	CTACAATGGGAGCACGGTTTCGG	CCT1133sgEF	CG4226	GCTGCGTTATCTGACCCCGAGGG
CCT1025sgEF	CG33517	ACGGTGGCGCGCGAGACGCTGGG	CCT1133sgEF	CG4226	CCTCTATCAAGGATATGCCGTGG
CCT1025sgEF	CG33517	AGCACAAACTTGGCGGTGACGGG	CCT1133sgEF	CG4226	AATGACCCTTAACCTCTACCCGG
CCT1026sgEF	CG13094	GGGATATTCGGGTACCCAGGAGG	CCT1134sgEF	CG18039	GATCACCTAATGACCCGATACGG
CCT1026sgEF	CG13094	CTTGGCCATCTCGAGCATCGAGG	CCT1134sgEF	CG18039	GGATGCAGATTGAAACCATCCGG
CCT1026sgEF	CG13094	GCTTTGGACGCACCATCATACGG	CCT1134sgEF	CG18039	GTCATTGCCACCGTCGCGGAAGG
CCT1027sgEF	CG32843	GAGGTCTTCGAGATTTACGCAGG	CCT1135sgEF	CG31201	GAGTGTTTGGACCCTCGTCGCGG
CCT1027sgEF	CG32843	GTCCGGGCAGAGTTCGTAGGCGG	CCT1135sgEF	CG31201	CCGGCGGGTTCGAAAGTCCGTGG
CCT1027sgEF	CG32843	TCGCTGCCAATAACTCGTTGTGG	CCT1135sgEF	CG31201	TCGCATGTAATTCTTGAAGGAGG
CCT1028sgEF	CG18090	GACTAGTCTACAGAACGCTAAGG	CCT1136sgEF	CG14723	GATTTGCGTGTCATGCGGATAGG
CCT1028sgEF	CG18090	CATTCTCTCTATTCGGGGACAGG	CCT1136sgEF	CG14723	CCAGGGAGAGGACCGTGACATGG
CCT1028sgEF	CG18090	CACGCTGTTTATGCCACTCTGGG	CCT1136sgEF	CG14723	GGCAATATATTTGCACGCGCTGG
CCT1029sgEF	CG6440	CAGTTGATCGGAGTTCTCCAGGG	CCT1137sgEF	CG13586	CCGACTGGACCGCATCTGCGAGG
CCT1029sgEF	CG6440	TCCTGGCCGTGTCCAACACACGG	CCT1137sgEF	CG13586	TTCTTCGACCTGGAGTGCAAGGG

CCT1029sgEF	CG6440	GCTTGTTGTAGTTCTTCAACAGG	CCT1137sgEF	CG13586	CCACCGAGATCTTTATGTTGCGG
CCT1030sgEF	CG43745	ATGCCGGTGCCGCAATAATGCGG	CCT1138sgEF	CG7665	CGATGTCTACCCCAATCTCACGG
CCT1030sgEF	CG43745	GGCAGTTTGGCGGTACATAGCGG	CCT1138sgEF	CG7665	CTGCTGCTAACGTCGCTGAGTGG
CCT1030sgEF	CG43745	CTCGCGGCAGCCTTACACTGAGG	CCT1138sgEF	CG7665	AGCACCCGAGTCTGTCCCAGCGG
CCT1031sgEF	CG8348	GTTCCATCCGGGTAGTCCAGAGG	CCT1139sgEF	CG31096	GTGACCTCCGAACTGAGACGCGG
CCT1031sgEF	CG8348	GCTGTCCATTGTCAATCCGCTGG	CCT1139sgEF	CG31096	GGTCATCAGACAGAAGCCTACGG
CCT1031sgEF	CG8348	GGCCGTGCAGACGAGCCTTGTGG	CCT1139sgEF	CG31096	TAGAGGAGACCGCACTCCACCGG
CCT1032sgEF	CG8422	CTGCACAACCTAGATGGCATCGG	CCT1140sgEF	CG7918	TGTATCATTCTTACGGTGGGCGG
CCT1032sgEF	CG8422	GCCACTATCGTTGCCATAGGTGG	CCT1140sgEF	CG7918	CAAGCGAGTCCTGACGCACACGG
CCT1032sgEF	CG8422	AGGGTACCGCGAGCTGTCCTCGG	CCT1140sgEF	CG7918	GCTCAAGGGTTATTGGGACCTGG
CCT1033sgEF	CG12370	GCTGTTGACACTGTAGCGTGCGG	CCT1141sgEF	CG11144	GTTGAGGCCGGTGATACTTGAGG
CCT1033sgEF	CG12370	AGACGACGATTTGAGGGCACTGG	CCT1141sgEF	CG11144	GCGACCAAACGACTGAGACAAGG
CCT1033sgEF	CG12370	TAGTGATCCCACGTTCCGTTTGG	CCT1141sgEF	CG11144	CAAAAGAAGCCTAACGCTCGCGG
CCT1034sgEF	CG13480	CAGCGATTCCACTCGTGGGGCGG	CCT1142sgEF	CG4322	TATCCAATACGGAAACATAGGGG
CCT1034sgEF	CG13480	GGCTGGCTCCATAGACTTGACGG	CCT1142sgEF	CG4322	GGCCCTGCTGAAATGTCCCAAGG
CCT1034sgEF	CG13480	GGTGGGGCGTAGTGCCGGAAGGG	CCT1142sgEF	CG4322	GGAGGACGGCTATCCCCCCCTGG
CCT1035sgEF	CG10626	GGAATTCCTGCCCGGAGCCGAGG	CCT1143sgEF	CG8985	GATATTCAAGGTATTCGCGATGG
CCT1035sgEF	CG10626	TACACTCAGGGCCTGGACGAAGG	CCT1143sgEF	CG8985	GAAACTGAGCCGCTCTACTGCGG
CCT1035sgEF	CG10626	CTATGGGGGAATCAGTATCGTGG	CCT1143sgEF	CG8985	GATGTAGTCGTGTATGGTGTAGG
CCT1036sgEF	CG4128	GTGCTCTTGAAGATACCAGGGGG	CCT1144sgEF	CG17061	GCACAGCGAGGAGTAACCCACGG
CCT1036sgEF	CG4128	CAATACGCTGGAGCGACCCGTGG	CCT1144sgEF	CG17061	CCTGGAGGATCCCTATACTGCGG
CCT1036sgEF	CG4128	AACGGAATACGGCGGGGTCAAGG	CCT1144sgEF	CG17061	GAACGGATCCATGCTCCGTGTGG
CCT1037sgEF	CG33976	GCCCGGAGCCACCGCGGCAAAGG	CCT1145sgEF	CG32853	GCTGACGGATCCAACTTTAGCGG
CCT1037sgEF	CG33976	AACATTGGCGCGGGTCACGGCGG	CCT1145sgEF	CG32853	TCTTTATCCCGAAATCTACTCGG
CCT1037sgEF	CG33976	CAACATCGTTTGGGTGTTCAAGG	CCT1145sgEF	CG32853	GAAATTCCTGCCAACCTGACCGG
CCT1038sgEF	CG13758	TCTACGCCATGAAAGCCGCCAGG	CCT1147sgEF	CG30018	ACTCGATGATAATTCGACAGAGG
CCT1038sgEF	CG13758	GCATCGAAATCGTGCAGTAGTGG	CCT1147sgEF	CG30018	CTTGTGTGATATAATCCATATGG
CCT1038sgEF	CG13758	GACGCAAGCGTTAGATTCCAGGG	CCT1147sgEF	CG30018	TATGGATGAACTACGATTGTTGG
CCT1039sgEF	CG14358	GCTCATGGCAAGCGGTCCGGCGG	CCT1148sgEF	CG17795	GATACCGTTGATATCTCGGAAGG
CCT1039sgEF	CG14358	GAATACGGACATTCGTGTTGGGG	CCT1148sgEF	CG17795	GGTGCAAAGGCACTATAAGAAGG
CCT1039sgEF	CG14358	TCAGGTTCCTGCCTGGAATACGG	CCT1148sgEF	CG17795	TCATTAGCTTCTTAACGCACAGG
CCT1040sgEF	CG30106	GAGACACCCTACGTGCCCTACGG	CCT1149sgEF	CG6536	GTGATTGCAGTCATGATTAGCGG
CCT1040sgEF	CG30106	CATCCTTCATGAACTCCGACAGG	CCT1149sgEF	CG6536	GCATACAACTTATACGCCTGGGG
CCT1040sgEF	CG30106	TTCGCATCTGTCGCACACTGAGG	CCT1149sgEF	CG6536	GACTAAACTTAATCCGCAAGTGG
CCT1041sgEF	CG13575	GCTCGAGTTGTACCTAGAATGGG	CCT1150sgEF	CG6965	CCGATGTTCACCAGCTATGGAGG
CCT1041sgEF	CG13575	CCAGTGAGATGAGGCAGGCCCGG	CCT1150sgEF	CG6965	ACCAGTCATGTCACTAGCGCCGG
CCT1041sgEF	CG13575	CCCTCGATCCAGCCGTATCCGGG	CCT1150sgEF	CG6965	TGGCCAATATACCACTATGCTGG
CCT1042sgEF	CG13995	TCTAGGCAATCCGTATGACGTGG	CCT1151sgEF	CG16992	GAATTCGGATCTTCCAAACGGGG
CCT1042sgEF	CG13995	TTGCCATAGTCGTAGTCCGCGGG	CCT1151sgEF	CG16992	GATTAGCTCCTCGTACGCATAGG
CCT1042sgEF	CG13995	GAGGGCGAGATGCAGCTCCGCGG	CCT1151sgEF	CG16992	GAAGGTTGTTTCGGTACAGGAGG
CCT1043sgEF	CG33495	CTAAACTTAGGACCCTACCTCGG	CCT1152sgEF	CG7476	TGAGTGGTACTCGTGCCTGTAGG
CCT1043sgEF	CG33495	AGGATCGAAATGATACGGAGTGG	CCT1152sgEF	CG7476	CTAAGGATCCAGGAGATATGTGG
CCT1043sgEF	CG33495	ACGACCAAGAGGAGAAATAGCGG	CCT1152sgEF	CG7476	GTGTCGTAGTAGTTGCACCCGGG
CCT1044sgEF	CG31720	GGTTCCATCGATCTTGCAATAGG	CCT1153sgEF	CG32475	GCAAACATAACGGGGAGCTACGG

CCT1044sgEF	CG31720	TACGAATACTCAGTACTGCGTGG	CCT1153sgEF	CG32475	GAGGCAGTGCTTAGTCCCTGTGG
CCT1044sgEF	CG31720	AAACGTAAATAAATCCCTGTGGG	CCT1153sgEF	CG32475	GATGGTCTACCTTATGTGTTCGG
CCT1045sgEF	CG30361	ATGCACCGCGACCTGTGCGGCGG	CCT1154sgEF	CG12414	ACATCTGTCGTATTAACAACAGG
CCT1045sgEF	CG30361	AGTACACCGAGGGCGAGCTGCGG	CCT1154sgEF	CG12414	AATATAATAATACCGTGCATGGG
CCT1045sgEF	CG30361	CATCCACTTCAAGCAGTCCCAGG	CCT1154sgEF	CG12414	TTGGCAGTTGGACTTATGATGGG
CCT1046sgEF	CG10342	GCCGGCGGCTAGGAGGGCAAGGG	CCT1155sgEF	CG32975	CGTGCTGATGTACAACAGTGCGG
CCT1046sgEF	CG10342	TTGACATCGTTCTTTCGCGGAGG	CCT1155sgEF	CG32975	AATACTGAACTCATTGTCGCTGG
CCT1046sgEF	CG10342	GACAGAGCCCGCGTTCGGTTCGG	CCT1155sgEF	CG32975	GTCATTGCTTCTACCGTGGTTGG
CCT1047sgEF	CG1147	TGGACCCGGTGCTTATCGATAGG	CCT1156sgEF	CG32538	ATCTCGTTCTATCCTGACCAGGG
CCT1047sgEF	CG1147	GCTGATGAGCATGTGGTACCAGG	CCT1156sgEF	CG32538	TTGGTTCGTGGACCTACGATGGG
CCT1047sgEF	CG1147	GCGTGCGCTATCTGGACGACCGG	CCT1156sgEF	CG32538	TGGAGTAGCCGCTTCTCATGGGG
CCT1048sgEF	CG13061	AGAGGAGATCCGACAACGGTGGG	CCT1157sgEF	CG11822	GGACGCGGGTGTGTAGATGACGG
CCT1048sgEF	CG13061	CAGAGGAGAAGGATGCACCTGGG	CCT1157sgEF	CG11822	GATCGGCTCCTGGGGCCTGAAGG
CCT1048sgEF	CG13061	GATCAAGAGCGTCCATGGCCTGG	CCT1157sgEF	CG11822	AGTTCGTGAACAGGCCGGCGTGG
CCT1049sgEF	CG8795	GGTGTCATCGGGGTCACCGTGGG	CCT1158sgEF	CG34388	AGGCGGCCTTGAGCCACCAACGG
CCT1049sgEF	CG8795	AAATCATGTCGGATATAGCGAGG	CCT1158sgEF	CG34388	GGAGGAGCTGGCCCCAGAATCGG
CCT1049sgEF	CG8795	GGAGAGCGTTCTCTCGGAAACGG	CCT1158sgEF	CG34388	GCTGGCCCCAATACCGATGAGGG
CCT1050sgEF	CG16752	GATCCGCGTCAGATGGTCCGCGG	CCT1159sgEF	CG3441	GCACTCACAATAATGGACCGTGG
CCT1050sgEF	CG16752	GGCATACAGTAGCCATAGAGCGG	CCT1159sgEF	CG3441	GGAGGAGGACAAACGTTCGGTGG
CCT1050sgEF	CG16752	GCTCAAAACGAGCACAATCAGGG	CCT1159sgEF	CG3441	GAAGCTGGTACTCGGGACTGGGG
CCT1051sgEF	CG14871	TTATGGCCTGCGAACTGGGGGGG	CCT1160sgEF	CG11051	GAATTCGTTGAAATCACCCTGGG
CCT1051sgEF	CG14871	GTAGTTAAAGCAGCATGTGCTGG	CCT1160sgEF	CG11051	CAGGATTGGATTCCTCACGGGGG
CCT1051sgEF	CG14871	TGACTAAGACAACGATGCATTGG	CCT1160sgEF	CG11051	GTCCGCCCGCGTCCCCCGTGAGG
CCT1052sgEF	CG34381	TCCGTCCCCCGAGAGTCCGGTGG	CCT1161sgEF	CG15361	GATTGGGGCGGGATTGGCACGGG
CCT1052sgEF	CG34381	CCACCGGACAACAACCGCCCCGG	CCT1161sgEF	CG15361	CTAGCTCCGTAGTAGTACTGGGG
CCT1052sgEF	CG34381	AGTGGACAAACTGGTACATGCGG	CCT1161sgEF	CG15361	AGCAAACAACATGTTCAAGCTGG
CCT1053sgEF	CG16720	GGAGCGGAATCTACAAAACGTGG	CCT1162sgEF	CG3856	GATGAACTCGAGTACGGCCAGGG
CCT1053sgEF	CG16720	GGCCACCAGATGCAAAATCGAGG	CCT1162sgEF	CG3856	GGCCAAACCCACCAGAAGATCGG
CCT1053sgEF	CG16720	TGGTCCTGACCATCTACATTCGG	CCT1162sgEF	CG3856	TCTCTGGTGCCGCATTTGGCTGG
CCT1054sgEF	CG15113	TGGTCGATGACGAACAAGAGCGG	CCT1163sgEF	CG7485	GGCGGCGGCTCTAACCGCTGCGG
CCT1054sgEF	CG15113	TCTATTTCCAAAATGCTCGCTGG	CCT1163sgEF	CG7485	ACTCAATGCCGCGGTAACGGTGG
CCT1054sgEF	CG15113	AATGGCCACCAGGTGCAGTATGG	CCT1163sgEF	CG7485	CAACGTGGCTTACTCGATCCTGG
CCT1055sgEF	CG12073	CAGCTGGATAGCCTATGCGGCGG	CCT1164sgEF	CG13565	GCGTTAAGAGAATTGTGTAACGG
CCT1055sgEF	CG12073	GCAAATTCCTCCAGGAGCAAAGG	CCT1164sgEF	CG13565	GGAACACCGATACCACCGCCAGG
CCT1055sgEF	CG12073	TCCGTCTCGCCTTCCACGAGCGG	CCT1164sgEF	CG13565	CATTCACGCAGCGCCCGGTGTGG
CCT1056sgEF	CG14919	GGTCCTGTTTCGGCACCCGAAGG	CCT1165sgEF	CG15284	GAACTGCGAGACTCTCAAGTCGG
CCT1056sgEF	CG14919	CCTCGCTGAGGGCAAAGAACAGG	CCT1165sgEF	CG15284	AGGGCATTGCGATATAGCCAAGG
CCT1056sgEF	CG14919	GACGTGCGAGGCGCCTATGGAGG	CCT1165sgEF	CG15284	GCATTGGGGCACTAGGATCGCGG
CCT1057sgEF	CG14575	TCCTCTCCAAATCCATGGGATGG	CCT1166sgEF	CG31660	CGATGAGCCGACACGTGCGGAGG
CCT1057sgEF	CG14575	GGTCTGTGGTCCAAGCACAAAGG	CCT1166sgEF	CG31660	TGTGTCCGCTCTCAGTCGGGCGG
CCT1057sgEF	CG14575	TAAGAGATTACCAACGACCCCGG	CCT1166sgEF	CG31660	CAACATTATCCGAATCCACTAGG
CCT1058sgEF	CG33344	TGCGATATCACACGTGATGCTGG	CCT1167sgEF	CG7105	GCTGTGGAAGTGGACACAGGTGG
CCT1058sgEF	CG33344	GGACGCCAGCCCCGAGGATTCGG	CCT1167sgEF	CG7105	GCGACCTTGTCGGCAGGTAACGG
CCT1058sgEF	CG33344	GTCAAATTCGCCGGGGTCGCTGG	CCT1167sgEF	CG7105	CTCCACAATGAGGCCACCGGTGG

CCT1059sgEF	CG13579	GTATGTAGGCCGCATAGCGGCGG	CCT1168sgEF	CG6986	AGTCCAATAACAAAAACGCACGG
CCT1059sgEF	CG13579	GGAAAGCGCCCCTCGGAGCAGGG	CCT1168sgEF	CG6986	GTAGAGCTTGAAATGATACTTGG
CCT1059sgEF	CG13579	TGACAGAAGATCTCTCCGTATGG	CCT1168sgEF	CG6986	GATTAACTGGCACGTCAGGTAGG
CCT1060sgEF	CG31760	GATAGGGCTCCGCCTCGCATTGG	CCT1169sgEF	CG10537	GGTGTAGAAACACTATCGGTTGG
CCT1060sgEF	CG31760	GCCCACTTCCTGGAGTATCGAGG	CCT1169sgEF	CG10537	ACGGATCCATACAGTGCAAGCGG
CCT1060sgEF	CG31760	GTCCTACGTCTGGTGGGTCAAGG	CCT1169sgEF	CG10537	TTTGTCGTAACTAACACTAAAGG
CCT1061sgEF	CG32547	GTAGGGCGAGAGCTGCGTACTGG	CCT1170sgEF	CG8930	GAAAACCTCCCAGGTCCAGGAGG
CCT1061sgEF	CG32547	GTTGACATGGAGCGACTTAGTGG	CCT1170sgEF	CG8930	AAGTCCTTGCAGGAATACCATGG
CCT1061sgEF	CG32547	CAGATTGATGATGAACGCATGGG	CCT1170sgEF	CG8930	GCGCAGGGTAGAAAAGGTCCTGG
CCT1062sgEF	CG18314	GCAGGAAATGAGCTACCTACAGG	CCT1171sgEF	CG40733	AGAAAGAAATGCTCGTTTCGAGG
CCT1062sgEF	CG18314	GTAGTAGTTGATCACCTCTGTGG	CCT1171sgEF	CG40733	TTCTTTCTTGGCTCTCGGTACGG
CCT1062sgEF	CG18314	TATCGGTATACACCTTCATGTGG	CCT1171sgEF	CG40733	AGGTACGATGAAAATGCGTCTGG
CCT1063sgEF	CG9652	GGATGTTTCCGGCCACCGAAAGG	CCT1172sgEF	CG5811	CGACTATGACCTTCTATCGGAGG
CCT1063sgEF	CG9652	AATCACACCAGTGGGAGCACCGG	CCT1172sgEF	CG5811	GACCGTGCGCATGCGAGGTGTGG
CCT1063sgEF	CG9652	CGTCGAGCACATGACATCAAAGG	CCT1172sgEF	CG5811	GACGATGAAGGGTCCAACTATGG
CCT1064sgEF	CG3022	ATACGGTCCATGGCCGGCCGTGG	CCT1173sgEF	CG4545	GAGAGGACTCGCGAGACCTGGGG
CCT1064sgEF	CG3022	CGTCCGTTTGTACTTCCAATCGG	CCT1173sgEF	CG4545	GGGATTCGAGCGGCCCGTCGTGG
CCT1064sgEF	CG3022	GGCCCTTGCCTGGGCAACGTCGG	CCT1173sgEF	CG4545	TGGACTGCCCCTGTTCTACATGG
CCT1065sgEF	CG3454	CTATATGCGCCAGTTACTGCCGG	CCT1174sgEF	CG33527	AAGATGCTGCCGTTGAACGGAGG
CCT1065sgEF	CG3454	GACAGTACTCACCCCTTTGGCGG	CCT1174sgEF	CG33527	GCTCCAGTGAGGCAGCCTACAGG
CCT1065sgEF	CG3454	GCAGGCCGGCGAGCTCGCCCAGG	CCT1174sgEF	CG33527	CTGCGACCAGGATCGTGACCAGG
CCT1066sgEF	CG4395	TGACTCAGCACAGTGCCGGCCGG	CCT1175sgEF	CG10823	GCTGGGCACGGTTCTCACTACGG
CCT1066sgEF	CG4395	GCGGCATTCTCCAGATATCGCGG	CCT1175sgEF	CG10823	CCATTCCGACCATGGCGCCGGGG
CCT1066sgEF	CG4395	CCAGAATGTCACATACGATACGG	CCT1175sgEF	CG10823	GTAGGCCACGCAGTAGACCATGG
CCT1067sgEF	CG4356	CGGGCTATACGATCCCTATTCGG	CCT1176sgEF	CG3171	ATGCGGGTAGATCGATTGCGTGG
CCT1067sgEF	CG4356	GCCAATGCCAGACTCATGACCGG	CCT1176sgEF	CG3171	ACATTGCCATAGAAGATCACCGG
CCT1067sgEF	CG4356	AGCCAGGTGTCGCAGACGATGGG	CCT1176sgEF	CG3171	GCTCAAGAGCCCCACGATACGGG
CCT1068sgEF	CG6456	CTATGGCTCACACTAAGACGCGG	CCT1177sgEF	CG7431	GTAGGAGGTGGATATCCCAGCGG
CCT1068sgEF	CG6456	CCACCCTCTAATGAACCAGGAGG	CCT1177sgEF	CG7431	GTAGAAGTGCGCCCATTCGGCGG
CCT1068sgEF	CG6456	ACGGCAACAATAAGCGCGCCTGG	CCT1177sgEF	CG7431	GAAGATGCCCACGAGAAGGTCGG
CCT1069sgEF	CG4521	GGATCCTCCAGAGCATTGATCGG	CCT1178sgEF	CG16766	GGCGTGTGGTCAGAACGGCGAGG
CCT1069sgEF	CG4521	GCATGGTGATAGCAAGCGTATGG	CCT1178sgEF	CG16766	CAGACCAGTGCGGCACCAGGTGG
CCT1069sgEF	CG4521	GGCAGCTATCAGACTAGCTACGG	CCT1178sgEF	CG16766	GGATGGAGCCGCTGCAGAGCAGG
CCT1070sgEF	CG6530	GCCGCTAAATGAATTCCAGAGGG	CCT1179sgEF	CG8394	CATTCCGGAACGCCGGTAGCTGG
CCT1070sgEF	CG6530	GAAATATCCCAGGAACAAGGAGG	CCT1179sgEF	CG8394	AAAGACTACGAGCAACCGCCGGG
CCT1070sgEF	CG6530	CATTTAGCGGCAACTCCAGCTGG	CCT1179sgEF	CG8394	CCTTCAATGAGTACGACGGCAGG
CCT1071sgEF	CG5610	GCAGAAGGATTTGTAAATGGCGG	CCT1180sgEF	CG3822	GCGAGGTCACCAGGTAGCTATGG
CCT1071sgEF	CG5610	GACCGTCTCACCGTCAAGATGGG	CCT1180sgEF	CG3822	GGACATTGTCGAGCTCACTCCGG
CCT1071sgEF	CG5610	ACTACTACATCTCCGTGGAGTGG	CCT1180sgEF	CG3822	TCCCCACTTGGAGAATCGCTGGG
CCT1072sgEF	CG6844	GTGACGCCGCCATACTCCGAGGG	CCT1182sgEF	CG5549	ATAGACGGCCACGGGACCCAGGG
CCT1072sgEF	CG6844	GGATACGGTTCGGCACAGCAGGG	CCT1182sgEF	CG5549	TCGCTGCTCGGATACTCAGTGGG
CCT1072sgEF	CG6844	TCGCCTGAACGGTTTCGCAGAGG	CCT1182sgEF	CG5549	AGGCGTGGTCTGCCCCTCTACGG
CCT1073sgEF	CG2302	GAGCTCCTGCGAAATCGACGTGG	CCT1183sgEF	CG5621	GATGCTCATCGCGTGACGGGCGG
CCT1073sgEF	CG2302	GTCCGGACGCCAGATGTGATCGG	CCT1183sgEF	CG5621	GGTCTCCTTTAGCATGCCATAGG

CCT1073sgEF	CG2302	TTCGACGGACGTATAGAACTCGG	CCT1183sgEF	CG5621	CAAACCGAATGGGTCCCGTGAGG
CCT1074sgEF	CG11348	GGCTTCCAAACCTTGTCGGGGGG	CCT1184sgEF	CG7446	GATCCGGGGCCGATGGACCAGGG
CCT1074sgEF	CG11348	ATGTGATGTCAGTCTCCGTGGGG	CCT1184sgEF	CG7446	GGTGGCTCGGGGTCGACCACCGG
CCT1074sgEF	CG11348	ATAACGGCCCTTGCCCGAAAGGG	CCT1184sgEF	CG7446	CGTCGGATGTCATCTACCGTTGG
CCT1075sgEF	CG6798	GGAGTATTACCCCGATACACTGG	CCT1185sgEF	CG7589	GTCTTTCCAGTCGATCATAGCGG
CCT1075sgEF	CG6798	TTCTCCCGTATACTTCAGAGTGG	CCT1185sgEF	CG7589	GATCATCTCCACGCGCATGCAGG
CCT1075sgEF	CG6798	ACTTGCACTAGGTTACTGCCAGG	CCT1185sgEF	CG7589	TCGTAGTGTTGTGCCAGAACTGG
CCT1076sgEF	CG6919	GACCACGTCTTCAACGGATACGG	CCT1186sgEF	CG8681	GGTCGAGGCCAACATAACTACGG
CCT1076sgEF	CG6919	TTCGTCAAGTGTTTCATTATTGG	CCT1186sgEF	CG8681	TTTATTGTATCCTCACGCCTGGG
CCT1076sgEF	CG6919	TAATGCTTCCGTCATGATCTCGG	CCT1186sgEF	CG8681	ACAGTAAAACAACTGGGGCCGGG
CCT1077sgEF	CG9918	GGCCGTAATCGTTAGCACCGTGG	CCT1187sgEF	CG9935	GAACTTCTCCGTGAAATGACCGG
CCT1077sgEF	CG9918	GGCCATCGTGATACCCGTAACGG	CCT1187sgEF	CG9935	GGGCAGACCGGCCTATGTTTGGG
CCT1077sgEF	CG9918	CCTGCGGAACGCCCGACAACAGG	CCT1187sgEF	CG9935	CCAGCCTGGAATGTATAACTCGG
CCT1078sgEF	CG7395	GGACATTTCCGAAGACACCCAGG	CCT1188sgEF	CG11155	TCTTCTTTAACCATAACATACGG
CCT1078sgEF	CG7395	ATGGCACAGACTCCTGCCGAAGG	CCT1188sgEF	CG11155	ATCATTCCAGGTTTGGTCGGAGG
CCT1078sgEF	CG7395	CAACTGGAGCCTAACGTCGCCGG	CCT1188sgEF	CG11155	CTAGCTAAAAGAGCATCTGTTGG
CCT1079sgEF	CG11895	GTCTCCGTGAATCACAAGGATGG	CCT1189sgEF	CG12344	TTAGGCGGAAGAACTACTCGCGG
CCT1079sgEF	CG11895	TTTAAGGTAGATTCCAGGACAGG	CCT1189sgEF	CG12344	CTACGTGACGCTGCTTCCAGAGG
CCT1079sgEF	CG11895	GAGATCCGTCGATGCAGGGCGGG	CCT1189sgEF	CG12344	CGAAGCGGAAGTATACGGTGAGG
CCT1080sgEF	CG9122	GTTTCCCACCTGGTTACGCAGGG	CCT1190sgEF	CG32848	GGGCTATCGATACAATCACGAGG
CCT1080sgEF	CG9122	CTACACTTCCGTGAACACGCAGG	CCT1190sgEF	CG32848	CCCGTGATATTATCCCTCAACGG
CCT1080sgEF	CG9122	CAGGCCCAGAAGACTCTTCCCGG	CCT1190sgEF	CG32848	TCGACGGCAGTCTTTGCTTGTGG
CCT1081sgEF	CG1056	TTTCTGGACTACAGTCCCCACGG	CCT1191sgEF	CG7535	GCCTTCGTATAGGAAACGGGCGG
CCT1081sgEF	CG1056	ACTGTTGCGATGGCCGTACGAGG	CCT1191sgEF	CG7535	GAGCAGATCTGTCTATCCAGCGG
CCT1081sgEF	CG1056	ATGCAAAGCTACTCTGGTCGTGG	CCT1191sgEF	CG7535	AAAGTATCTGACCCTGACGGAGG
CCT1082sgEF	CG42796	GCACCTGGTCCTGTGGGAGGAGG	CCT1192sgEF	CG17336	GAGGCGCTGATAGACTCCAGTGG
CCT1082sgEF	CG42796	CATCCAGGCAGATCCAGGTGAGG	CCT1192sgEF	CG17336	GTAGTGCAGATCCATCATGCAGG
CCT1082sgEF	CG42796	TCGTCCTGGGAACAGCGGCCGGG	CCT1192sgEF	CG17336	GTATTGGCGCGACGAGCGTTTGG
CCT1083sgEF	CG9753	GTTTCTGGGTAGTCCCATGGAGG	CCT1194sgEF	CG11236	ACTGGCAACACCATTAACCCCGG
CCT1083sgEF	CG9753	GGTGTAGGGTATGTTCAGCTCGG	CCT1194sgEF	CG11236	TGGGGTCCGTACCTTCTGGGCGG
CCT1083sgEF	CG9753	GGCGTCGCAACTTTCTTTCCCGG	CCT1194sgEF	CG11236	CATAAAGGTGACGATCATATCGG
CCT1084sgEF	CG18208	CGTCTTCTCGACCGGAAAGCCGG	CCT1195sgEF	CG12338	CTCCTTCTGGAGTTCTAAGGCGG
CCT1084sgEF	CG18208	TCGCTGGCCAATGAGCTAATGGG	CCT1195sgEF	CG12338	TAGTGGCATAGGGCAAGAAGAGG
CCT1084sgEF	CG18208	CGAATCACACAGAAGTCCACTGG	CCT1195sgEF	CG12338	ATCCCAGTAGTTGAAGGCATCGG
CCT1085sgEF	CG18741	AGGAGCCGGCGCGCCCCTCCTGG	CCT1196sgEF	CG4827	GGTGCCCTTCCTAAATGCCGTGG
CCT1085sgEF	CG18741	CCGTGTGCAAGTACCGCTCCCGG	CCT1196sgEF	CG4827	GAATCCCATTGCACCCCGGGCGG
CCT1085sgEF	CG18741	CCTCCTGTTGCCACCATCGCAGG	CCT1196sgEF	CG4827	GTTCCGAAAGGCAAGCACCTTGG
CCT1086sgEF	CG32476	AGACAACCCGTTAGATCCGGCGG	CCT1197sgEF	CG30104	TATCGTAAGGAGGCTCAGGAGGG
CCT1086sgEF	CG32476	GCAAATAACTAACTAATAGCAGG	CCT1197sgEF	CG30104	TCAGTTGGGGAACCTTGCTTAGG
CCT1086sgEF	CG32476	CAACGAATCATACACTGTGAAGG	CCT1197sgEF	CG30104	TGGCCACTCGGGTTATTTGAAGG
CCT1087sgEF	CG42244	CATTGCGGTGGATAACCAGGCGG	CCT1198sgEF	CG8129	GGCCATGCGAATGTCCCGCGAGG
CCT1087sgEF	CG42244	GCCTATAACATCGCAATTTGTGG	CCT1198sgEF	CG8129	ATCTATTAGCGGCATTGCGGTGG
CCT1087sgEF	CG42244	AACGCCTCCGTGGAACTGTCCGG	CCT1198sgEF	CG8129	TTTAACGGCTGTGGCAATACCGG
CCT1088sgEF	CG7411	GGAATACCGCCTGCTCGAGGTGG	CCT1199sgEF	CG3011	GGCCTGGATCTGCCCGATGGCGG

CCT1088sgEF	CG7411	GGGGCGTTGTTGGATCCCACTGG	CCT1199sgEF	CG3011	AGGGATATCCCGGCAAGAGGTGG
CCT1088sgEF	CG7411	GTTCACCCTTAAGCGTCGTTTGG	CCT1199sgEF	CG3011	GTCTCCGGGTTCACTTTGTACGG
CCT1089sgEF	CG1543	GGTGAGACGGGACTACCAGCAGG	CCT1200sgEF	CG13317	GCCGCTGATACCCACGCCGGAGG
CCT1089sgEF	CG1543	CAATGTGACGGCACCGCACGAGG	CCT1200sgEF	CG13317	TTTTGTTGCGCCGTGTCAGTCGG
CCT1089sgEF	CG1543	TGTGATGATGATAAGCCAGTTGG	CCT1200sgEF	CG13317	AGTTGACAACTCACCGCTCGCGG
CCT1090sgEF	CG10118	GGAGTCCCGTCAGTCGCGCGTGG	CCT1201sgEF	CG14049	GATATGCGTAAGCGGAACGGTGG
CCT1090sgEF	CG10118	GAGGCGTGCTTGGGGAACCACGG	CCT1201sgEF	CG14049	TATCACATCGCTGAGGCCGGTGG
CCT1090sgEF	CG10118	ATCCCGCCGTCGCAGCCTGGTGG	CCT1201sgEF	CG14049	GGCCACCTTGTTCGCCGTGGCGG
CCT1091sgEF	CG7285	TGTCCTCCAGTTTGTGAAAGGGG	CCT1202sgEF	CG14059	GTGCGAGCACCTCTTTCAGGCGG
CCT1091sgEF	CG7285	GCTATGCAATGTTGATAGGTGGG	CCT1202sgEF	CG14059	ACTCGATGGACCTTCTGTCGCGG
CCT1091sgEF	CG7285	ATATATCCTGAATCTGGCGGTGG	CCT1202sgEF	CG14059	CATCGGAGTCTGTTGCCTGATGG
CCT1092sgEF	CG13702	CATACTGAATCTGGCTATCGCGG	CCT1203sgEF	CG14167	CTACTAATCCTTATGATCGGCGG
CCT1092sgEF	CG13702	TGTAGCTGTACGAACAGTCCGGG	CCT1203sgEF	CG14167	GCGGCCGCACAACTTCATGGTGG
CCT1092sgEF	CG13702	GTCCAGGTGGGGTCGCACACTGG	CCT1203sgEF	CG14167	GTAGGAGTAGGCTAGGTAGCAGG
CCT1093sgEF	CG13968	TTATCATAGAGATTGCTCAGGGG	CCT1204sgEF	CG14173	CCCGGAAACCACAAACTCTGCGG
CCT1093sgEF	CG13968	GATGCAGCAGCCCGCCCAGGCGG	CCT1204sgEF	CG14173	TGCAGGATGATAGCAGCATGTGG
CCT1093sgEF	CG13968	ACTGAGTCAAGGCTGCGCCTTGG	CCT1204sgEF	CG14173	GCATGTGGCAGACACTGGACGGG
CCT1094sgEF	CG11937	TACAACGCGTCGCCGCAACGCGG	CCT1205sgEF	CG14920	AAATCTCCTCCGGCTGACTGGGG
CCT1094sgEF	CG11937	TTCGGCTCTCTCTCTTCGGCTGG	CCT1205sgEF	CG14920	AGAAGTTGCACAAGTCTTGCCGG
CCT1094sgEF	CG11937	TTCGAAAGGTAGCGCAGCACTGG	CCT1205sgEF	CG14920	AGCCGGAGAGGTGACATTGCCGG
CCT1096sgEF	CG13419	GCTCCGCCACGAGAACAACAAGG	CCT1206sgEF	CG17673	TCCAGGCCTGGGAATGGCCGTGG
CCT1096sgEF	CG13419	TCAAATACCATTATCCGTGGCGG	CCT1206sgEF	CG17673	TTTGTAGGCTTCCTATTCCACGG
CCT1096sgEF	CG13419	CAGCATTCTGAAACTCTGCACGG	CCT1206sgEF	CG17673	ACTCGGCTTGGTCCAGGCCTGGG
CCT1097sgEF	CG15520	GACCACGACAAGAACCGACGAGG	CCT1207sgEF	CG17878	CATTGGCCAACGCTCACCACTGG
CCT1097sgEF	CG15520	GAAGGCATAGAGCCCCATGTTGG	CCT1207sgEF	CG17878	CAGTTGAGAAGACCCCATCTCGG
CCT1097sgEF	CG15520	ATCGCCGAATTCAGTACAGCTGG	CCT1207sgEF	CG17878	ACTCAATGGGAAAGGACGCTTGG
CCT1098sgEF	CG4910	CGTCCATGAGGATTTCCCTGAGG	CCT1208sgEF	CG33273	GGAGAACTGGGATCACGGAGCGG
CCT1098sgEF	CG4910	AGCTAAGTGGCGTTATACAATGG	CCT1208sgEF	CG33273	TCAGCATGTCCATCAAGGCGGGG
CCT1098sgEF	CG4910	GAACAACGAGGGCACCAATATGG	CCT1208sgEF	CG33273	AGCTATCCAAATCCGCCAAGTGG
CCT1099sgEF	CG11318	GTACGTTTCCACTCCAGTAGTGG	CCT1209sgEF	CG40041	TATACGTGTATACACGACGATGG
CCT1099sgEF	CG11318	TATGAAACCTGGTCAACTGAGGG	CCT1209sgEF	CG40041	GTTGGGACTATGTAAGCGTTTGG
CCT1099sgEF	CG11318	TGGAGAGGAACGTAATTCATCGG	CCT1209sgEF	CG40041	CGCTGGGCGTGGACACAAACAGG
CCT1100sgEF	CG12290	GCAGTCCCAGGAACAAAGTGGGG	CCT1210sgEF	CG6736	GATTTACACGCCGTGTCAGGCGG
CCT1100sgEF	CG12290	CTCCGTGGGTAAGCTCTCAAAGG	CCT1210sgEF	CG6736	CGGCTGCAGTAACTGCGACACGG
CCT1100sgEF	CG12290	GGGATCCGTAACGGCACACCAGG	CCT1210sgEF	CG6736	GTGCGGCGAGGCTCTGATCCAGG
CCT1101sgEF	CG12796	GATTGGAGATGACCGATCGCAGG	CCT1211sgEF	CG8167	CTGCAGTGAAAAGCTCAACGAGG
CCT1101sgEF	CG12796	GAGCTTCGATAATCCCAAGCGGG	CCT1211sgEF	CG8167	GAAGGACAAAGGCTTGCTCATGG
CCT1101sgEF	CG12796	CAGCAGGCAGGGACCTCTCATGG	CCT1211sgEF	CG8167	GCGCGCTTGTGTGGAATCACGGG
CCT1102sgEF	CG13229	TGTCGTTGAAAGGAACCCGCTGG	CCT1212sgEF	CG17777	TATGGACACGGTCACTACGGCGG
CCT1102sgEF	CG13229	AGATTTGAGCTACACCTGGGCGG	CCT1212sgEF	CG17777	CGTCTTCTTCTCATCCACGGCGG
CCT1102sgEF	CG13229	TTCCAGCATCACAAACATATCGG	CCT1212sgEF	CG17777	CGCCGTAGCCGCCATAGCCGTGG
CCT1103sgEF	CG15556	GGATCACGTGACCTGTAGGTCGG	CCT1213sgEF	CG45777	CGTGTCTTGGGCGAGCACGGAGG
CCT1103sgEF	CG15556	TATGAGACCTGGCTTAGCGATGG	CCT1213sgEF	CG45777	GGAGGCGAGTGCCGTGCCCACGG
CCT1103sgEF	CG15556	TGAGTCGGAACGATGTACTCTGG	CCT1213sgEF	CG45777	GGAGCGTTGCTAAAGGAAGCGGG

CCT1104sgEF	CG15614	GATGCAGTCCATCCACGAAAGGG	CCT1214sgEF	CG34136	GAAGAATGCAAGGCACAGTAGGG
CCT1104sgEF	CG15614	TCACCAGCTCAGAATCCGGTTGG	CCT1214sgEF	CG34136	GAATGAGGTGAGCGGAAGACAGG
CCT1104sgEF	CG15614	AAAGTTCGTACACAGTCCAAAGG	CCT1214sgEF	CG34136	TTGCCCAAGCGAAGAATGCAAGG
CCT1105sgEF	CG15744	GCTCTCCCTGGGCACACCAATGG	CCT1215sgEF	CG43117	GAATTGGTCTGGGCTGAGGAAGG
CCT1105sgEF	CG15744	GCCATTAGCCACATCTATGAGGG	CCT1215sgEF	CG43117	ATCCACCAACACCACAACCACGG
CCT1105sgEF	CG15744	CGCCTGGCCCCCCTCTGCTGCGG	CCT1215sgEF	CG43117	GCAGGCAGAATCCGGCGAATAGG
CCT1107sgEF	CG30340	CTGGCTGCACAAGCCCAATGGGG			
CCT1107sgEF	CG30340	GACTACCGAGAGATTGAGCACGG			
CCT1107sgEF	CG30340	CTTCTATCAGAACTACCAGTTGG			

Table S4 CCT gene expression profile of clock neurons

	s-LNv		l-LNv		5th		LNd		LPN		DN1		DN2		DN3	
Gene symbol	GFP+	N#	GFP+	N#	GFP+	N#	GFP+	N#	GFP+	N#	GFP+	N#	GFP+	N#	GFP+	N#
AstC	/	/	/	/	/	/	1 ± 0	6	/	/	/	/	1.83 ± 0.41	6	1 ± 0	1
CCHa1	/	/	/	/	/	/	/	/	/	/	1.6 ± 0.55	5	/	/	/	/
ChAT	3 ± 1.41	2	/	/	/	/	2.3 ± 1.06	10	1 ± 1	1	1 ± 0	1	1 ± 0	10	1 ± 0	7
CNMa	/	/	/	/	/	/	/	/	/	/	4 ± 1.41	2	/	/	1 ± 0	2
Dh31	3.64 ± 0.5	11	/	/	/	/	1.2 ± 0.42	10	/	/	3.8 ± 0.63	10	/	/	/	/
Dh44	/	/	1.67 ± 0.58	3	/	/	3 ± 1	3	/	/	5 ± 0	3	1.67 ± 0.58	3	1.67 ± 0.58	3
GlyT	2.8 ± 1.64	5	3.88 ± 0.35	8	1 ± 0	3	1 ± 0	3	/	/	1.57 ± 0.79	7	1 ± 0	6	2 ± 0.93	8
HisCl1	/	/	/	/	/	/	0 ± 0	/	/	/	9 ± 0	1	/	/	/	/
ITP	/	/	/	/	/	/	/	/	/	/	/	/	/	/	1 ± 0	2
NPF	1 ± 0	2	/	/	/	/	1 ± 0	3	/	/	/	/	/	/	/	/
Nplp1	/	/	/	/	/	/	/	/	/	/	5 ± 0	2	/	/	2 ± 0	2
Proc	/	/	/	/	/	/	1 ± 0	12	/	/	/	/	/	/	/	/
sNPF	4 ± 0	7	/	/	/	/	1.63 ± 0.52	8	/	/	/	/	/	/	/	/
TH	1.5 ± 0.71	2	/	/	/	/	1 ± 0	2	/	/	3.5 ± 0.71	2	/	/	/	/
Trh	/	/	/	/	/	/	/	/	/	/	1.75 ± 0.5	4	/	/	/	/
Trissin	/	/	/	/	/	/	1.82 ± 0.4	11	/	/	/	/	/	/	/	/
VGlut	/	/	1.2 ± 0.45	5	/	/	1.17 ± 0.41	6	/	/	3.5 ± 0.55	6	2 ± 0	1	2.2 ± 0.45	5
CG13229	/	/	3.5 ± 0.55	6	1 ± 0	1	1.5 ± 0.55	6	/	/	/	/	/	/	1 ± 0	3
CG32547	/	/	2.71 ± 0.95	7	/	/	1.86 ± 0.9	7	/	/	3.29 ± 1.8	7	1 ± 0	5	/	/
CG43795	/	/	/	/	/	/	/	/	/	/	/	/	1 ± 0	6	/	/
5-HT2B	/	/	/	/	/	/	1.62 ± 0.65	13	/	/	/	/	1 ± 0	1	/	/
CCHa1-R	1.5 ± 0.71	2	/	/	/	/	/	/	/	/	/	/	/	/	/	/
CNMaR	/	/	/	/	/	/	/	/	/	/	/	/	/	/	15.67 ± 0.58	3
CrzR	/	/	/	/	/	/	/	/	/	/	2 ± 0	2	1.5 ± 0.71	2	2.5 ± 0.71	2
D2R	/	/	/	/	/	/	1 ± 0	6	/	/	/	/	/	/	/	/
Dh31-R	2 ± 0	2	3.43 ± 0.53	7	1 ± 0	2	/	/	/	/	1 ± 0	3	/	/	/	/
Dh44-R2	/	/	/	/	/	/	1 ± 0	6	/	/	/	/	/	/	/	/
FMRFaR	/	/	/	/	/	/	/	/	/	/	/	/	1 ± 0	6	/	/
GABA-B-R2	3.43 ± 0.53	7	3.63 ± 0.52	8	1 ± 0	4	4.29 ± 1.7	7	/	/	3 ± 0	6	1 ± 0	1	1 ± 0	1
GABA-B-R3	/	/	/	/	/	/	1 ± 0	4	/	/	/	/	/	/	/	/

GluRIB	/	/	/	/	/	/	/	/	/	/	1.56 ± 1.01	9	1.5 ± 0.58	4	1 ± 0	2
mAChR-B	1.33 ± 0.58	3	3.33 ± 0.87	9	/	/	1.5 ± 0.53	8	/	/	3.38 ± 2.33	8	1 ± 0	5	/	/
MsR1	/	/	3.29 ± 0.49	7	/	/	1 ± 0	7	1 ± 1	1	/	/	2 ± 0	1	/	/
nAChRα1	3 ± 0	2	/	/	/	/	5.6 ± 0.89	5	2 ± 1	3	12.4 ± 1.52	5	/	/	1 ± 0	2
nAChRα2	/	/	3.8 ± 0.45	5	1 ± 0	1	2 ± 0.89	6	/	/	2.17 ± 1.17	6	/	/	2 ± 0.71	5
nAChRβ2	/	/	3 ± 1	3	/	/	/	/	/	/	1 ± 0	2	/	/	1 ± 0	5
Nmdar1	1 ± 0	2	3.64 ± 0.5	11	/	/	1.88 ± 0.35	8	/	/	1.5 ± 0.58	4	1.11 ± 0.33	9	1.4 ± 0.84	10
NPFR	/	/	/	/	/	/	1 ± 0	10	/	/	/	/	/	/	1.14 ± 0.38	7
Oct-TyrR	/	/	/	/	/	/	/	/	/	/	/	/	/	/	2 ± 0	2
Octβ2R	/	/	/	/	/	/	/	/	/	/	10.5 ± 0.71	2	1.5 ± 0.71	2	2.5 ± 0.71	2
Pdfr	/	/	1.14 ± 0.38	7	/	/	1 ± 0	2	/	/	2.29 ± 1.11	7	1 ± 0	6	1.33 ± 0.58	3
PK2-R1	/	/	/	/	/	/	1.5 ± 0.71	2	/	/	/	/	1 ± 0	3	/	/
SIFaR	/	/	3.21 ± 0.43	14	/	/	2 ± 0.39	14	/	/	1 ± 0	5	1 ± 0	6	1.22 ± 0.44	9
spab	/	/	/	/	/	/	1 ± 0	4	/	/	/	/	1 ± 0	2	/	/
CG13995	/	/	3 ± 0	1	/	/	1 ± 0	1	/	/	/	/	/	/	/	/

N# represents GFP positive brain number

/ represents no GFP found in corresponding clock neuron subset

Table S5 List of CCT genes intersected with Clk856 drivers

RaoLab Stock No.	CG No.	Gene Symbol	Driver	Intersection with Clk856
DKI0289	CG42796	5-HT2B	LexA	Clk856-GAL4
DKI0317	CG14919	AstC	LexA	Clk856-GAL4
DKI0292	CG43795	CG43795	LexA	Clk856-GAL4
DKI0303	CG13229	CG13229	LexA	Clk856-GAL4
DKI0073	CG13995	CG13995	LexA	Clk856-GAL4
DKI0110	CG12345	ChAT	LexA	Clk856-GAL4
DKI0254	CG32547	CG32547	LexA	Clk856-GAL4
DKI0121	CG33517	Dop2R	LexA	Clk856-GAL4
DKI0309	CG12370	Dh44-R2	LexA	Clk856-GAL4
DKI0060	CG13094	Dh31	LexA	Clk856-GAL4
DKI0105	CG32843	Dh31-R	LexA	Clk856-GAL4
WCKI1122	CG2114	FMRFaR	LexA	Clk856-GAL4
DKI0305	CG5549	GlyT	LexA	Clk856-GAL4
DKI0322	CG6706	GABA-B-R2	LexA	Clk856-GAL4
DKI0312	CG3022	GABA-B-R3	LexA	Clk856-GAL4
DKI0191	CG43743	GluRIB	LexA	Clk856-GAL4
DKI0212	CG6798	nAChRβ2	LexA	Clk856-GAL4
DKI0221	CG7918	mAChR-B	LexA	Clk856-GAL4
DKI0201	CG6844	nAChRα2	LexA	Clk856-GAL4
WCKI1173	CG8985	MsR1	LexA	Clk856-GAL4
WCKI1006	CG1147	NPFR	LexA	Clk856-GAL4
WCKI1018	CG7105	Proc	LexA	Clk856-GAL4
DKI0093	CG2902	Nmdar1	LexA	Clk856-GAL4
WCKI1089	CG10823	SIFaR	LexA	Clk856-GAL4
WCKI1080	CG8784	PK2-R1	LexA	Clk856-GAL4
DKI0059	CG13968	sNPF	LexA	Clk856-GAL4
DKI0082	CG14871	Trissin	LexA	Clk856-GAL4
DKI0248	CG9122	Trh	LexA	Clk856-GAL4
DKI0265	CG9887	VGlut	LexA	Clk856-GAL4
DKI0165	CG13586	ITP	Gal4	Clk856-p65AD
DKI0111	CG10118	TH	Gal4	Clk856-p65AD
DKI0168	CG3441	Nplp1	Gal4	Clk856-p65AD
DKI0287	CG14723	HisCl1	Gal4	Clk856-p65AD
DKI0203	CG5610	nAChRα1	Gal4	Clk856-p65AD
WCKI1015	CG10342	NPF	LexA	Clk856-GAL4
DKI0099	CG14358	CCHa1	LexA	Clk856-GAL4
WCKI1017	CG33976	Octβ2R	Gal4	Clk856-p65AD
WCKI1019	CG10698	CrzR	Gal4	Clk856-p65AD
DKI0078	CG30106	CCHa1-R	LexA	Clk856-GAL4
DKI0029	CG13936	CNMa	p65AD	Clk856-GAL4
DKI0288	CG33696	CNMaR	p65AD	Clk856-GAL4
WCKI1095	CG8348	Dh44	GAL4	Clk856-p65AD

DKI0134	CG13758	Pdfr	LexA	Clk856-GAL4
WCKI1199	CG7485	Oct-TyrR	Gal4	Clk856-p65AD
DKI0262	CG8216	spab	LexA	Clk856-GAL4
DKI0013	CG10537	Rdl	LexA	Clk856-GAL4
DKI0069	CG1056	5-HT2A	LexA	Clk856-GAL4
WCKI1162	CG10626	Lkr	LexA	Clk856-GAL4
DKI0251	CG11318	CG11318	LexA	Clk856-GAL4
WCKI1030	CG11325	AkhR	LexA	Clk856-GAL4
WCKI1201	CG1171	Akh	LexA	Clk856-GAL4
DKI0215	CG11822	nAChRβ3	LexA	Clk856-GAL4
CG11883-L-LexA	CG11883	CG11883	LexA	Clk856-GAL4
CG11883-S-LexA	CG11883	CG11883	LexA	Clk856-GAL4
WCKI1180	CG11937	amn	LexA	Clk856-GAL4
DKI0307	CG12344	CG12344	LexA	Clk856-GAL4
Nplp3-LexA	CG13061	Nplp3	LexA	Clk856-GAL4
L53-T5-W-	CG13480	Lk	LexA	Clk856-GAL4
DKI0302	CG13565	Orcokinin	LexA	Clk856-GAL4
DKI0050	CG13575	CG13575	LexA	Clk856-GAL4
DKI0160	CG13579	CG13579	LexA	Clk856-GAL4
DKI0286	CG13579	CG13579-RB	LexA	Clk856-GAL4
DKI0091	CG13633	AstA	LexA	Clk856-GAL4
DKI0096	CG14375	CCHa2	LexA	Clk856-GAL4
DKI0086	CG14575	CapaR	LexA	Clk856-GAL4
DKI0007	CG14593	CCHa2-R	LexA	Clk856-GAL4
DKI0094	CG14734	Tk	LexA	Clk856-GAL4
DKI0020	CG14994	gad1	LexA	Clk856-GAL4
DKI0089	CG15113	5-HT1B	LexA	Clk856-GAL4
DKI0187	CG15274	GABA-B-R1	LexA	Clk856-GAL4
DKI0055	CG15284	Pburs	LexA	Clk856-GAL4
Tβh-LexA	CG1543	Tβh	LexA	Clk856-GAL4
DKI0143	CG15520	Capa	LexA	Clk856-GAL4
WCKI1196	CG15614	CG15614	LexA	Clk856-GAL4
DKI0159	CG15744	CG15744	LexA	Clk856-GAL4
DKI0030	CG16720	5-HT1A	LexA	Clk856-GAL4
DKI0146	CG16752	SPR	LexA	Clk856-GAL4
DKI0156	CG16992	mthl6	LexA	Clk856-GAL4
DKI0294	CG17061	mthl10	LexA	Clk856-GAL4
WCKI1120	CG17084	CG17084	LexA	Clk856-GAL4
DKI0031	CG17795	mthl2	LexA	Clk856-GAL4
DKI0196	CG18039	GluRIID	LexA	Clk856-GAL4
DKI0148	CG18090	Dsk	LexA	Clk856-GAL4
WCKI1097	CG18208	CG18208	LexA	Clk856-GAL4
DKI0321	CG18314	DopEcR	LexA	Clk856-GAL4
DKI0123	CG18741	DopR2	LexA	Clk856-GAL4

DKI0205	CG2302	nAChR α3	LexA	Clk856-GAL4
WCKI1184	CG2346	FMRFa	LexA	Clk856-GAL4
DKI0225	CG2872	AstA-R1	LexA	Clk856-GAL4
DKI0290	CG30018	mthl13	LexA	Clk856-GAL4
DKI0066	CG30340	CG30340	LexA	Clk856-GAL4
DKI0151	CG31096	Lgr3	LexA	Clk856-GAL4
DKI0231	CG31147	mthl11	LexA	Clk856-GAL4
DKI0232	CG31760	CG31760	LexA	Clk856-GAL4
DKI0234	CG32447	CG32447	LexA	Clk856-GAL4
DKI0259	CG32475	mthl8	LexA	Clk856-GAL4
WCKI1107	CG32476	CG32476	LexA	Clk856-GAL4
DKI0252	CG32540	CCKLR-17D3	LexA	Clk856-GAL4
DKI0206	CG32975	nAChR α5	LexA	Clk856-GAL4
DKI0101	CG33344	CCAP-R	LexA	Clk856-GAL4
DKI0284	CG33495	Dup99B	LexA	Clk856-GAL4
DKI0087	CG33495	Dup99B	LexA	Clk856-GAL4
DKI0128	CG33513	Nmdar2	LexA	Clk856-GAL4
DKI0315	CG33527	SIFa	LexA	Clk856-GAL4
DKI0180	CG33639	CG33639	LexA	Clk856-GAL4
DKI0246	CG34388	natalisin	LexA	Clk856-GAL4
DKI0175	CG34411	CG34411	LexA	Clk856-GAL4
DKI0102	CG3454	HDC	LexA	Clk856-GAL4
WCKI1101	CG3856	oamb	LexA	Clk856-GAL4
DKI0208	CG4128	nAChR α6	LexA	Clk856-GAL4
WCKI1044	CG42244	Octβ3R	LexA	Clk856-GAL4
DKI0193	CG4226	GluRIIC	LexA	Clk856-GAL4
DKI0173	CG42301	CCKLR-17D1	LexA	Clk856-GAL4
WCKI1166	CG4313	CG4313	LexA	Clk856-GAL4
DKI0276	CG4356	mAChR-A	LexA	Clk856-GAL4
DKI0016	CG43745	MsR2	LexA	Clk856-GAL4
WCKI1169	CG4395	hec	LexA	Clk856-GAL4
NT5E1-lexA	CG4827	NT5E-1	LexA	Clk856-GAL4
WCKI1176	CG5400	Eh	LexA	Clk856-GAL4
WCKI1203	CG5811	RYa-R	LexA	Clk856-GAL4
WCKI1205	CG5911	ETHR	LexA	Clk856-GAL4
WCKI1055	CG6371	CG6371	LexA	Clk856-GAL4
WCKI1009	CG6440	Ms	LexA	Clk856-GAL4
WCKI1011	CG6456	Mip	LexA	Clk856-GAL4
WCKI1192	CG6530	mthl3	LexA	Clk856-GAL4
WCKI1194	CG6536	mthl4	LexA	Clk856-GAL4
WCKI1049	CG6919	oa2	LexA	Clk856-GAL4
WCKI1118	CG6965	CG6965	LexA	Clk856-GAL4
DKI0192	CG6992	GluRIIA	LexA	Clk856-GAL4
WCKI1093	CG7285	AstC-R1	LexA	Clk856-GAL4

DKI0071	CG7411	Ort	LexA	Clk856-GAL4
DKI0311	CG7431	TyrR	LexA	Clk856-GAL4
DKI0299	CG7446	Grd	LexA	Clk856-GAL4
DKI0320	CG7497	CG7497	LexA	Clk856-GAL4
WCKI1094	CG7665	Lgr1	LexA	Clk856-GAL4
DKI0240	CG8380	DAT	LexA	Clk856-GAL4
DKI0047	CG8394	vGAT	LexA	Clk856-GAL4
WCKI1181	CG8422	Dh44-R1	LexA	Clk856-GAL4
DKI0269	CG8442	GluRIA	LexA	Clk856-GAL4
WCKI1174	CG8795	PK2-R2	LexA	Clk856-GAL4
WCKI1060	CG10001	CG10001	Gal4	Clk856-p65AD
DKI0130	CG14723	HisCl1	Gal4	Clk856-p65AD
DKI0041	CG15361	Nplp4	Gal4	Clk856-p65AD
WCKI1198	CG15556	CG15556	Gal4	Clk856-p65AD
DKI0255	CG18105	ETH	Gal4	Clk856-p65AD
DKI0198	CG31201	GluRIIE	Gal4	Clk856-p65AD
WCKI1164	CG3171	Tre1	Gal4	Clk856-p65AD
DKI0300	CG4910	CCAP	Gal4	Clk856-p65AD
DKI0226	CG6936	mth	Gal4	Clk856-p65AD
WCKI1178	CG6986	Proc-R	Gal4	Clk856-p65AD
DKI0297	CG7476	mthl7	Gal4	Clk856-p65AD
WCKI1053	CG9918	PK1-R	Gal4	Clk856-p65AD

Table S6 Phenotypes of CCT genes knocking out in clock neurons

Target Gene	LD condition				DD conditon		
	MAI	MAPI	EAI	EAPI	Power	Period	AR
Pdfr	**0.087 ± 0.119**	-0.047 ± 0.175	0.34 ± 0.076	**0.101 ± 0.071**	**3.45 ± 7.54**	**22.41 ± 0.51**	17/22
Pdf	**0.11 ± 0.124**	0.026 ± 0.12	0.383 ± 0.065	**0.114 ± 0.094**	**15.46 ± 34.25**	**22.31 ± 0.4**	13/23
nAChRα1	0.316 ± 0.121	**0.14 ± 0.145**	0.352 ± 0.094	-0.094 ± 0.068	**37.83 ± 27.68**	**23.18 ± 0.43**	1/14
Dh44	0.339 ± 0.111	0.042 ± 0.106	0.367 ± 0.09	-0.138 ± 0.088	**44.22 ± 45.84**	23.55 ± 0.24	7/19
CNMaR	0.345 ± 0.063	0.062 ± 0.129	0.342 ± 0.132	-0.042 ± 0.061	**71.37 ± 39.43**	24.01 ± 0.8	1/22
SIFaR	0.296 ± 0.076	0.062 ± 0.098	0.381 ± 0.08	-0.041 ± 0.078	**75.56 ± 66.38**	23.32 ± 0.33	4/24
ITP	0.277 ± 0.103	0.015 ± 0.106	0.357 ± 0.058	-0.06 ± 0.075	80.74 ± 39.06	23.75 ± 0.29	2/24
CG17777	0.272 ± 0.096	-0.025 ± 0.18	0.453 ± 0.068	-0.114 ± 0.048	81.81 ± 49.34	23.74 ± 0.29	1/22
Dh31	**0.205 ± 0.122**	-0.035 ± 0.134	0.405 ± 0.075	-0.092 ± 0.094	82.44 ± 51.16	23.5 ± 0.29	1/22
CG13995	0.346 ± 0.087	0.011 ± 0.152	0.414 ± 0.055	-0.072 ± 0.099	87.7 ± 36.53	23.56 ± 0.33	1/24
nAChRα2	0.26 ± 0.1	0 ± 0.145	0.348 ± 0.088	-0.042 ± 0.078	88.15 ± 50.2	23.7 ± 0.24	1/22
NPFR	0.269 ± 0.174	0.042 ± 0.092	0.403 ± 0.089	-0.072 ± 0.073	88.69 ± 46.62	23.35 ± 0.33	2/24
CrzR	0.324 ± 0.087	0.026 ± 0.122	0.415 ± 0.068	-0.028 ± 0.083	91.63 ± 54.11	23.35 ± 0.39	2/24
HisCl1	0.306 ± 0.075	0.08 ± 0.097	0.398 ± 0.04	-0.04 ± 0.096	93.7 ± 48.07	23.8 ± 0.39	1/23
AstC-R2	0.363 ± 0.074	-0.073 ± 0.164	0.465 ± 0.082	-0.136 ± 0.073	94.45 ± 57.72	24.04 ± 0.38	1/24
VGAT	0.249 ± 0.093	0.078 ± 0.118	0.402 ± 0.054	-0.106 ± 0.078	98.11 ± 52.33	23.42 ± 0.36	1/21
MsR1	0.31 ± 0.069	**0.091 ± 0.089**	0.336 ± 0.086	-0.099 ± 0.077	99.46 ± 46.48	24.14 ± 0.65	1/24
CCAP	0.321 ± 0.075	-0.028 ± 0.191	0.464 ± 0.06	-0.105 ± 0.074	99.76 ± 57.98	23.84 ± 0.37	0/22
CG34136	0.278 ± 0.084	0.022 ± 0.099	0.388 ± 0.052	-0.037 ± 0.085	101.43 ± 54.01	23.7 ± 0.43	1/22
GABA-B-R2	0.277 ± 0.078	-0.016 ± 0.108	0.337 ± 0.074	-0.084 ± 0.071	101.92 ± 30.51	23.95 ± 0.4	0/20
Hug	0.337 ± 0.073	0.013 ± 0.093	0.41 ± 0.042	-0.059 ± 0.081	102 ± 51.47	23.55 ± 0.39	1/23
nAChRβ2	0.254 ± 0.095	0.035 ± 0.121	0.355 ± 0.079	**-0.011 ± 0.07**	104.34 ± 42.52	23.91 ± 0.3	0/22
AstC	0.329 ± 0.102	-0.005 ± 0.178	0.36 ± 0.098	-0.017 ± 0.057	104.4 ± 48.76	23.71 ± 0.4	2/23
Nplp3	0.38 ± 0.06	0.023 ± 0.102	0.415 ± 0.041	-0.124 ± 0.076	105.02 ± 47.1	23.66 ± 0.35	1/22
Ptth	0.377 ± 0.069	-0.028 ± 0.127	0.409 ± 0.057	-0.061 ± 0.085	105.4 ± 35.61	23.49 ± 0.32	0/24
GluRIB	0.317 ± 0.079	-0.016 ± 0.137	0.363 ± 0.057	-0.059 ± 0.077	106.25 ± 41.48	23.78 ± 0.25	0/18
CCHa1-R	0.307 ± 0.1	0.052 ± 0.088	0.419 ± 0.041	-0.064 ± 0.073	106.83 ± 46.29	**23.28 ± 0.4**	0/23
TβH	0.257 ± 0.103	0.037 ± 0.123	**0.31 ± 0.061**	-0.05 ± 0.079	107.86 ± 44.06	23.74 ± 0.38	0/19
Oct-TyrR	0.343 ± 0.085	0.013 ± 0.107	0.387 ± 0.061	-0.088 ± 0.1	108.19 ± 56.73	23.94 ± 0.32	2/22
Clk856-GAL4>Cas9.M9	***0.3 ± 0.076***	***0.016 ± 0.09***	***0.38 ± 0.048***	***-0.066 ± 0.074***	***108.37 ± 30.19***	***23.8 ± 0.25***	***0/24***
Dop2R	0.357 ± 0.075	0.063 ± 0.137	0.425 ± 0.084	-0.076 ± 0.073	109.27 ± 69.88	23.51 ± 0.51	2/24
Mip	0.316 ± 0.052	0 ± 0.134	0.402 ± 0.048	-0.068 ± 0.066	111.37 ± 42.75	23.47 ± 0.42	1/22
TrH	0.26 ± 0.124	0.05 ± 0.124	0.365 ± 0.051	-0.024 ± 0.07	111.5 ± 41	23.7 ± 0.44	0/23
Trissin	0.261 ± 0.086	0.056 ± 0.116	0.362 ± 0.065	-0.073 ± 0.056	111.89 ± 54.79	23.4 ± 0.29	2/22
CG43795	0.333 ± 0.113	0.007 ± 0.114	0.415 ± 0.054	-0.099 ± 0.071	111.9 ± 57.29	23.57 ± 0.35	0/22
CG7589	0.327 ± 0.061	0.013 ± 0.12	0.474 ± 0.065	-0.092 ± 0.07	112.13 ± 45.66	23.8 ± 0.38	0/23
CNMa	0.284 ± 0.086	**0.082 ± 0.12**	0.364 ± 0.041	-0.091 ± 0.085	112.6 ± 41.9	23.97 ± 0.22	0/24
CG32547	0.249 ± 0.098	-0.015 ± 0.116	0.344 ± 0.078	-0.049 ± 0.072	112.98 ± 63.4	23.69 ± 0.29	2/23
CG45777	0.36 ± 0.067	-0.047 ± 0.154	0.484 ± 0.065	-0.119 ± 0.077	113.47 ± 68.45	23.55 ± 0.25	0/24
Octβ2R	0.319 ± 0.081	0.028 ± 0.065	0.434 ± 0.07	-0.061 ± 0.071	114.28 ± 63.82	23.55 ± 0.41	1/24
Dh44-R2	0.357 ± 0.058	0.054 ± 0.067	0.403 ± 0.047	-0.039 ± 0.07	115.91 ± 61.1	23.51 ± 0.39	1/23
VAChT	0.284 ± 0.095	-0.118 ± 0.116	0.401 ± 0.084	-0.154 ± 0.058	116.69 ± 74.92	23.93 ± 0.3	1/21
CCHa1	0.352 ± 0.058	0.002 ± 0.086	0.39 ± 0.062	-0.119 ± 0.081	116.75 ± 44.06	23.73 ± 0.32	1/22
mGluRA	0.321 ± 0.065	-0.005 ± 0.078	0.49 ± 0.047	-0.062 ± 0.073	116.82 ± 50.26	24.04 ± 0.25	1/23
PK2-R1	0.333 ± 0.079	0.037 ± 0.121	0.429 ± 0.046	-0.099 ± 0.093	117.33 ± 50.14	23.95 ± 0.27	1/22
spab	0.253 ± 0.08	-0.005 ± 0.094	0.363 ± 0.046	**0.002 ± 0.057**	117.38 ± 46.52	23.64 ± 0.26	0/22

Dh31-R	0.321 ± 0.103	-0.021 ± 0.161	0.412 ± 0.043	-0.09 ± 0.072	118.71 ± 50.62	23.6 ± 0.23	1/20
FMRFaR	0.294 ± 0.092	-0.013 ± 0.099	0.373 ± 0.033	-0.111 ± 0.074	119.47 ± 42.54	23.86 ± 0.32	0/21
CG13229	0.359 ± 0.069	0.059 ± 0.098	0.421 ± 0.049	-0.068 ± 0.066	122.46 ± 60.2	23.36 ± 0.37	2/21
mAChR-B	0.242 ± 0.112	**0.09 ± 0.087**	0.388 ± 0.037	-0.047 ± 0.081	122.88 ± 40.64	23.77 ± 0.42	0/23
5-HT2B	0.293 ± 0.085	0.035 ± 0.123	0.373 ± 0.042	-0.095 ± 0.084	124.65 ± 34.31	24.03 ± 0.29	0/24
TH	0.3 ± 0.101	0.016 ± 0.131	0.349 ± 0.11	-0.032 ± 0.086	125.71 ± 44.74	23.94 ± 0.33	1/23
Proc	0.362 ± 0.072	0.028 ± 0.142	0.437 ± 0.03	-0.086 ± 0.095	128.13 ± 61.01	23.57 ± 0.37	0/23
AstA	0.312 ± 0.092	-0.025 ± 0.113	0.412 ± 0.051	-0.082 ± 0.089	131.22 ± 35.09	23.63 ± 0.31	0/24
5-HT1B	0.313 ± 0.072	0.047 ± 0.117	0.402 ± 0.062	-0.083 ± 0.091	132.29 ± 41.37	23.5 ± 0.29	0/20
sNPF-R	0.283 ± 0.112	0.035 ± 0.069	0.387 ± 0.035	-0.089 ± 0.056	133.38 ± 41.77	23.74 ± 0.4	0/21
CG43117	0.285 ± 0.084	-0.03 ± 0.134	0.333 ± 0.081	-0.095 ± 0.092	134.98 ± 58.52	23.72 ± 0.33	0/21
NMDAR1	0.341 ± 0.066	0.065 ± 0.134	0.408 ± 0.052	-0.084 ± 0.083	135.01 ± 45.81	23.76 ± 0.23	1/19
GABA-B-R3	0.314 ± 0.104	0.041 ± 0.097	0.362 ± 0.061	-0.081 ± 0.056	135.49 ± 37.61	23.79 ± 0.24	0/23
CG12344	0.327 ± 0.062	-0.043 ± 0.154	0.465 ± 0.099	-0.121 ± 0.067	138.31 ± 63.27	23.98 ± 0.35	0/23
Gpb5	0.268 ± 0.058	-0.006 ± 0.12	0.424 ± 0.077	-0.078 ± 0.068	138.41 ± 42.42	23.69 ± 0.29	0/23
Nplp1	0.248 ± 0.115	0.072 ± 0.087	0.414 ± 0.023	-0.071 ± 0.103	138.54 ± 40.39	23.92 ± 0.3	0/23
Grd	0.26 ± 0.091	0.008 ± 0.132	0.448 ± 0.075	-0.065 ± 0.064	139.49 ± 78.28	23.65 ± 0.39	1/24
NPF	0.329 ± 0.086	0.007 ± 0.147	0.404 ± 0.067	-0.071 ± 0.05	139.57 ± 44.27	23.72 ± 0.3	0/23
sNPF	0.346 ± 0.084	-0.007 ± 0.118	0.414 ± 0.062	-0.111 ± 0.065	146.16 ± 58.23	23.6 ± 0.45	0/17
GlyT	0.273 ± 0.111	-0.119 ± 0.117	0.395 ± 0.076	-0.193 ± 0.105	105.325 ± 60.615	23.548 ± 0.245	5/43

VGlut and ChAT presented in Table S7

Table S7 Phenotypes of candidate CCT genes knockout in clock neurons

Genotype	LD condition				DD condition		
	MAI	MAPI	EAI	EAPI	Power	Period	AR
sgRNA^{Dh44}, Cas9.M6	0.329 ± 0.086	-0.058 ± 0.119	0.38 ± 0.058	-0.081 ± 0.065	66.38 ± 40.4	23.18 ± 0.31	2/22
Clk856> sgRNA^{Dh44}	0.354 ± 0.093	0.03 ± 0.131	0.444 ± 0.045	-0.085 ± 0.066	94 ± 45.35	23.61 ± 0.34	2/20
Clk856> sgRNA^{Dh44}, Cas9.M6	0.346 ± 0.096	-0.02 ± 0.165	0.397 ± 0.059	-0.085 ± 0.077	74.64 ± 27.25	23.75 ± 0.31	0/20
sgRNA$^{nAChR\alpha1}$, Cas9.M6	0.29 ± 0.089	-0.064 ± 0.139	0.363 ± 0.056	-0.071 ± 0.064	58.35 ± 43.82	23.53 ± 0.45	2/13
Clk856> sgRNA$^{nAChR\alpha1}$	0.318 ± 0.096	0.019 ± 0.137	0.401 ± 0.052	-0.08 ± 0.071	56.89 ± 45.03	23.66 ± 0.43	1/12
Clk856> sgRNA$^{nAChR\alpha1}$, Cas9.M6	0.307 ± 0.154	-0.031 ± 0.099	0.381 ± 0.056	-0.074 ± 0.074	69.21 ± 52.1	23.71 ± 0.29	2/13
sgRNA^{ChAT}, Cas9.M6	0.292 ± 0.096	0.026 ± 0.155	0.291 ± 0.092	-0.1 ± 0.055	91.48 ± 55.18	23.43 ± 0.41	3/19
Clk856> sgRNA^{ChAT}	0.298 ± 0.098	-0.016 ± 0.157	0.353 ± 0.071	-0.079 ± 0.051	78.66 ± 41.65	23.54 ± 0.25	1/22
Clk856> sgRNA^{ChAT}, Cas9.M6	0.22 ± 0.137	0.003 ± 0.123	0.318 ± 0.078	-0.124 ± 0.075	49.35 ± 42.11	23.7 ± 0.2	4/14
sgRNA^{CNMa}, Cas9.M6	0.342 ± 0.076	-0.141 ± 0.138	0.35 ± 0.091	-0.088 ± 0.079	92.81 ± 39.89	23.98 ± 0.44	1/23
Clk856> sgRNA^{CNMa}	0.355 ± 0.181	0.019 ± 0.093	0.431 ± 0.05	-0.121 ± 0.079	18.96 ± 22.19	23.8 ± 0.27	7/14
Clk856> sgRNA^{CNMa}, Cas9.M6	0.354 ± 0.11	**0.113 ± 0.169**	0.353 ± 0.086	-0.072 ± 0.066	93.51 ± 48.39	24.17 ± 0.42	1/20
sgRNA^{VGlut}, Cas9.M6	0.254 ± 0.114	-0.115 ± 0.14	0.32 ± 0.066	-0.073 ± 0.043	56.28 ± 39.85	23.41 ± 0.38	1/20
Clk856> sgRNA^{VGlut}	0.306 ± 0.102	-0.026 ± 0.146	0.369 ± 0.074	-0.104 ± 0.067	63.82 ± 48.6	23.6 ± 0.36	5/20
Clk856> sgRNA^{VGlut}, Cas9.M6	**0.179 ± 0.1****	-0.087 ± 0.107	0.27 ± 0.07	-0.158 ± 0.063	45.09 ± 41.35	23.7 ± 0.27	6/21
sgRNA$^{mAChR\text{-}B}$, Cas9.M6	0.37 ± 0.062	-0.047 ± 0.109	0.374 ± 0.064	-0.076 ± 0.054	110.16 ± 32.99	23.78 ± 0.47	0/21
Clk856> sgRNA$^{mAChR\text{-}B}$	0.358 ± 0.095	-0.003 ± 0.109	0.442 ± 0.038	-0.143 ± 0.087	73 ± 36	23.48 ± 0.45	0/17
Clk856> sgRNA$^{mAChR\text{-}B}$, Cas9.M6	0.259 ± 0.1	-0.109 ± 0.139	0.357 ± 0.066	-0.088 ± 0.074	109.35 ± 45.07	23.71 ± 0.36	0/22
sgRNA^{MsR1}, Cas9.M6	0.339 ± 0.078	-0.011 ± 0.175	0.368 ± 0.061	-0.072 ± 0.087	55.68 ± 49.3	23.77 ± 0.55	5/22
Clk856> sgRNA^{MsR1}	0.378 ± 0.098	-0.023 ± 0.114	0.4 ± 0.036	-0.143 ± 0.075	55.05 ± 43.19	23.89 ± 0.4	3/19
Clk856> sgRNA^{MsR1}, Cas9.M6	0.276 ± 0.085	-0.04 ± 0.123	0.313 ± 0.063	-0.085 ± 0.083	78.21 ± 50.06	23.85 ± 0.48	2/21
sgRNA^{SIFaR}, Cas9.M6	0.254 ± 0.104	-0.075 ± 0.14	0.34 ± 0.047	-0.072 ± 0.052	82.85 ± 42.29	23.63 ± 0.35	0/23
Clk856> sgRNA^{SIFaR}	0.329 ± 0.122	-0.058 ± 0.121	0.375 ± 0.059	-0.096 ± 0.05	81.71 ± 41.2	23.82 ± 0.36	0/21
Clk856> sgRNA^{SIFaR}, Cas9.M6	0.219 ± 0.143	-0.142 ± 0.172	0.299 ± 0.095	-0.117 ± 0.088	94.45 ± 32.78	24.04 ± 0.38	0/19
Clk856> Cas9.M6	0.295 ± 0.12	-0.043 ± 0.109	0.325 ± 0.081	-0.118 ± 0.048	90.64 ± 43.86	23.7 ± 0.27	1/16

Clk856> sgRNA^{VGlut}, Cas9.M6 vs Clk856> sgRNA^{VGlut}, ** $P < 0.01$

Clk856> sgRNA^{VGlut}, Cas9.M6 vs Clk856> Cas9.M6, ** $P < 0.01$

Clk856> sgRNA^{VGlut}, Cas9.M6 vs sgRNA^{VGlut}, Cas9.M6, $P = 0.0921$

Table S8 Conditional knockout of VGlut in DN1s

Genotype	LD condition				DD condition		
	MAI	MAPI	EAI	EAPI	POWER	PERIOD	AR
sgRNA^{VGlut},Cas9.M6	0.268 ± 0.124	-0.072 ± 0.106	0.328 ± 0.071	-0.065 ± 0.035	79.06 ± 49.45	22.89 ± 0.19	1/23
R18H11>sgRNA^{VGlut}	0.258 ± 0.085	-0.093 ± 0.104	0.327 ± 0.05	-0.124 ± 0.069	67.49 ± 42.52	23.38 ± 0.36	1/21
R18H11>sgRNA^{VGlut},Cas9.M6	**0.136 ± 0.148 ****	-0.109 ± 0.116	0.284 ± 0.106	-0.084 ± 0.061	61.9 ± 42.35	23.18 ± 0.27	4/24
R18H11>Cas9.M6	0.25 ± 0.093	-0.068 ± 0.124	0.387 ± 0.055	-0.048 ± 0.057	55.46 ± 49.14	23.33 ± 0.43	5/20
R51H05>sgRNA^{VGlut}	0.348 ± 0.067	-0.078 ± 0.078	0.398 ± 0.051	-0.103 ± 0.047	122.02 ± 38.89	23.4 ± 0.37	0/20
R51H05>sgRNA^{VGlut},Cas9.M6	0.26 ± 0.097	-0.16 ± 0.116	0.312 ± 0.073	-0.062 ± 0.059	82.56 ± 48.06	23.23 ± 0.33	2/22
R51H05>Cas9.M6	0.251 ± 0.098	-0.118 ± 0.143	0.349 ± 0.087	-0.055 ± 0.072	45.76 ± 41.2	23.19 ± 0.39	3/17
R79A11>sgRNA^{VGlut}	0.172 ± 0.131	-0.11 ± 0.102	0.378 ± 0.055	-0.087 ± 0.062	88.87 ± 40.43	23.43 ± 0.31	1/21
R79A11>sgRNA^{VGlut},Cas9.M6	0.178 ± 0.11	-0.131 ± 0.083	0.325 ± 0.08	-0.068 ± 0.037	75.67 ± 45.37	23.3 ± 0.29	1/19
R79A11>Cas9.M6	0.19 ± 0.132	-0.128 ± 0.114	0.346 ± 0.052	-0.082 ± 0.065	31.29 ± 32.62	23.16 ± 0.47	3/21
R91F02>sgRNA^{VGlut}	0.233 ± 0.099	-0.108 ± 0.1	0.341 ± 0.069	-0.081 ± 0.049	97.13 ± 41.94	23.73 ± 0.39	0/21
R91F02>sgRNA^{VGlut},Cas9.M6	0.301 ± 0.109	-0.109 ± 0.056	0.381 ± 0.071	-0.061 ± 0.042	112.28 ± 47.81	23.45 ± 0.31	0/24
R91F02>Cas9.M6	0.26 ± 0.166	-0.078 ± 0.107	0.366 ± 0.065	-0.035 ± 0.04	72.82 ± 45.83	23.43 ± 0.41	2/22
CNMa-KI-GAL4>sgRNA^{VGlut}	0.28 ± 0.123	-0.058 ± 0.088	0.357 ± 0.043	-0.063 ± 0.019	54.7 ± 43.96	23.03 ± 0.33	3/23
CNMa-KI-GAL4>sgRNA^{VGlut},Cas9.M6	0.268 ± 0.094	-0.117 ± 0.119	0.331 ± 0.055	-0.048 ± 0.086	51.21 ± 36.91	22.83 ± 0.29	3/18
CNMa-KI-GAL4>Cas9.M6	0.261 ± 0.066	-0.155 ± 0.114	0.342 ± 0.051	-0.088 ± 0.08	54.14 ± 36.21	22.85 ± 0.21	2/24
Clk4.1M>sgRNA^{VGlut}	0.281 ± 0.116	-0.052 ± 0.102	0.4 ± 0.057	-0.174 ± 0.043	61.29 ± 46.5	23.45 ± 0.39	3/23
Clk4.1M>sgRNA^{VGlut},Cas9.M6	0.181 ± 0.111	-0.074 ± 0.07	0.313 ± 0.101	-0.112 ± 0.047	77.13 ± 38.86	23.44 ± 0.38	0/21
Clk4.1M>Cas9.M6	0.294 ± 0.102	-0.096 ± 0.098	0.41 ± 0.035	-0.087 ± 0.051	80.18 ± 40.76	23.51 ± 0.25	0/24

***** P <0.01***